Stony Brook University

Understanding the effects of multivalent glycopolymer structure on molecular recognition

A Dissertation Presented

by

Eunjung Lee

to

The Graduate School

in Partial Fulfillment of the

Requirements

for the Degree of

Doctor of Philosophy

in

Chemistry

Stony Brook University

May 2012

Stony Brook University

The Graduate School

Eunjung Lee

We, the dissertation committee for the above candidate for the

Doctor of Philosophy degree, hereby recommend

acceptance of this dissertation.

Nicole S. Sampson – Dissertation Advisor
Professor of Chemistry

Kathlyn A. Parker – Chairperson of Defense
Professor of Chemistry

Benjamin S. Hsiao– Third member of Defense
Professor of Chemistry

Suzanne Scarlata– Outside Member of Defense
Professor of Physiology & Biophysics
Stony Brook University

This dissertation is accepted by the Graduate School

Lawrence Martin
Dean of the Graduate School

Abstract of the Dissertation

Understanding the effects of multivalent

glycopolymer structure on molecular recognition

by

Eunjung Lee

Doctor of Philosophy

in

Chemistry

Stony Brook University

2012

Carbohydrate-protein interactions are involved in a large number of important physiological and pathological processes. The weak binding affinity of a monovalent carbohydrate is compensated by multivalency in which multimeric recognition elements interact with a cell surface display of two or more receptors. In order to study lectin-carbohydrate interactions and find analytical and diagnostic applications, a large number of synthetic glycoconjugates have been investigated in the last decade.

In order to explore the effects of structural features of glycopolymers on the binding events, a series of polymers were synthesized. Multivalent ligands with pendant saccharide moieties were prepared from two different types of backbones via ruthenium catalyzed ring-opening metathesis polymerization (ROMP). Several functional groups and neutral and charged spacers were introduced onto the backbone to explore binding of glycopolymers to cholera toxin B subunit (CT B_5)

The interactions of cholera toxin and the polymers were determined using the intrinsic fluorescence of the Trp 88 residue in the cholera toxin binding site. As sugar epitopes in

polymers bind to CT B_5, a variable decrease in fluorescence was observed. The improvement in inhibition over glycopolymers was also observed using competitive ELISA experiments.

The interesting insight we found was that self-assembly of glycopolymers was involved in lectin binding events. Since glycopolymers have hydrophobic backbone and hydrophilic sugar moieties, glycopolymers form micelles and aggregates which derive from hydrophobic interactions of polymer backbone and inter- or/and intra-molecular hydrogen bonding of sugars.

Further studies to identify polymer behaviors in aqueous solution were carried out by measuring their critical micelle concentration (CMC) and determining their size and morphology by dynamic light scattering (DLS) and transmission electron microscopy (TEM). These studies revealed that norbornene-based and cyclobutene-based polymers containing sugar moieties self-assemble into micelles and vesicles. The polymer particles were spherical and their size was heterogeneous. Binding of the cholera toxin B5 protein did not induce further aggregation.

In glycopolymer particles, hydrophilic sugar moieties are located on the surface and hydrophobic backbones which composed of backbones of polymers are inside. In the recognition of lectin by synthetic glycopolymers, the binding affinity of glycopolymer was significantly inversely correlated with the self-assembled polymeric structure.

List of Contents

List of Abbreviations

ATRP	atom transfer radical polymerization
Ac	acetyl
AcOH	acetic acid
Ac_2O	acetic anhydride
bd	broad doublet
bs	broad singlet
CH_2Cl_2	dichloromethane
CMC	critical micelle concentration
CT B_5	cholera toxin B subunit
DBU	1, 8-diazabicyclo[5.4.0]undec-7-ene
DIEA	*N*,*N*- diisopropylethylamine
DLS	dynamic light scattering
DMAP	4-dimethylaminopyridine
DMF	*N*,*N*-dimethylformamide
DMSO	dimethyl sulfoxide
DPH	1,6-diphenyl-1,3,5-hexatrien
EDC	1-ethyl-3-[3-dimethylaminopropyl]carbodiimide hydrochloride
ESI-MS	electrospray ionization mass spectormetry
ELISA	enzyme-linked immunosorbent assay
Et	ethyl

Et_2O	diethyl ether
EtOAc	ethyl acetate
GM1	Galβ1-3GalNAc β1-4[NeuAcα2-3] Gal β1-4Glcβ1-ceramide
GPC	gel permeation chromatography
h	hour
H_2	hydrogen
HBTU	*O*-benzotriazole-*N*,*N*,*N'*,*N'*-tetramethyluronium hexafluorophosphate
HOBt	*N*-Hydroxybenzotriazole
HRP	horseradish peroxidase
Ig	immunoglobulin
MALDI-TOF	matrix-assisted laser desorption ionization
M_n	number-average molecular weight
M_w	weight-average molecular weight
NMR	nuclear magnetic resonance
NOESY	nuclear Overhauser effect spectroscopy
PBS	phosphate-buffered saline
Pd/C	palladium on carbon
PDI	polydispersity index
PNA	N-phenyl-1-napthylamine
ROMP	ring opening metathesis polymerization
RPM	rotation per minute
Ru	ruthenium
SDS-PAGE	sodium dodecyl sulfate-polyacrylamide gel electrophoresis

TEM	transmission electron microscopy
THF	tetrahydrofuran
TLC	thin layer chromatography
Trp	tryptophan
UV	ultraviolet
Z,Cbz	benzyloxycarbonyl

List of Figures

List of Schemes

List of Tables

Chapter I

Introduction

I. Glycopolymers

II. Synthetic multivalent ligands and their interactions with biological molecules

III. Cholera toxin B subunit

IV. Self-assembly of polymers

IV. Specific aims

I. Glycopolymers

Carbohydrates are involved in numerous biological processes, especially cell-cell interactions such as fertilization, immune defense, cell migration, viral infection, inflammation and cancer metathesis.[1-3] The specific mechanisms for numerous carbohydrate - lectin interactions still need to be unraveled. Therefore synthetic polymers containing carbohydrates, "glycomimics" have been developed as a promising tool in the biomedical and pharmaceutical fields.[4-8]

Glycopolymers can be defined, in a broad sense, as natural and chemically modified natural sugar–based polymers, and synthetic carbohydrate-containing polymers. In a narrow sense, they are synthetic polymers containing sugar moieties, which act as specific biological functional groups similar to those of naturally occurring glycoconjugates.[9,10]

There are two methodologies to synthesize glycopolymers. The first method is post-polymerization modification with the sugar moiety. This method is convenient, but results in heterogeneous conjugation because of incomplete reaction of sugar molecules due to steric hindrance. The other method is the polymerization of sugar-containing monomers. This is more widely used method because it gives glycopolymers of controlled and defined structures.

Glycopolymers have been synthesized from popular polymer synthetic methods, radical polymerization, ionic polymerization, ring opening metathesis polymerization (ROMP).

Free radical polymerization is a common method for the synthesis of glycopolymers. The advantage of this method is that high purity of solvent and monomer are not always necessary. In addition, the chemistry is tolerant of a variety of monomer functionalities and reaction

conditions. However, control of molecular weight is difficult. High polydispersity (PDI) values are observed (> 2.0). The high values are due to chain transfer reactions.

There are two ionic polymerization methods, cationic and anionic polymerization. Ionic polymerization yields polymers with well-defined molecular weights and low polydispersities. However, both techniques are very sensitive to reaction solvent and oxygen. Generally, anionic polymerization should be reacted in aprotic solvents to prevent interaction of the solvent with the growing polymer. In addition, polymerization methods require the highest purity of monomers and reactants.

Atom transfer radical polymerization (ATRP) and ring opening metathesis polymerization (ROMP) are popular methods in synthetic polymer chemistry because the methods use living catalysts which allow the formation of polymers with controllable molecular weights and narrow polydispersities.

Controlled/living radical polymerization (CRP)

Newly developed radical methods are controlled/living radical polymerization (CRP) techniques such as atom transfer radical polymerization (ATRP),[11-13] reversible addition-fragmentation chain transfer (RAFT) polymerization,[14,15] and nitroxide-mediated polymerization (NMP).[16] ATRP is one of the most widely used CRP methods due to convenient experiment setup and its compatibility with functional groups (Scheme 1-1).

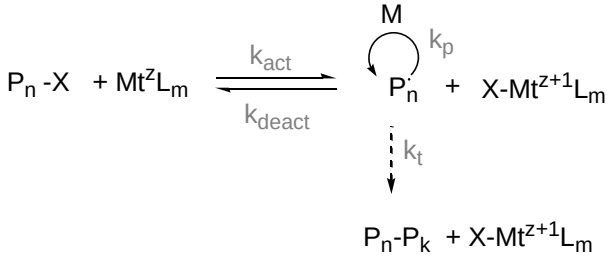

Scheme 1-1. Transition-Metal-Catalyzed ATRP (P_nX: alkyl halide initiators or dormant species, Mt^zL_m: low-oxidation-state metal complexes).[17]

Polymer brushes have been synthesized by controlled/living radical polymerization (CRP) via one of three routes: ″grafting through″, ″ grafting onto″ and ″ grafting from″.[18]

″Grafting through″ is mediated by polymerization of macromonomers. In this method, control of side chain density is easier than with other routes. However, degree of polymerization depends on the types of macromonomers. In ″grafting onto″ route, side chains are attached to the polymer backbone via coupling reactions. It is advantageous that polymers containing various functional groups are prepared. However, grafting density of side chain is limited due to steric hindrance. In ″grafting from″ route, side chains are polymerized from initiating sites in polymer backbones. This method allowed high grafting density and low molecular weight distribution. However, radical-radical couplings result in cross-linked polymers.

″Grafting through″ is the most popular route to synthesize glycopolymers. Homopolymers, poly[2-(β-D-glucosyloxy)ethyl acrylate] (PGEA) and copolymers, poly[2-(β-D-(glucosyloxy)ethyl acrylate-co-stearyl acrylate] were synthesized by ATRP following grafting through route. Molecular distributions of the polymers were relatively high (1.7 to 1.9). However, the polymers form micelle structures which exhibit favorable interactions with their target protein, Concanavalin A (ConA).[19]

As an example of grafting onto route, a combination of click chemistry and ATRP was used to synthesize glycopolymers.[20] Polymers functionalized with alkyne side chains were prepared from ATRP of trimethylsilyl methacrylate monomers. For both homopolymerization and copolymerization with methyl methacrylate, this method resulted in low polydispersity

(<1.5) and high monomer conversion (>80%). The attachment of sugar molecules by click reaction produced glycopolymers targeted to Con A. Coclicking of different sugar molecules enables the production of polymers varying in density of sugar in the same polymer backbones. Interactions of polymers with Con A increased with sugar density from 0% to 75%. At a higher sugar density than 75%, interactions remain constant due to steric hindrance of side chains.

″Grafting from″ method was developed to synthesize polymers functionalized with sugar molecules.[21-24] In addition, this method was applied to modify the surface of membrane, nanoparticles and carbon nanotubes.[25-28] The ″grafting from″ method via ATRP allows the formation of polymers with high grafting density and lengths of polymer side chains are easily controllable.

Ring opening metathesis polymerization (ROMP)

The synthesis of glycopolymers by ring opening metathesis polymerization (ROMP) has gained attention as a promising polymerization method.[29] The polymerization process is living and affords polymers with low polydispersity. ROMP catalysts have been developed to be tolerant of a wide range of monomer functionalities, which allows the polymerization reaction to take place in water. (Figure 1-1)[30-33] In addition, highly functionalized polymers can be easily generated.[34-40] The limitation of this method is that further purification may be required to remove the transition metal catalyst.

ROMP converts cyclic olefins into linear polymers containing new olefins in the polymer chain (Scheme 1-2).[41] In the initiation step, a cyclic olefin coordinates with a metal alkylidene complex. [2+2] cycloaddition generates a metallacyclobutane intermediate which undergoes

cycloreversion to produce a new metal alkylidene. The propagation step is the repetition of the cycloaddition-cycloreversion step until all monomers are consumed. The reaction is commonly terminated by addition of ethylvinyl ether to release the catalyst from the polymer terminus.

(a) (b)

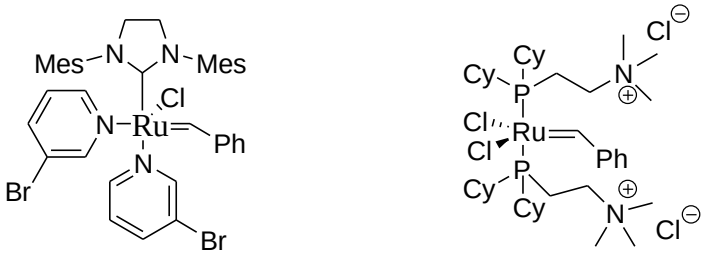

Figure 1-1.Structure of Ru alkylidene ligated to a N-heterocyclic carbene (a) and water soluble Ru alkylidenes.[29]

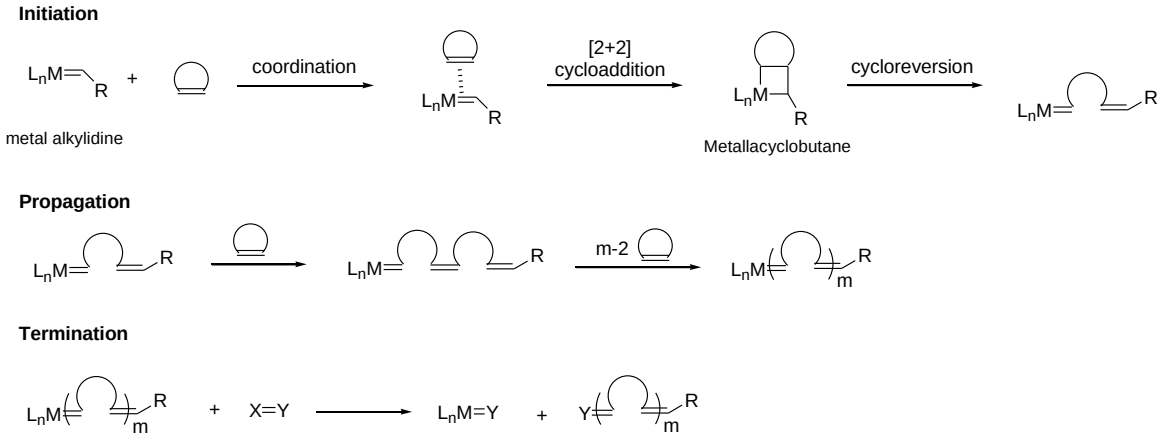

Scheme 1-2. Mechanism of ROMP.[41]

ROMP monomers are generally strained cyclic olefins with no bulky groups around the double bond (Figure 1-2).[29,41] The most popular monomers for ROMP are cyclic olefins which have considerable ring strain (>5 kcalmol^{-1}) such as cyclobutene, cyclopentene, cis-cyclooctene and norbornene.[42]

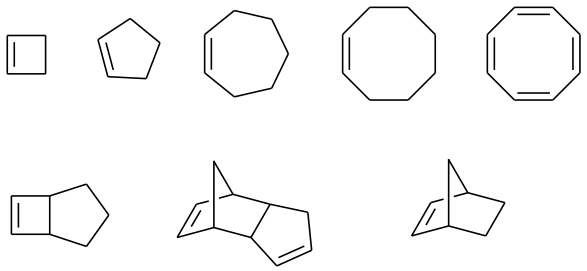

Figure 1-2.Cyclic olefin ROMP monomers.[41]

The initial study of ROMP to synthesize glycopolymers was performed with norbornene monomers containing glucose derivatives. (Figure 1-3 (a)) They were polymerized at 50℃, which resulted in glycopolymers with narrow PDI (1.1-1.2).[34]

(a) (b)

Figure 1-3. (a) Norbornene monomers containing glucose derivatives (R=glucose) (b), 7-oxonorbonene derivatives (R_1,R_2= glucose).

The ring opening metathesis polymerization (ROMP) of 7-oxonorbornene derivatives (Figure 1-3(b), was carried out. The biological activities of the resulting polymers were tested against Concanavalin A. The polymers were prepared from monomers with different linkages, α-*C*-glycoside or α-*O*-glycoside and their inhibition potencies as function of sugar densities was compared. Polymers with higher sugar densities showed higher inhibition than polymers with lower sugar density.[35] Another binding study of glycopolymers found that polymers with low density of sugar molecules are more efficient than polymers presenting low density of sugar molecules due to steric hindrance.[43] The results revealed that the density is important

to enhance the interactions between protein and polymers. However, microstructures of ligand-receptor complexes should be considered in designing multivalent ligands.

II. Synthetic multivalent ligands and their interactions with biological molecules

Detecting receptor complexes

Many methods to identify receptors involved in complex cellular processes have been utilized and developed. In immunoprecipitation, a specific antibody is used to detect a specific antigen. Föerster resonance energy transfer (FRET) is used to explore protein conformational changes in multiprotein complexes. Fluorescence microscopy images can show interactions of ligands with cell surface receptors. However, these techniques cannot explain molecular details for signaling complexes. For example, the density and aggregation of receptor complexes varies between cell types. The $\alpha_v\beta_3$ integrin is upregulated on both cancer cells and tumor-associated vessels, but it is absent or present at only low levels on normal tissues.[44] Using synthetic multivalent ligands, we can identify the structure and function of molecules involved in receptor signaling.[45]

Synthetic multivalent ligands as inhibitors, effectors and detectors

Multivalent ligands in cells are hard to characterize due to their heterogeneous features and complex mechanisms. Mimics of natural multivalent ligands can be helpful in understanding and exploring how the ligands function in biological systems. Synthetic multivalent ligands act as inhibitors to block the attachment of the natural ligand to its target

receptor in cell-cell, cell-virus, and cell-toxin interactions. Additionally, synthetic multivalent ligands act as effectors. Ligand binding initiates a particular signaling path, for example, it can stimulate an immune response.[46]

A variety of synthetic scaffolds have been considered such as small molecules (sugars and peptides), dendrimers, liposomes, and linear polymers. These various synthetic ligands have different characteristics including size, shape, flexibility, and bioavailability that can affect the binding affinity to cell-surface receptors. In the case of small molecules, the architecture is very similar to the natural ligand. However, most small molecules form dimers, which are too small to generate the multimeric effect. Liposomes are prepared by noncovalent assemblies of various compositions and display multiple recognition elements. They are used less frequently than other synthetic scaffolds because this is complicated by the difficulty in regulating the arrangement of ligands. Liposomes are susceptible to changes in the orientation of ligands due to interactions with the cell membrane.[47] Dendrimers are good candidates for multivalent ligands due to the high density of ligand moieties and the valency of the ligand can be controlled easily. However, in some dendrimers, accessibility to the target molecule is reduced due to the steric bulk of high-density ligands. Linear polymers are more attractive as synthetic ligands in comparison to dendrimers as linear polymers are more accessible. Polymers of this type are prepared by several kinds of synthetic methods such as radical, ionic or ROMP.[48,49] Among these methods, ROMP is an attractive method to generate well-defined synthetic multivalent ligands. The living polymerization by ruthenium catalyst generates polymers having narrow PDI and allows control over the degree of polymerization. The fast-initiation of ROMP facilitates making block copolymers with varying density and length.[50,51]

Examples of various synthetic multivalent ligands are summarized in Table 1-1.

Table 1-1. Examples of synthetic multivalent ligands

Target	Natural ligand	Description of synthetic ligand	IC_{50}	Enhancement in Activity observed	Assay*	Ref.
Inhibitors						
Shiga-like toxins	P^k tris-accharide	• Dimeric bridged P^k trisaccharide	STARFISH -SLT I ; 4×10^{-5} M	~ 40	a	52
		• decameric saccharide (STARFISH)	STARFISH -SLT II ; 6×10^{-9} M	~ 10^6		
		Bivalent trisaccharide	5×10^{-5} M	~38	b	53
Anthrax - toxin	PA_{63}				c	54
		Polyacrylamide -peptide derivatives	20 nM	7500		
		Poly-L-Glutamic acid	20 nM	4	c	55
		Poly(N-acryloyl succinimide)	2 μM		c	56
Con A	Mannose	ROMP		10	d,e,f	38,43
		PAMAM dendrimer		~ 5000	g	57
		Glycodendrimer-cyclodextrin	10-12 μM	113~136	h	58
		Neoglycopolymer (combination of click chemisty and living radical olymerization)		~ 60	e	20
Cholera-	GM1	Glutamic acid	0.058 mM for 11% sugar	640	I,j	59

toxin		based glycopolymer	0.05 mM for 21% sugar			
		Pentavalent ligand	6 nM	10^7	i	[60]
			1 μM	10^5		[61]
		Protein-based glycopolymer	350 μM 68 mM for galactose	200	k	[62]
		Large cyclic peptide	1-2 μM	10^5	i	[63]
		Bivalent ligand	9 μM	10^4	i	[64]
Fertili-zation	fertilin β	ROMP containing oligopeptide	1.1 μM by peptide	500-1700	l	[65]
Influenza Virus	HA	polyacrylamide with SA-containing side chains prepared by copolymerization		$10^4 – 10^5$	g	[66]
		Linear –dendron and dendrimer polymers		500-5000	g,m	[67]
Effectors						
	L-selectin	trisaccharide	2mM	3	n	[68]
	$\alpha_v\beta_3$ integrin	RGD-based peptidomimetic	0.55nM		o	[45,69]
	Chemoreceptor, MCP	ROMP		100~1000	p	[70]
	Anti-β_2GPI	Cyclic thioether peptide	$1\text{-}2\times10^{-4}$ M		q,r	[71]

*Assay method

a. Solid-phase inhibition assay; b. Competitive solid-phase assay; c. Cytotoxicity assay; d.Turbidity assay; e. Quantitative precipitation; f. FRET; g. Hemmagglutination Inhibition assay; h. Enzyme-linked lectin assay (ELLA); i. CT GD1b Enzyme-linked adhesion assay; j. Fluorescence titration assay; k. Non-linear regression methods; l. Fertilization index via IVF assay; m. ELISA infection assay; n. capture ELISA; o. Integrin binding assay; p. Motion analysis (mean angular velocity); Fluorescence microscopy, q. ELISA assay for anticardiolipin antibodies (ACA); r. *in vivo* assay

Multivalent ligands are used as tools to investigate complex cellular processes. They are also designed with variable structural features, shape, valency, orientation of ligand, flexibility and size of backbone. As multivalent ligands bind specific receptors, cellular signaling can be altered depending on the structure of the multivalent ligand. From these changes, how the receptors interact with each other spatially and how they regulate signaling events can be predicted. For example, integrins are cell-cell adhesion receptors and mediate intracellular signaling pathways. They can switch their binding abilities between low- and high-affinity modes. To identify the ability of integrin clustering, a group of synthetic ligands are used as chemical inducers of dimerization (CIDs).

In early work, FK506, a low-molecular weight drug that was converted a dimeric form, FK1012, was tested for dimerization of FKBP. After addition of FK1012, drug-mediated dimerization of target protein was observed.[72]

In the case of T-cells, T-cell receptors (TCRs) play an important role in recognizing foreign antigens leading to activation of cellular signal cascades. However, it is not clear whether they act monovalently or multivalently for antigen recognition. For this study, a streptavidin- based tetravalent ligand was tested.[73] Mono-, di-, tri-, or tetrameric ligands were

prepared by changing the peptide which binds to the TCR. When the tetramer was treated, T-cell activation was significantly increased.

In addition, the relationship between function and structure of receptors involved in signaling was investigated with respect to receptor orientation and composition of receptors. Several results show that orientation is less important than receptor clustering. Additionally, the affinity of receptor depends on the number of ligands. Nevertheless, it is unclear how many ligands are needed for effective receptor-ligand interactions. This was studied by preparing multivalent ligands that vary in the density and valency of ligands. The relationship between binding affinity and stoichiometry of ligand-receptor complexes suggests there is an improved binding affinities of *L*-selectin with increasing number of multivalent ligands.[74]

How synthetic multivalent ligands work

The major limitation of monovalent ligands is their weak binding affinity which comes from single site recognition. In particular, most saccharides bind to their receptors with low binding affinity in the μM to mM range. Many biological systems achieve tight binding through multivalency - multimeric recognition elements that interact with the cell surface. In human biology, multivalent events occur by interaction of a virus, bacterium, or cells to the cell surface.[75] Several mechanisms related with receptor binding of multivalent ligand have been suggested (Figure 1-4) including chelate effect, clustering, subsite binding and statistical rebinding.[43,46]

Chelate effect occurs when ligands bind to a specific receptor, its freedom to translate in solution is lost. However, there is no additional entropic cost for subsequent binding. Clustering is when the multivalent ligand causes receptors to cluster by altering the proximity

or orientation of receptors. In case of subsite binding, once a primary receptor-ligand interaction occurs, it facilitates the access of another ligand to the subsites and increases the binding affinity on subsites.

Statistical rebinding is a result of multimeric ligands forming high local concentration around binding sites. This allows more chances for ligands to interact with their receptors.

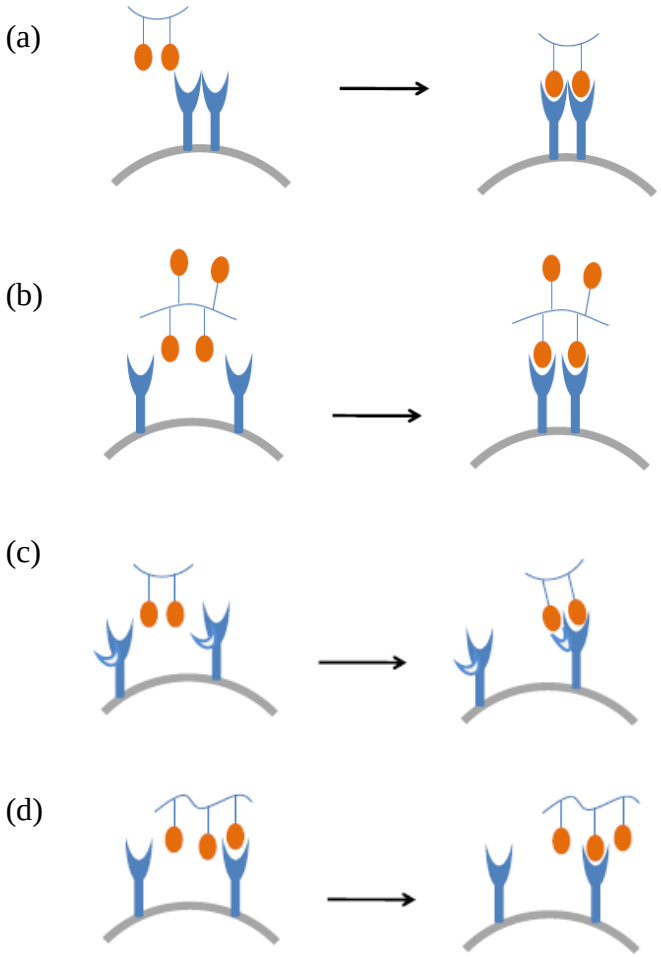

Figure 1-4. Possible mechanism of receptor-ligand interactions on cell surface. a) chelate effect, b) clustering, c) subsite binding and d) statistical rebinding. Figure adapted from Kiessling, et al.[74,76]

III. Cholera toxin B subunit

The classes of AB_5 bacterial toxins have been a threat to human health by causing mild traveler's diarrhea from infection by *E .coli* heat-labile enterotoxin (LT). Serious diarrhea can be cuased by infection of *Vibrio cholera* and the equally serious hemolytic uremic syndrome from infection by *Shiga toxin* family. [77,78] The cholera toxin (CT) family includes cholera toxin (CT) and *E.coli* heat-labile enterotoxin (LT and LT-II). CT consists of a catalytic activity in A subunit and a function of receptor binding and delivery of the toxin in pentameric B subunit. The B subunits bind to the oligosaccharide of GMI on the surface of epithelial cells. The toxin is then internalized into the cell and transported into the Golgi.[79,80] The A subunit is separated from the B subunit by reduction of a disulfide bridge and the A subunit translocates to the cytosol.[81] Inside the intestinal cell, the A subunit modified Gsα by irreversible ADP ribosylation which cause a continuous stimulation of adenylate cyclase, resulting in a massive efflux of fluids from intestinal cells.[82]

The oligosaccharide portion of ganglioside GM1 is a branched pentasaccharide (Galβ1-3GalNAc β1-4[NeuAcα2-3]Gal β1-4Glcβ1).[83] Ganglioside GM1 recognizes B subunits via direct and solvent-mediated hydrogen bonding.[84,85] Major contributions to toxin binding come from the two terminal sugars, galactose and sialic acid, in GM1 pentasaccharide (Figure 1-5). The O2, O3 and O4 in hydroxyl groups of galactose form hydrogen bonds with nitrogen in the side chains of Asn 90 and Lys 91. They make additional direct and solvent-mediated hydrogen bonds to residues Asn 14 and Glu 51. The sialic acid moiety interacts with the backbone of residues of Glu 11 and His 13 through hydrogen bonds. However, the other sugars, *N*-acetyl galactosylamine, central galactose and glucose residues are not involved in

toxin binding. When cholera toxin B:GM1 complexes are formed, their binding mode is proposed that the Gal (β1-3) GalNAc is inserted deeply into B-subunits as a "forefinger" and the sialic acid occupies a shallower depression on the surface of the toxin. This conformation allows the ceramide lipid tail attached to the glucose to be oriented far from the central pore so that the A subunit is located on the opposite site of cell surface.

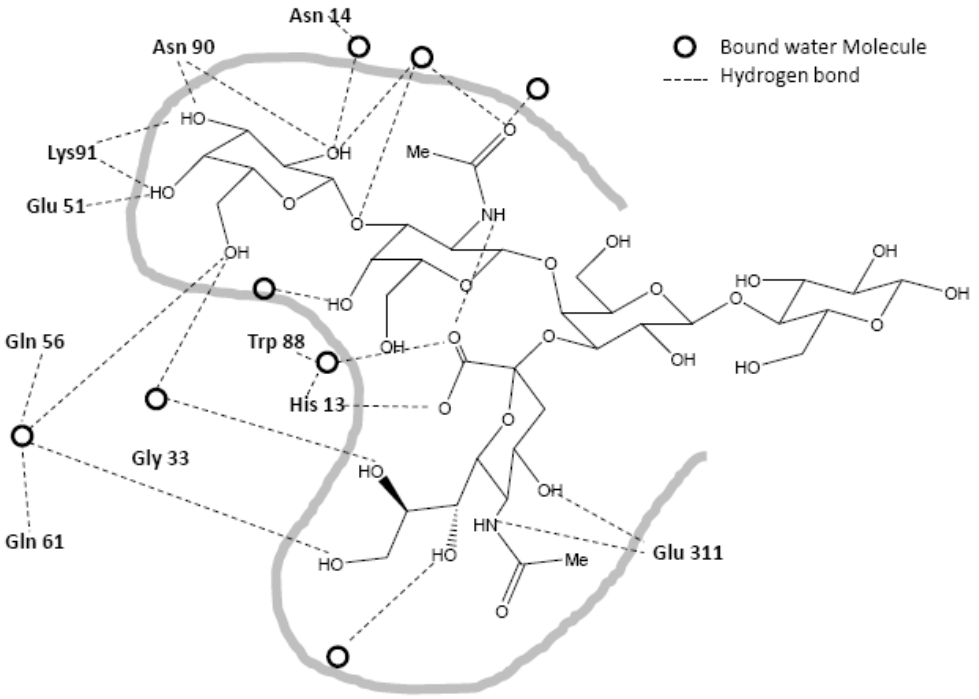

Figure 1-5. Structure GM1 pentasaccharide binding sites. Figure adapted from Lecommandoux et al.[90]

IV. Self-assembly of polymers

Formation of self-assembly

Lipids are biomolecules that form lamellar bilayer structures in nature. The extending study of mimicking of cell membrane resulted in several types of self-assembled structures such as “liposome”, “virosome”, “polymersome” and “peptosome”.

Several factors are involved in formation of polymer vesicles such as average MW of the polymer, the mass or volume fraction of each block and the effective interaction energy between monomers in the block.[86] One rule for the shape of surfactant is determined by the value of the surfactant packing parameter $P=\nu/a_0 l$, where ν and l are the volume and length of the hydrophobic moiety (alkyl chain), and a_0 is the optical surface area occupied by one surfactant at the micelle-water interface. Surfactants with value of $P<1/3$ produce spherical micelles. Whereas those with the value of $1/3<P<1/2$ and $1/2<P<1$ form elongated micelles and disk-like micelle, respectively. Regarding the formation of polymer vesicles, a general rule is followed a ratio of phospholipids-like ratio of hydrophilic to total mass ($f_{\text{hydrophilic}}$). Typical polymersomes form when $f_{\text{hydrophilic}}$ is $\approx$35% in water. Cylindrical shape and micelle form for molecules with $f_{\text{hydrophilic}}<50$ % and $f_{\text{hydrophilic}}>45\%$, respectively. Other factors involved in vesicle formation are free energy of amphiphilic polymers, interfacial energy of the hydrophobic-hydrophilic area and the loss of entropy. Polymers with low conformational energy, stiff polymer chains with low internal degrees of freedom, associate into structures to minimize the interfacial energy. In addition, strong secondary interactions such as charge interactions, hydrogen bonding, and dipolar interactions are involved in polymer vesicles.

Those effects are the driving force of lipid vesicle formation which restrict the intermolecular conformation and lead to bilayer formation.

Self-assembly of glycopolymer

Glycopolymers have self-assembled structures comparable to those observed for synthetic block polymers, which have attracted attention due to their potential in material and pharmaceutical areas.[87] It is known that polysaccharides form self-assemblies. For example, rod-like or worm-like chains are expected for cellulose, chitosan and hyaluronan. The conformation leads to the stiffness in asymmetry of polysaccharide conjugated diblock copolymers, which facilitate self-assembly in comparison to coil-coil block-copolymers.[88,89] Hyaluronan-co-poly(γ-benzyl L-glutamate) (PBLG) was studied for its self-assembly into vesicles.[90] The rigid and hydrophobic α-helical PBLG and hydrophilic hyaluronan blocks support formation of membranes. The resulting structures are copolymer bilayers having interdigitated PBLG blocks stacked in antiparallel orientation.

Additionally, self-assembled structures were found in glycopolymers which were synthesized via polymerization of sugar-containing monomers or addition of sugar molecules onto preformed polymer chain. Photoaddition of 2,3,4,6-tetra-O-acetyl-1-thio-β-D-glucopyranose onto 1,2-polybutadieneblock-poly(ethylene oxide) forms polymer vesicles spontaneously ("glycosome").[91,92]

Glycopolymers are used as drug carriers.[93] The glycopolymers were synthesized from sugar containing cyclic carbonate monomers by ring-opening polymerization, which self-assemble into micelles. These micelles containing doxorubicin were utilized as carriers for drug delivery.

V. Specific aims

In recent years, multivalent ligands have attracted considerable attention due to their increased activities compared to monovalent ligands. Thus, their potential as therapeutic agents has been suggested for several diseases. In the field of synthetic multivalent ligands, an important issue is to design multivalent ligands, which can act more efficiently in biological systems to understand molecular biological mechanisms. Another issue which has been rarely reported is the architecture of multivalent ligands in multivalent ligand-receptor systems. Here, we explain how the structures of multivalent ligands enhance binding activities.

Design and synthesis of glycopolymers as multivalent ligands

Our new synthetic multivalent ligands present multimeric sugar moieties which can span the cholera toxin B subunit and are designed to fit to the receptors based on the well-known crystal structure of the cholera toxin. Knowledge of the protein structure aids in structure-based design approaches.[61,78]

Glycopolymers were prepared with two types of polymers, homopolymer and block copolymer via ruthenium catalyzed ring-opening metathesis polymerization (ROMP). The living polymerization method facilitates making block copolymers, and the length of polymer can be manipulated by varying the ratio of monomers to the catalyst. A small set of glycopolymers was evaluated for their binding activities and their structures in aqueous solution in terms of length, valency and functional groups.

Evaluation binding activities of glycopolymers

In order to assess the interactions between sugars in the glycopolymer and CTB, two types of assay methods, fluorescence titration assay and competitive ELISA were applied. The fluorescence spectrum of CTB shows a change in intensity and a shift in its wavelength for maximum emission because the indole ring of tryptophan (W88) stacks against the hydrophobic α-face of the galactosyl moiety. In competitive ELISA, the binding of glycopolymers to CTB was evaluated over GM1 coated on the plate walls in a competitive assay. The potency of a series of glycopolymers was observed to be inversely proportional to the affinity of glycopolymer. Further support that glycopolymers bind to CTB was sought through NMR analyses.

Identifying architectures of glycopolymers in the process of toxin binding

Multivalent ligands have been developed to provide a key to identify receptor complexes. Polymer libraries as multivalent ligands are one of preferred tools for studying cell surface receptor topology. Therefore characterization of polymer behavior is essential to understand how polymers act in solution. However, polymer behavior in aqueous solution is complicated even though we designed synthetic ligand based on crystal structure of target receptor. The purpose of this study is to characterize the architectures of glycopolymers and elucidate how their structural features affect the binding efficiency of glycopolymers. Based on the result of biological assays, the glycopolymers are proposed to form self-assembled structures. This is not a common feature for homopolymers, but several groups have reported that homopolymers form micelles or vesicles. The dependency of glycopolymers behaviors on length, composition and valency was assessed.

Chapter II

Synthesis of glycopolymers as multivalent ligands targeting cholera toxin B subunits

I. Introduction

II. Results

III. Discussion

I. Introduction

To study the interactions between GM1 and CT B_5, numerous GM1 (Galβ1-3GalNAc β1-4[NeuAcα2-3] Gal β1-4Glcβ1) oligosaccharide mimics have been synthesized.[94-99] The synthesis of ganglioside GM1 (Galβ1-3GalNAc β1-4[NeuAcα2-3] Gal β1-4Glcβ1-ceramide) is very challenging. Thus one promising approach was synthesis of galactose derivatives or GM1 oligosaccharide analogues.

An example of potent modified-galactose inhibitors is *m*-nitrophenyl-α-D-galaotopyranoside (MNPG) (Figure 2-1).[94,95] Screening the ACD3D (Available Chemicals Directory) database for potential ligands of cholera toxin resulted in 35 candidate galactose derivatives. ELISA showed that *m*-nitrophenyl α-D-galactoside is the best ligand with 100 times higher potency (K_d= 0.5 mM) than galactose. Based on the crystal structure, one of the oxygen atoms of the nitro group displaces water #2 from the binding site to make a hydrogen bond with the backbone N-H of Gly 33 residing in a neighboring subunit of the pentamer. The displacement of water into bulk solution increases the entropy of the system, which leads to enhanced affinity.[100]

(a) (b)

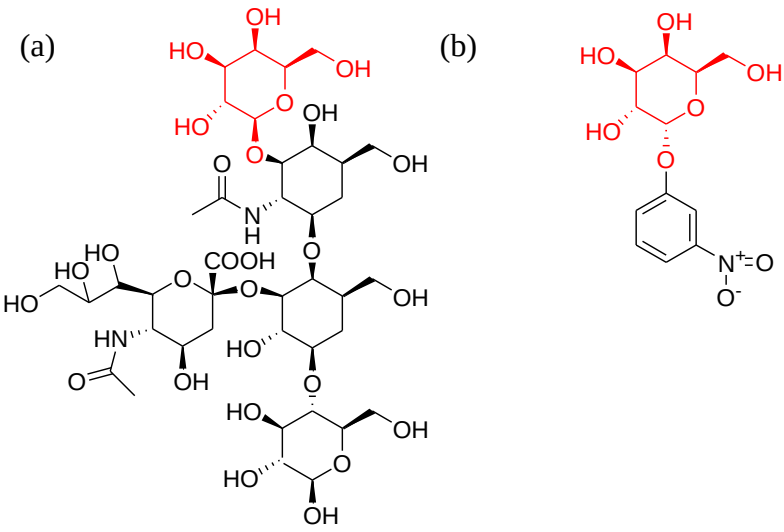

Figure 2-1. Chemical structure of GM1 oligosaccharide (a) and MNPG (b). [101]

Pseudo-oligosaccharide was synthesized as first generation of mimic of GM1 (Figure 2-2 (a)).[102,103] Since crystal structures of complexes showed that the terminal galactose and sialic acid (NeuAc) are essential for CT B_5 binding, a synthetic sugar was designed to contain the same core trisaccharide(Galβ1-3GalNAcβ1-4(NeuAcα2-3)) as GM1 and to replace the other two sugars with conformationally locked cyclohexanediol (CHD). Binding of pseudo-oligosaccharide to CT was evaluated by ELISA inhibition assay. The results showed that the inhibition profile of pseudo-oligosacchraride was clearly overlapped with that of GM1.

Second generation mimic of GM1 was designed to simplify the synthetic method by replacing the sialic acid with α-hydroxyacids (Figure 2-2 (b)).[104] In a direct binding assay, these modified sugars did not bind cooperatively to CT B_5. This loss might be due to missing NeuAc. Among second generation mimics, an ((R)-lactic acid derivative displayed the strongest affinity with a K_d of 190 μM.

(a)

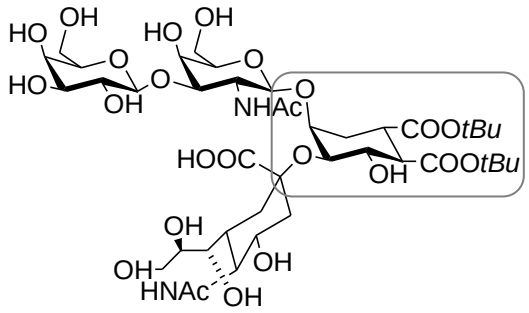

Galβ(1-3)GalNAc(1-4)
|
CHD
|
Neu5Acα(2-3)

(b)

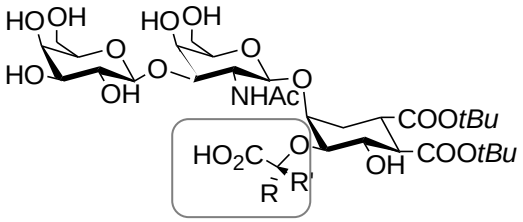

Galβ(1-3)GalNAc(1-4)
|
CHD
|
(R)-lactic acid

Figure 2-2. Structure of ganglioside GM1 mimics[96,102] (a) Pseudo-oligosaccharide, (b) Second generation mimic of GM 1 (R=Me, R′=H).

Another successful approach to targeting CT B_5 with synthetic ligands is modular structure-based design.[105] In this report, pentavalent ligands composed of three parts, core, linker and finger, fit into the five identical carbohydrate binding sites of CT B_5 so that the ligands form 1:1 complexes with CT B_5. The finger containing 1-β-amidated D-galactose which binds to CT B_5. The effects of the linker length on pentavalent ligand affinity were evaluated by incorporating different length carbon chains or peptides.[63,105] The results indicated that the ligand with lowest IC_{50} was detected when ligand effective dimension is matched with LT's binding site distribution.

Glycodendrimers have been developed as multivalent ligands displaying varieties of building blocks with different properties.[97,106,107] Lactose-functionalized dendrimers were synthesized and tested for their ability to bind CT B_5.[106] Enhanced cooperative binding efficiencies were observed as the generation of glycodendrimers became higher. In addition, Hill cooperativity coefficients of glycodendrimers were similar even though the dendrimers had different generations. It was suggested that multivalent effects were achieved by a model in which glycodendrimers bridge binding sites rather bind a single toxin.

Polymer-based linear ligands were reported as macromolecular inhibitors.[59,108,109] Poly (L-glutamic acid)-based glycopolymers were synthesized with varying saccharide densities and linker lengths to explore binding of the glycopolymers to CT B_5.[59] The highest inhibition efficiencies were achieved when the calculated average distance between adjacent saccharides in the glycopolymers matched the receptor spacing of CT B_5 (35 Å). Similar results were obtained with glycopolypeptides in which galactose-bearing glycopolypeptides were prepared via a combination of protein engineering and chemical strategies.[108] In this study, three

different polypeptides were prepared to identify the effects of saccharide spacing, backbone composition and charge. Glycopolypeptides with different saccharide spacings were prepared by varying the degree of substitution with saccharide. Inhibition results showed that appropriate saccharide spacing is more important than sugar density by comparing polymers with similar density of sugar molecules and different spacing between the sugar molecules.

II. Results

We undertook a rational approach to determine the interactions of glycopolymers and CT B_5. A series of glycopolymers was synthesized as multivalent ligands to fit the binding sites of CT B_5. The design of glycopolymers was based on the well-known crystal structure of the cholera toxin.[110] In order to characterize our multivalent systems, two types of glycopolymers, homopolymer and triblock copolymer, were synthesized with different backbone flexibilities, valences, polymer lengths and functional groups. For specific interactions of glycopolymers with CT B_5, galactose moieties are incorporated because it is a major component of GM1 in CT B_5 binding. Since the sugar binding pockets in CT B_5 are narrow and hydrophobic ligands show favorable interactions with the protein,[111] the B block of glyco-copolymers was designed to contain different linkers and backbones based on hydrphobicity and rigidity (Figure 2-3).

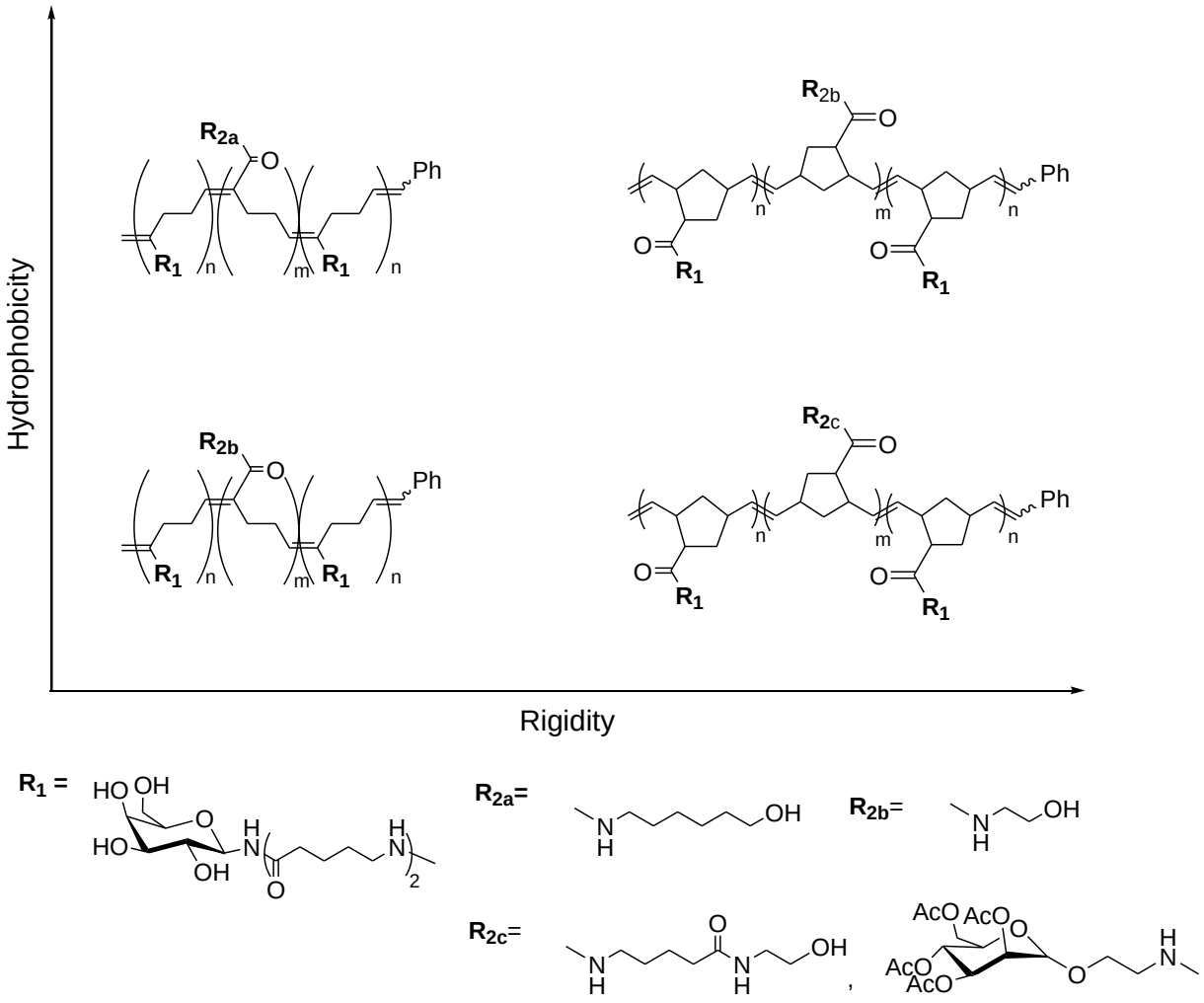

Figure 2-3. Design for comparing hydrophobicity and rigidity of polymers. Hydrophobicity was determined from ClogP values of polymers. Norbornene-based polymer backbone is more rigid than cyclobutene-based polymer backbone.

Preparation of protected sugars

β-Azido-2,3,4,6-tetraacetyl-D-galactose, **3** was synthesized following a procedure reported in the literature.[112] Pentaacetyl-D-galactose **1** was synthesized by peracetylation of D-galactose with acetic anhydride in pyridine in the presence of a catalytic amount of DMAP. Then the anomeric position of **1** was converted to bromide **2** with HBr/AcOH. 1-β-Azido-

2,3,4,6-tetraacetyl-D-galactose **3**, was obtained by treatment of **2** with NaN_3 under phase-transfer catalysis conditions (Scheme 2-1).

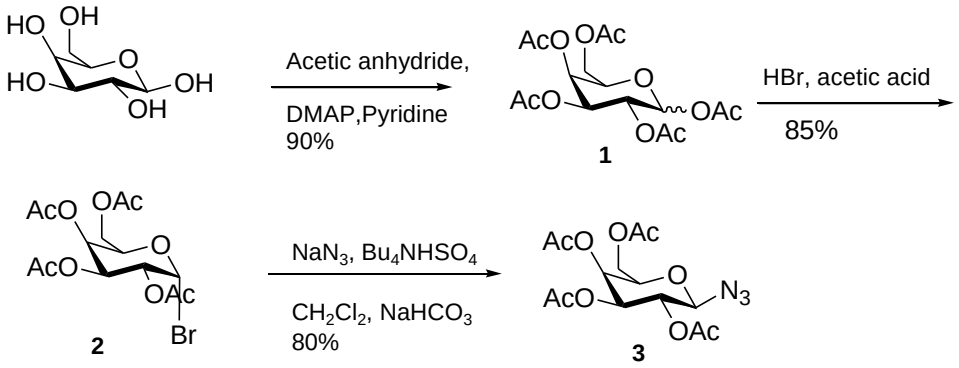

Scheme 2-1. Preparation of β-azido-2,3,4,6-tetraacetyl-D-galactose.

D-mannose was treated with acetic anhydride in pyridine in the presence of catalytic DMAP to afford pentaacteyl-D-mannose **4**. Selective deprotection of the anomeric acetyl group was carried out with hydrazine acetate in DMF.[113] Addition of trichloroacetonitrile in the presence of a catalytic amount of DBU resulted in formation of trichloroacetimidate **5**.[113] Treatment with 2-chloroethanol and a Lewis acid provided chloroethyl mannoside **6**, which was transformed into azide **7** (Scheme 2-2).[114,115]

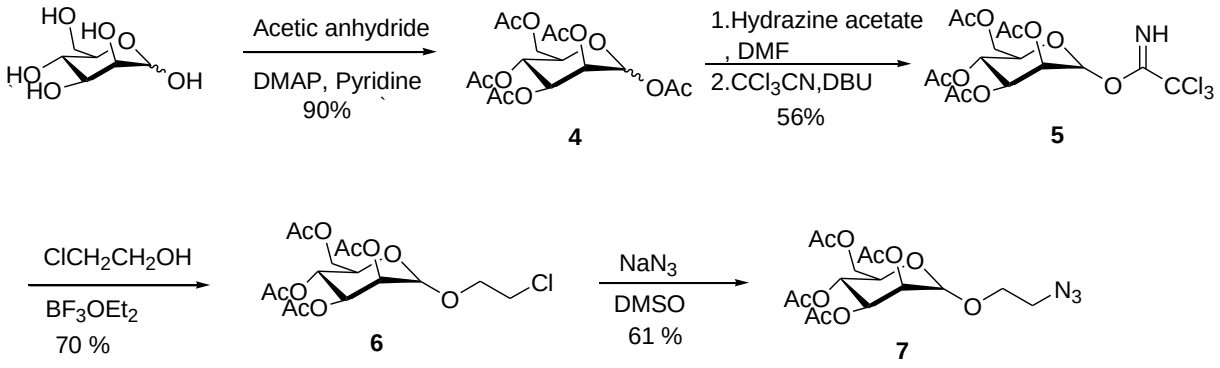

Scheme 2-2. Preparation of β-azido-2,3,4,6-tetraacetyl-D-mannose.

Preparation of monomers

Galactose monomers, **14** and **15** were synthesized from cyclobutene and norbornene carboxylic acid, respectively, with a 5-aminovaleric acid linker. The amine and carboxylic acid moieties of 5-aminovaleric acid were protected as the methyl ester and Cbz carbamate **8** and **9**, respectively. Coupling of **8** to **9** yielded compound **10**. After deprotection of the methyl ester of compound **10**, azido-2,3,4,6-tetraacetyl-D-galactose **3** was attached to compound **11** via Staudinger ligation.[116] The Staudinger ligation was the most efficient method to prepare amide-linked sugar derivatives. The traditional method to synthesize compound **12** is coupling of glycosylamines with an activated carboxylic group. The advantage of the Staudinger ligation is that conversion of the azide into an amine occurs in situ. In addition, glycosylamines are relatively unstable and were often obtained in low yield. Catalytic transfer hydrogenation of **12** in the presence of 10% Pd/C and 5% formic acid provided complete deprotection of the carbamates. Residual formic acid was removed on an ion-exchange column. The coupling of compound **13** with 5-norbornene-exo-carboxylic acid or cyclobutene-1-carboxylic acid afforded norbornene-based monomer, **14** or cyclobutene-based monomer, **15** (Scheme 2-3).

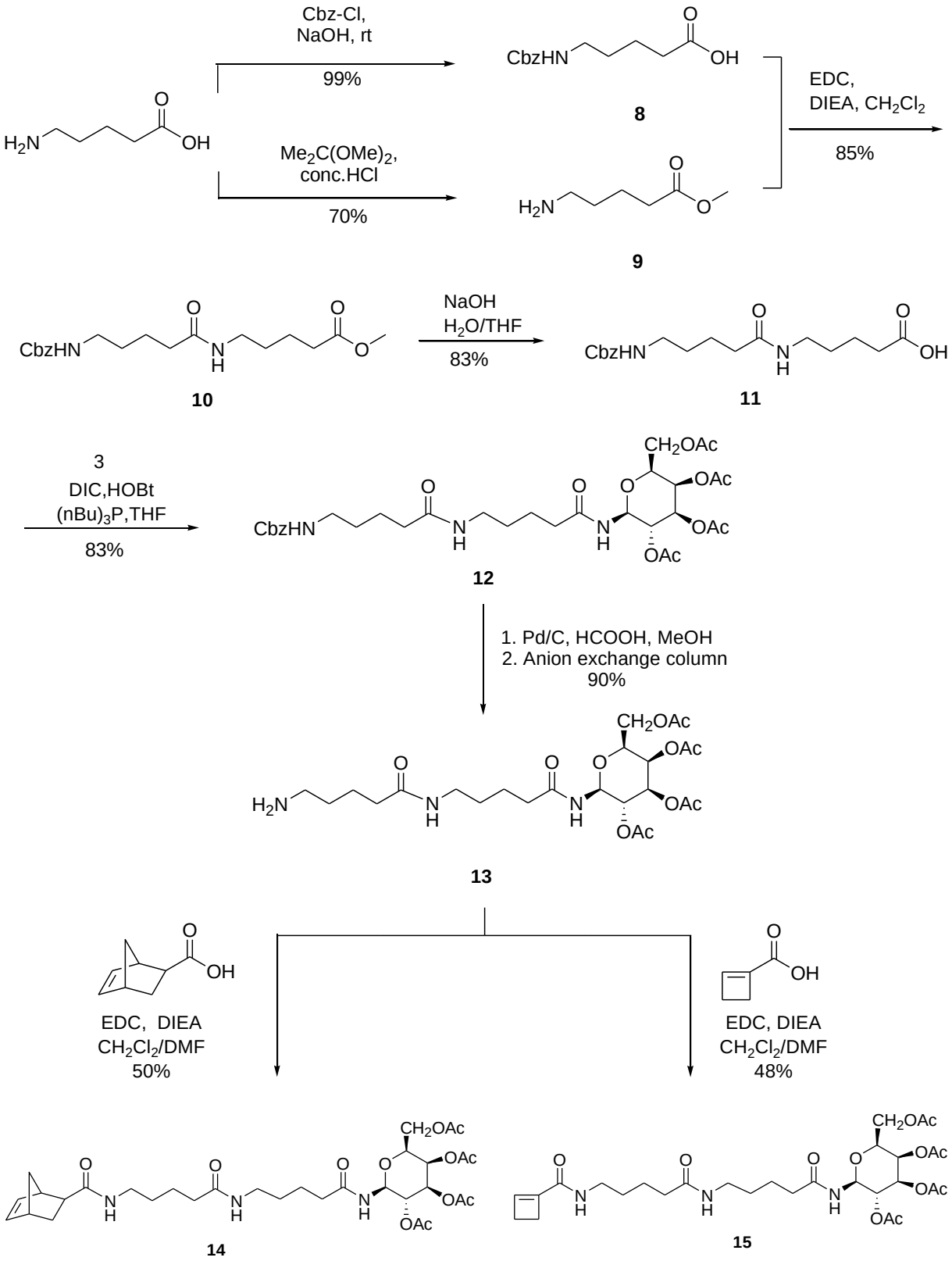

Scheme 2-3. Preparation of norbornene- and cyclobutene based monomers containing galactose.

Preparation of B monomer for ABA tri-block copolymers

To synthesize monomers **17** and **18**, 2-acetyloxyethylamine was synthesized from 2-hydroxyethylamine hydrochloride as reported in the literature.[117] Compound **16** was allowed to react with 5-norbornene-exo-carboxylic acid and cyclobutene-1-carboxylic acid to afford compounds **17** and **18** (Scheme. 2-5). Deacetylation was performed after polymerization because free hydroxyl groups on the monomers reduced the efficiency of the polymerization process (Scheme 2-4).

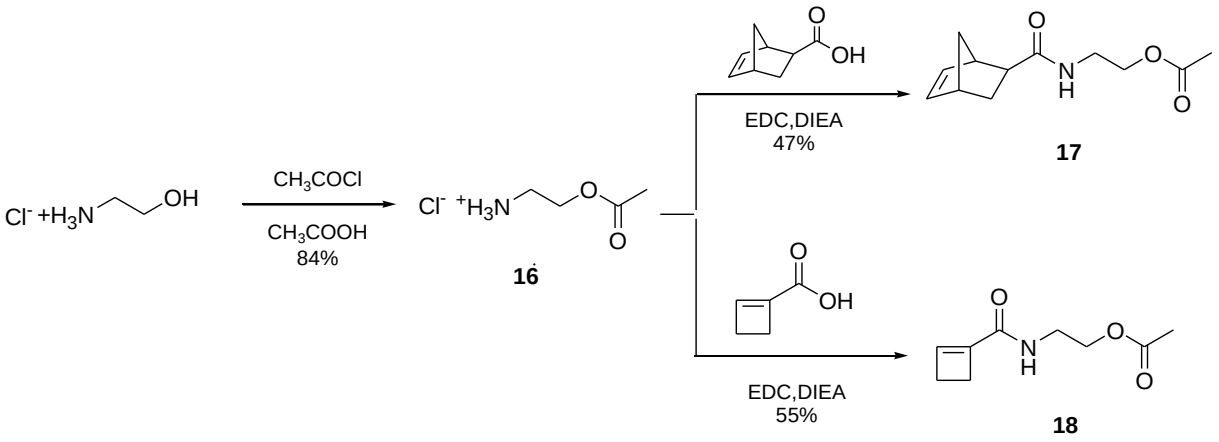

Scheme 2-4. Synthesis of monomers, **17** and **18**

For the preparation of monomer **20** (Scheme 2-5), compound **8** was coupled with 2-acetyloxyethylamine **16**, followed by deprotection of the carbamate in the presence of Pd/C and H_2. Then, compound **19** was coupled with 5-norbornene-exo-carboxylic acid to give compound **20** (Scheme 2-5).

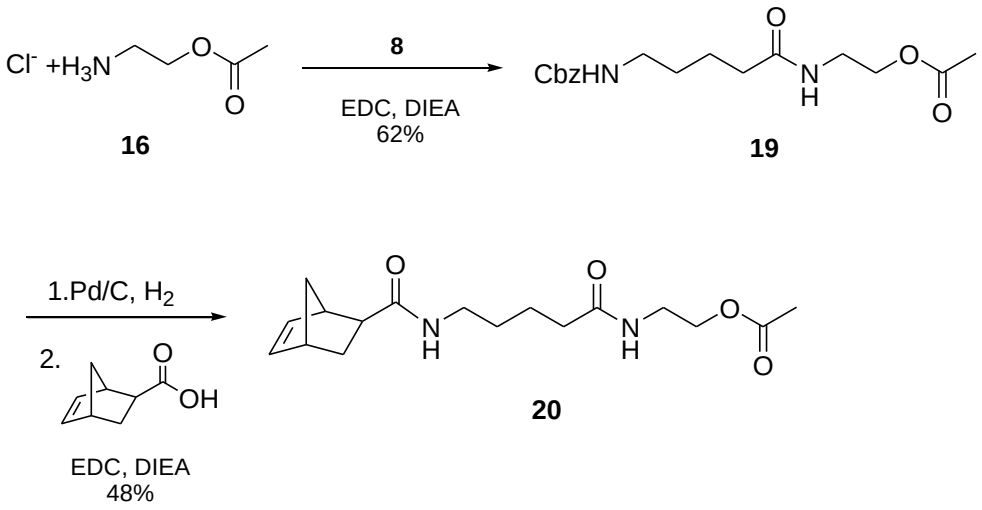

Scheme 2-5. Synthesis of monomer **20**.

To obtain norbornene derivatives containing negatively charged residues, glycine methyl ester was coupled to 5-norbornene-exo-carboxylic acid to provide compound **21**. After polymerization, the methyl esters were deprotected (Scheme 2-6).

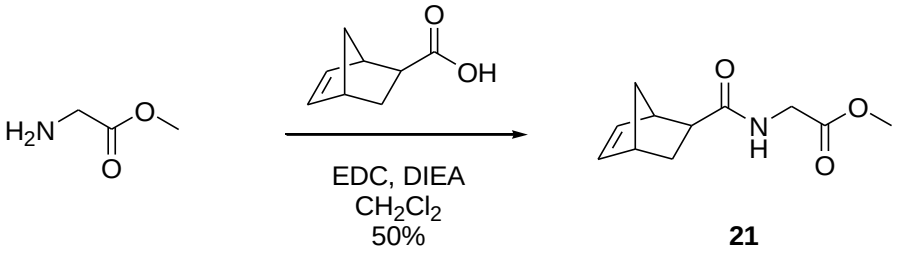

Scheme 2-6. Synthesis of norbornene monomer containing glycine methyl ester **21**.

Mannose monomer was synthesized via Staudinger ligation analogous to the preparation of compound **13**. Activation of azido-2,3,4,6-tetraacetyl-D-mannose **7** with tributylphosphine and subsequent reaction with 5-norbornene-exo-carboxylate active ester afforded compound **22** (Scheme 2-7).

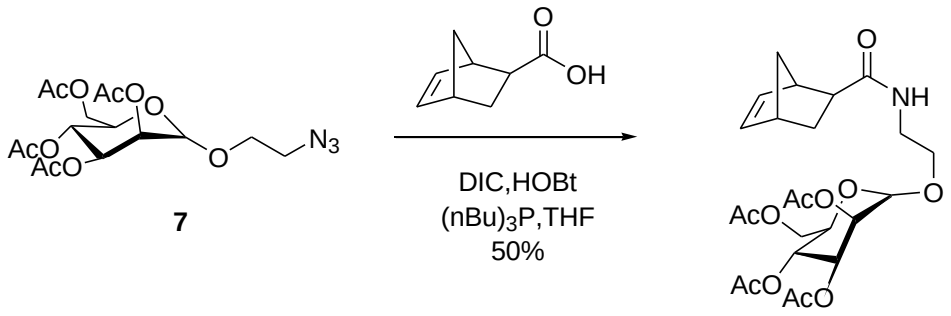

Scheme 2-7. Synthesis of norbornene mannose monomer **22**.

Preparation of homopolymers and triblock copolymers

The ring opening metathesis polymerization (ROMP) of monomers was conducted in CH_2Cl_2 with Grubbs′ N-heterocycliccarbene, dipyridyl ruthenium catalyst (Schemes 2-8 and 2-9). Homopolymers were synthesized from NB-$(ava)_2$-Ac_y-gal **14** and CB-$(ava)_2$- Ac_y-gal **15**. To obtain optimal reaction conditions, the polymerizations were run with various monomer/catalyst ratios, solvents, and reaction times. The conversion rate for each monomer, the molecular weight and the PDI are reported in Table 2-1.

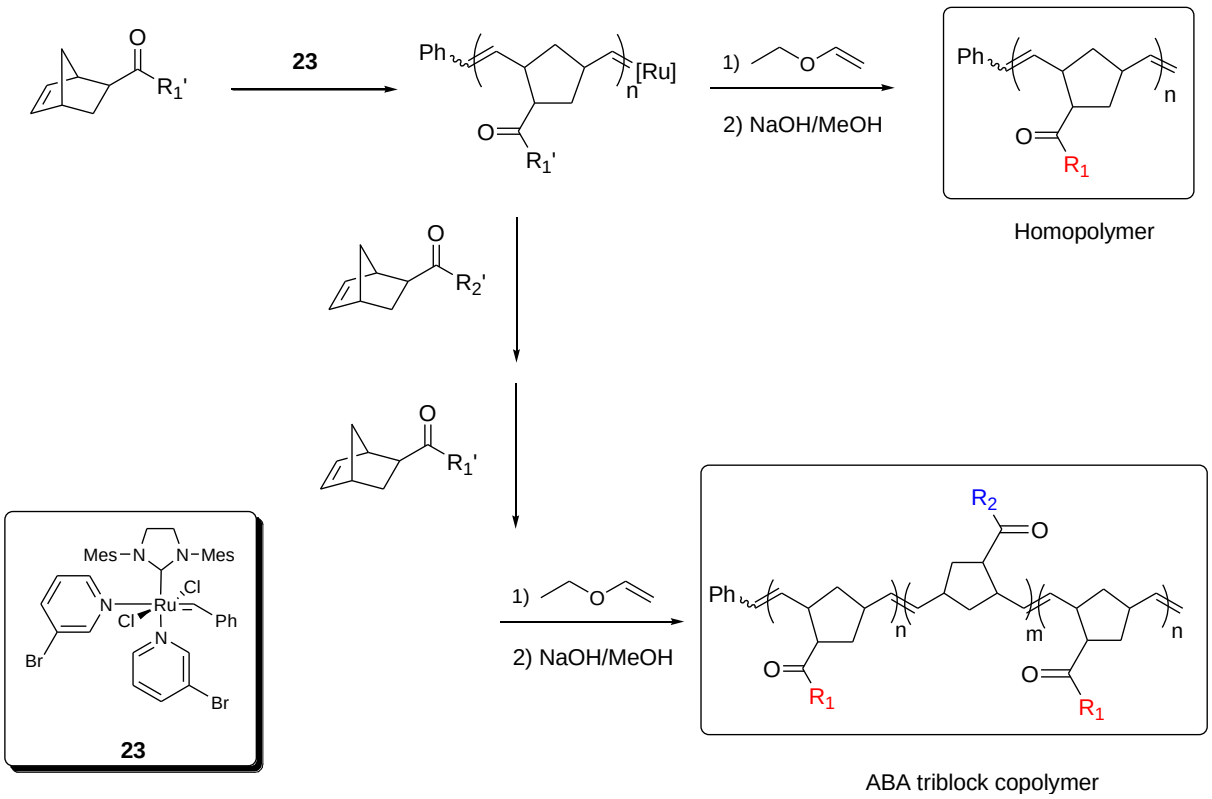

R_1'=-(ava)$_2$-tetraacetyl-D-galactose

R_2'= (a) (ava)-acetyloxyethylamine, (b) glycine methyl ester,

(c) tetraacetyl-mannose, (d) acetyloxyethylamine

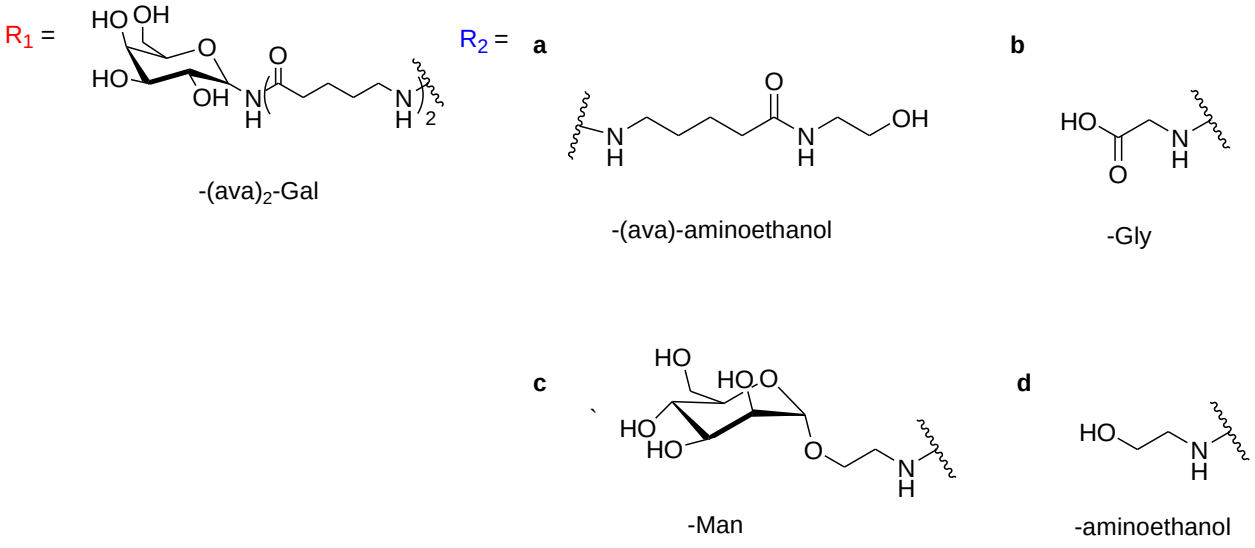

Scheme 2-8. Synthesis of glycopolymers from norbornene-based monomers.

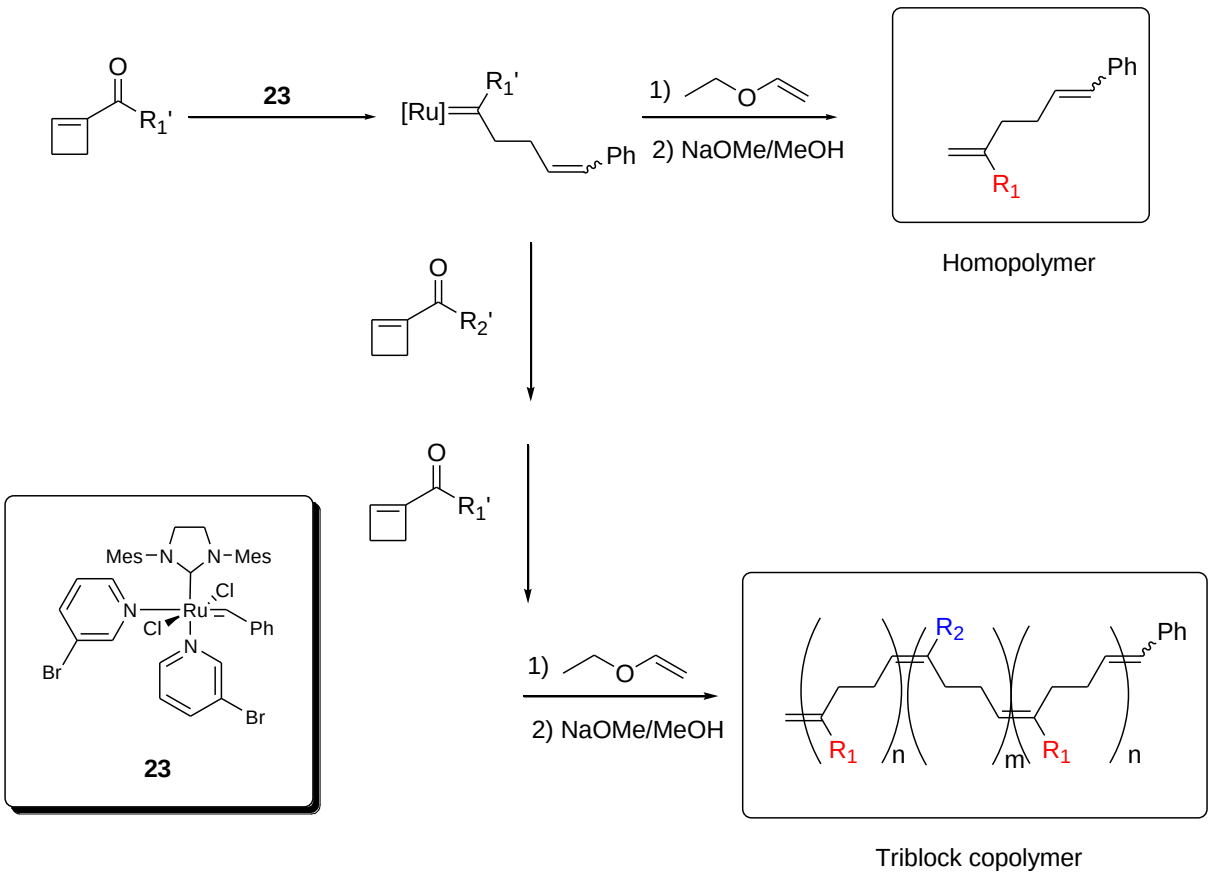

R_1'=-(ava)$_2$- tetraacetyl-D-galactose, R_2'=-acetyloxyethylamine

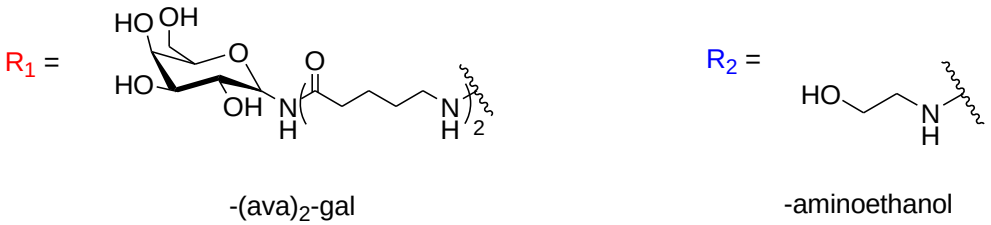

-(ava)$_2$-gal

-aminoethanol

Scheme 2-9. Synthesis of glycopolymers from cyclobutene-based monomers.

Table 2-1. Preparation of homopolymers via ROMP with monomer **14** (a) and **15** (b).

(a)

Entry[a]	Solvent	[**14**]/[Ru][b]	Conc. of catalyst (mM)	% Conversion yield [c] (time (h))	$M_{n,calc}$	$M_{n,GPC}$[d]	$M_{w,GPC}$[d]	PDI
1	CD_2Cl_2/CD_3OD (3/1)	10	5	100% (3.5)		6553	8468	1.29
2		10	10	100% (1.5)	6657	5432	6271	1.15
3	$CDCl_3$	10	10	100% (1.5)		4809.60	5370	1.11
4		15	10	100% (1.5)	9985	6937	7660	1.10
5	CH_2Cl_2	50	0.57	100% (2.5)	33345	34716	36121	1.04
6	CH_2Cl_2	100	0.57	100% (2.5)	66604	77047	83760	1.09

(b)

Entry[a]	Solvent	[**15**]/[Ru][b]	Conc. of catalyst (mM)	% Conversion yield[c] (time (h))	$M_{n,cald}$	$M_{n,GPC}$[d]	$M_{w,GPC}$[d]	PDI
7	CD_2Cl_2/MeOD (3/1)	10	5	20% (4)	6257	-	-	-
8		10	10	100% (0.5)	6257	4856	5732	1.18
9	CD_2Cl_2/CD_3OD (2/1)/ 2M LiCl	10	5	30-50% (3)	6257	-	-	-
10	$CDCl_3$	10	10	100% (1.5)	6257	4673	5243	1.12
11		15	10	100% (2)	9485	-	-	-
12	CH_2Cl_2	50	0.57	50% (3)	31370	-	-	-
13		100	0.57	50% (4)	62634	-	-	-

[a]Reaction temperature is 25℃.
[b][M]=concentration of monomer; [C]=concentration of Ru-catalyst.
[c]Calculated based on ^{1}H NMR spectra.
[d]Determined by UV detector using a polystyrene standard.

Polymerization progress was monitored by ^{1}H NMR spectroscopy. The reactions were quenched by addition of ethylvinyl ether. For polymerization of norbornene-based monomers,

it took 3.5 hours to reach complete polymerization in CD_2Cl_2/CD_3OD (3/1) (run 1). With higher concentrations of catalyst (0.01 M), the polymerization required a shorter reaction time (1.5 hours) for completion (run 2). In $CDCl_3$, the conversion yield was almost the same as in CD_2Cl_2/CD_3OD (3/1) and there was no significant difference in PDI between the two solvents. Polymerization of 50 or 100 equivalents of monomer resulted in high molecular weight polymers with low PDIs (run 5 and 6). Polymerization of cyclobutene monomers showed a greater dependence on solvents. In CD_2Cl_2/CD_3OD (3/1), only 20% of the monomer was converted into polymer with 5 mM catalyst concentration (run 7). LiCl was added to improve the solubility, but it only slightly improved reactivity (run 9). At a higher concentration of catalyst (10 mM), it took 1.5 hours and 0.5 hours for complete conversion of monomer in two solvents, CD_2Cl_2/CD_3OD (3/1) and $CDCl_3$. Initiation of polymerization in $CDCl_3$ was much faster than in CD_2Cl_2/CD_3OD (3/1) (Figure 2-4). In the case of cyclobutene monomer at monomer/catalyst ratio greater than 15, only 50% conversion of monomer occurred (runs 12 and 13).

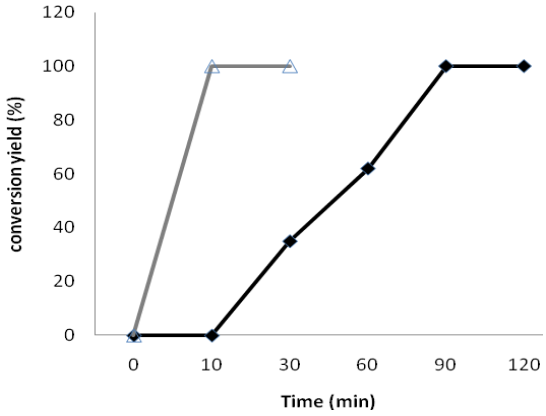

Figure 2-4. Polymerization rate of monomer **15** in different solvents: $CDCl_3$ (△) and CD_2Cl_2/CD_3OD (3/1,v/v) (◆).

The molecular weight of polymers was determined by GPC using THF with polystyrene standards. The obtained molecular weights were slightly different from the calculated molecular weights. In addition, PDI of homopolymers was lower than copolymers.Molecular weights of polymers also were analyzed by MALDI-TOF. Although MALDI-TOF is a powerful tool for molar mass determination of polymers, it depends on the ionization capability of molecules. Three different matrixes, CMBT (5-chloro-2-mercaptobenzothiazole), DHB (2,5-dihydroxybenzoic acid) and DHCA (3,5-dimethoxy-4-hydroxycinnamic acid) were used to measure molar masses of our polymers. The best result was obtained when the polymers were mixed with DHB. Although molecular weight repeats in MALDI-TOF spectra appear to correspond to the molecular weight of the monomer, we did not obtain spectra with sufficient resolution for further analysis. For longer polymers, the resolution of spectra was even lower.

The synthesis of triblock copolymer (ABA) was conducted by sequential addition of monomers (Figure 2-5). After n equivalents of A monomer containing sugar was polymerized, m equivalent of the second B monomer was added to establish B block (Schemes 2-8 and 2-9). Then another n equivalent of the first A monomer was added to complete the synthesis of triblock copolymer. Removal of protecting groups afforded free terminal alcohol and carboxylic acid moieties. Three monomers (**17**, **18** and **20)** were used to synthesize triblock copolymer containing hydroxyl groups in B block. Copolymer-1 and Copolymer-2 are triblock polymers of norbornene derivatives containing tetraacetyl galactose, **14** and glycine methyl ester, **21**. Copolymer 3 was synthesized from norbornene derivatives containing tetraacetyl galactose, **14** and tetraacetyl mannose, **22**. Cyclobutene-based triblock copolymers were synthesized from cyclobutene derivatives containing tetraacetyl galactose, **15** and 2-

acetyloxyethanolamine, **18**. The triblock polymers were characterized by ^{1}H NMR spectroscopy and GPC with polystyrene standards. The molecular weights of triblock copolymers are summarized in Table 2-2.

Table 2-2. Preparation of Triblock copolymers via ROMP

Polymer[a]	Conversion yield (%) (time(h))[b]	$M_{n,cald}$	$M_{n,GPC}$[c]	$M_{w,GPC}$[c]	PDI
Copolymer-1	100% (2h)	10615	3785.1	6615.2	1.75
Copolymer-2	100% (3h)	22077	9453.7	13300.5	1.4
Copolymer-3	100% (2h)	17274	9213.5	132351	1.43
Copolymer-4	100% (2h)	7690	3510.4	6006.5	1.71
Copolymer-5	100% (3h)	14749	8156.92	11114.6	1.36

[a]Reaction temperature is 25℃.
[b]Calculated based on ^{1}H NMR spectra.
[c]Determined by UV detector using polystyrene standard.

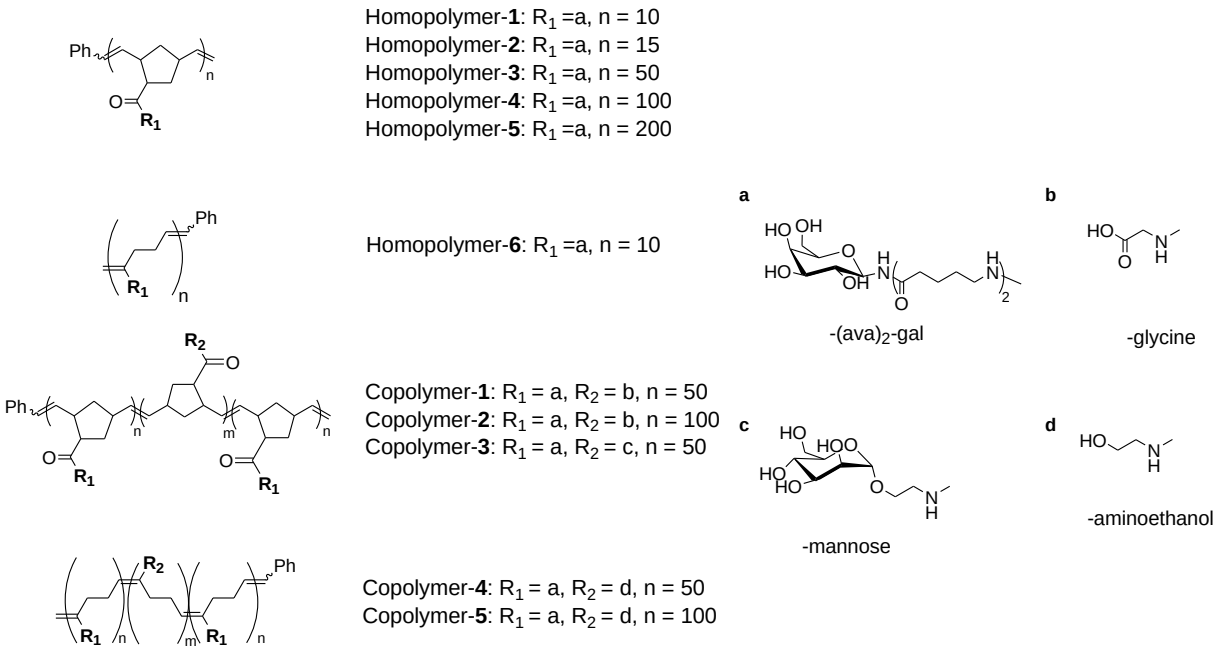

Figure 2-5. Summary of norbornene-based and cyclobutene-based glycopolymers.

III. Discussion

Rational design of glycopolymers

Cholera toxin B subunit (CT B_5) was chosen as a model protein to study the role of polymer backbones in ligand-receptor interactions. The crystal structures of CT B_5 and CT B_5-GM1 complexes enables the selection of small ligands to mimic GM1. Our glycopolymers utilized galactose in a multivalent format to examine the correlation of polymeric structures and binding efficiencies.

Several types of polymer structures have been used to investigate polymer behavior in multiple receptor complexes (Figure 2-6). Homopolymers display sugar moieties in each repeating unit to present multivalent ligands. Triblock copolymers (ABA) possess sugar moieties in the terminal A block and present bivalent ligands. The B block is a spacer of sufficient length and accessibility for favorable interactions of the ligands with CT B_5.

Triblock copolymer	Homopolymer having multiple copies of ligand
bivalent with single ligand 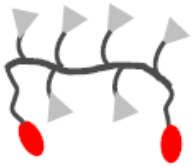 bivalent with multiple copies of ligand 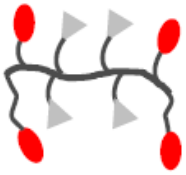	

Figure 2-6. Triblock copolymers and homopolymer presenting sugar moieties.

Spacers of triblock copolymers were designed based on the crystal structure of cholera toxin so that synthetic ligands have optimal spacial display.[64,84,118] The distance between two receptors in the B subunit is 35 Å for adjacent sites and 56 Å for non-adjacent sites. The galactose moieties interact with the B5 subunit in a cleft approximately 16 Å deep (Figure. 2-7). To estimate the precise distance of polymers, the distances between sugar molecules of triblock copolymers were calculated. The estimated effective length of linker and distance between two sugars was calculated based on equation (1). In a random-coil polymer, the root-mean square distance between the ends of the polymer for a freely joined chain is given by equation (1).[119]

$$(r^2)^{1/2} = l \times n^{1/2} \qquad (1)$$

Where n is the number of links or segments and l is the length of each segment.

Based on the calculation, distances between sugar molecules of norbornene-based triblock copolymers, 1-48-1 and 1-98-1 are 37 Å and 53 Å, respectively. Sugar spacing of cyclobutene-based triblock copolymers, 1-48-1 and 1-98-are estimated as 31 Å and 44 Å.

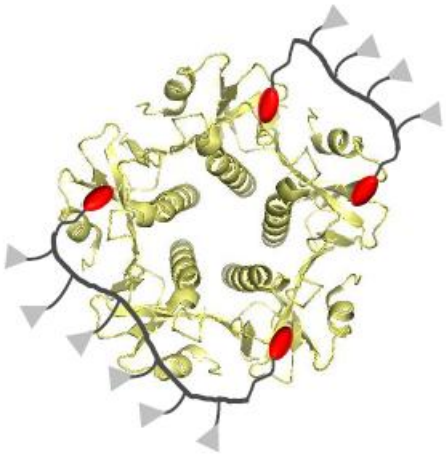

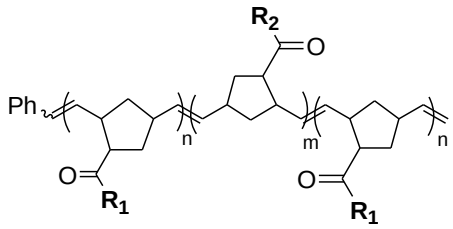

1-48-1; n=1, m=48
1-98-1 ; n=1, m= 98

Figure 2-7. CT B_5: glycopolymer complexes.

Even though multivalent ligands have advantages in protein-carbohydrate interactions, numerous factors are involved in a binding event such as structures of polymers, number of binding elements and the spacing of binding elements. Polymers with longer chain showed better binding efficiency, but the potency of polymers does not increase linearly as the length of polymers increase.[37,38,59] In addition, homopolymers have a much higher number of sugar molecules than block copolymers, but steric hindrance between sugar molecules needs to be considered.

Synthesis of monomers

Initially monomers having unprotected sugar were used in the polymerization synthesis as reported previously.[34] However, it was technically difficult to produce the monomers in high yield. To produce norbornene monomer containing galactose, norbornene-exo-carboxylic acid was allowed to react with galactosylamine derivatives. However, glycosylamines are relatively unstable and gave unsatisfactory results. The choices of solvents

for both reaction and purification are limited due to the high polarity of unprotected sugar. The resulting yields were relatively low. The most important issue is ROMP of the monomers with free sugars. Polymerization methods for monomers containing unprotected sugar have been developed, but they are still challenging. Sugar monomers are soluble in polar or aqueous solvent. However, the monomers are not soluble in solvents compatible with ruthenium catalyst. In addition, it was reported that the polymerization process with 1st generation grubbs catalyst is not efficient in mixture of CH_2Cl_2 and polar protic solvents.[34]

To overcome the difficulty with unprotected sugar monomers, the hydroxyl groups of galactose and mannose were acetylated. Azido-2,3,4,6-tetraacetyl-D-galactose, **3** was then conjugated to linkers to provide compound **13**, followed by coupling with 5-norbornene-exo-carboxylic acid and cyclobutene carboxylic acid to yield galactose-containing monomers **14** and **15**. Likewise, other functional groups in monomers were protected before coupling to 5-norbornene-exo-carboxylic acid. The functional groups on all monomers were retained during polymerization to avoid unfavorable interactions with ruthenium catalyst.

Synthesis of homopolymers and block copolymers

Homopolymers and block copolymers were synthesized from a series of monomers via ROMP. To determine optimal conditions of polymerization, several different conditions were tested in the homo-glycopolymer syntheses. The studies revealed the polymerization processes were slow in the solvent mixture $CDCl_2/CD_3OD$, perhaps because CD_3OD might coordinate with catalyst. The polymerization of cyclobutene-monomer, $CDCl_2/CD_3OD$ was incomplete at a low concentration of catalyst (0.005M) in the absence or presence of LiCl. $CDCl_2$ was found to be the best solvent for polymerization because monomer conversion is

fast even at a low concentration of catalyst and PDIs were narrow. Norbornene-based monomer was converted into high molecular weight polymer in $CDCl_2$, up to 200 monomer repeating units. However, long cyclobutene-based polymers were not obtained. Since the monomer showed fast initiation, propagation might not proceed quantitatively due to activity loss of catalyst.

Triblock copolymers with a spacer block having hydroxyl groups were designed in order to compare polymer properties based on hydrophobicity and rigidity. Relative hydrophobicity of monomers was compared based on ClogP of monomers. ClogP has been used to determine structure-activity relationships.[120-122] ClogP of cyclobutene-based monomer **18** is -0.643. ClogP of norbornene-based monomers, **17** and **20** are 0.417 and -0.297. For all triblock copolymers, A block contained same residue, galactose, thus the designed polymers were designed to compare how the hydrophobicity of linker involved in CT B_5-polymer interactions.

Cyclobutene-based monomers provided flexible linear polymers which have fewer covalent constraints than norbornene-based polymers. The difference in backbones of the two monomers comes from the repeating cyclopentene derived from norbornene monomers and flexible alkyl carbon chains in cyclobutene monomers.

All glycopolymers were successfully synthesized, but block copolymers which were polymerized from monomers **17** and **19** were not soluble in water after removal of their protecting groups. Therefore those polymers were not available for binding assays.

Incorporation of a mannose derivative into B block resulted in Copolymer-3. A mannose derivative was selected because mannose is not involved specific interactions with CT B_5. In addition, it provides polymers having high water solubility.

Triblock copolymers with a negative charge in the spacer block were generated from norbornene monomers containing galactose in A block and glycine in B block (Copolymer-1 and -2). It was reported that negative charged polymers exhibited enhanced binding affinity.[109] Those polymers are designed to study how charged molecule affects binding of polymers to CT B_5 as well as polymer structure.

Chapter III

Evaluation of interactions of glycopolymers with cholera toxin B subunit

I. Introduction

II. Results

III. Discussion

I. Introduction

Accompanying methods to evaluate carbohydrate-protein interactions have been studied with the development of synthetic ligands. It is known that a single carbohydrate has weak binding affinity for their receptors (association constant $\approx 10^6\ M^{-1}$). In biological systems, multimeric carbohydrates are involved in tight binding. Numerous synthetic ligands have been reported as mimics of nature and the assay methods to measure multivalent interactions are required.

The interactions between saccharide and cholera toxin B subunits (CT B_5) have been extensively studied with fluorescence titration assays.[123] From the crystal structure, it was found that galactose is the major sugar moiety in GM1-oligosaccharide (GM1-OS, Galβ1-3GalNAc β1-4[NeuAcα2-3]Gal β1-4Glcβ1) that binds to CT B_5. Fluorescence studies determined that galactose induces bathochromic shifts in the emission spectrum of W88 of CTB like GM1, because the indole ring of tryptophan (W88) stacks against the hydrophobic α-face of the galactosyl residue. Dissociation constants were determined to be 50 nM for GM1, 40 mM for galactose, and 81 mM for lactose. The binding of galactose is weaker than GM1 and is not cooperative, suggesting that GM1 communicate with adjacent CTB monomers to stabilize CTB structure and to facilitate cooperative binding. This method has been employed to determine the binding of synthetic ligands.

Another popular assay method to determine carbohydrate-CT B_5 interactions is enzyme-linked lectin assay (ELLA) which is a modified method of well-known enzyme-linked immunosorbent assay (ELISA).[78,124] This method is a competitive binding assay in which ligands compete for binding to lectin-enzyme conjugate with immobilized GM1 in microtiter plate wells. The development of color to detect concentration of lectin bound is inversely

proportional to the affinity of competitor ligands and is used to determine IC_{50}. However, the limitation of this method is that 100% of maximal inhibition is rarely observed. In addition, IC_{50} measured by ELLA is used to estimate dissociation constant, which is not always reasonable.[125] In spite of the limitations, ELLA is widely used because it is a simple and convenient assay.

Isothermal titration microcalorimetry (ITC) has been used to evaluate carbohydrate-CT B_5 interactions by measuring the heat caused by binding events as a function of ligand concentration. Direct interactions between ligands and receptors in solution provide enthalpy and free energy. Based on the thermodynamic parameters, binding constants are calculated, which is the major advantage of this method compared to other assays. However, ITC requires large amounts of materials and technically the assay method is quite sensitive to environment of samples such as temperature, buffer and concentration.[126-128]

New assay methods to evaluate CT B_5- multivalent ligands have been reported for better understanding of multivalency effects. Saturation transfer difference (STD) NMR spectroscopy measured the difference between a saturation transfer spectrum and a normal NMR spectrum.[129] This method is useful to monitor molecular mobility from ligand binding by measuring difference in its relaxation behavior. STD NMR has been developed mostly for small molecules. Recently, STD NMR studies were carried out to determine binding constants of bivalent ligands for CT B5 and binding epitope mapping.[130]

High-performance liquid affinity chromatography (HPLAC) was developed based on affinity chromatography in which differences in binding affinities of ligands were evaluated over cholera toxin bound column.[131] Retention time of synthetic ligands was used to calculate

K_d. However, the results of K_d was contradictory because interactions between multivalent ligands and CT B_5 resulted in broad peaks.

Real-time monitoring of protein-lectin interactions was performed by microarrays.[132] Glycodendrimers with different valencies were attached to porous aluminum oxide flow through microarray chip. The fluorescent signals detected when fluorophore-labeled lectins bind to their ligands. However, this method showed only specificity of lectins for certain sugars and whether it is multivalent or not, rather than measuring binding constant.

II. Results

A series of glycopolymers as multivalent ligands for CT B_5 was evaluated for their binding efficiency by fluorescence titration assay, ELISA and 1D ^{1}H NMR spectroscopy. CT B_5 was prepared following the procedure in literature.[133]

The interactions of glycopolymers with CT B_5 were measured by monitoring the intrinsic fluorescence of Trp 88, the only tryptophan residue in the B subunit. Emission spectra of protein were recorded with excitation wavelength at 280 nm. The spectrum of the protein in presence of short homo-glycopolymers exhibited a decrease in intensity as function of polymer concentration. The differences of intensity at 350 nm were normalized and plotted in Figure 3-1. The short homopolymers behave monovalently. Unfortunately, the glycopolymers are associated with problems around 310 nm in spectrum of CT B_5-polymer solutions and around 360 nm in spectrum of polymer solutions. It was supposed there are several reasons such as aggregations of polymers in buffer solution, absorbance of residual catalyst or end phenyl group of polymer. In addition, absorbance of polymer in emission spectrum increased as the molecular weight of the polymer increased. When cut-off filter (320

nm) was applied, signal around 310 nm was significantly reduced. DMSO was added to make the polymer solutions uniformly soluble (Figure 3-2). However, it was not effective to reduce emission intensity even in the presence of 10% DMSO.

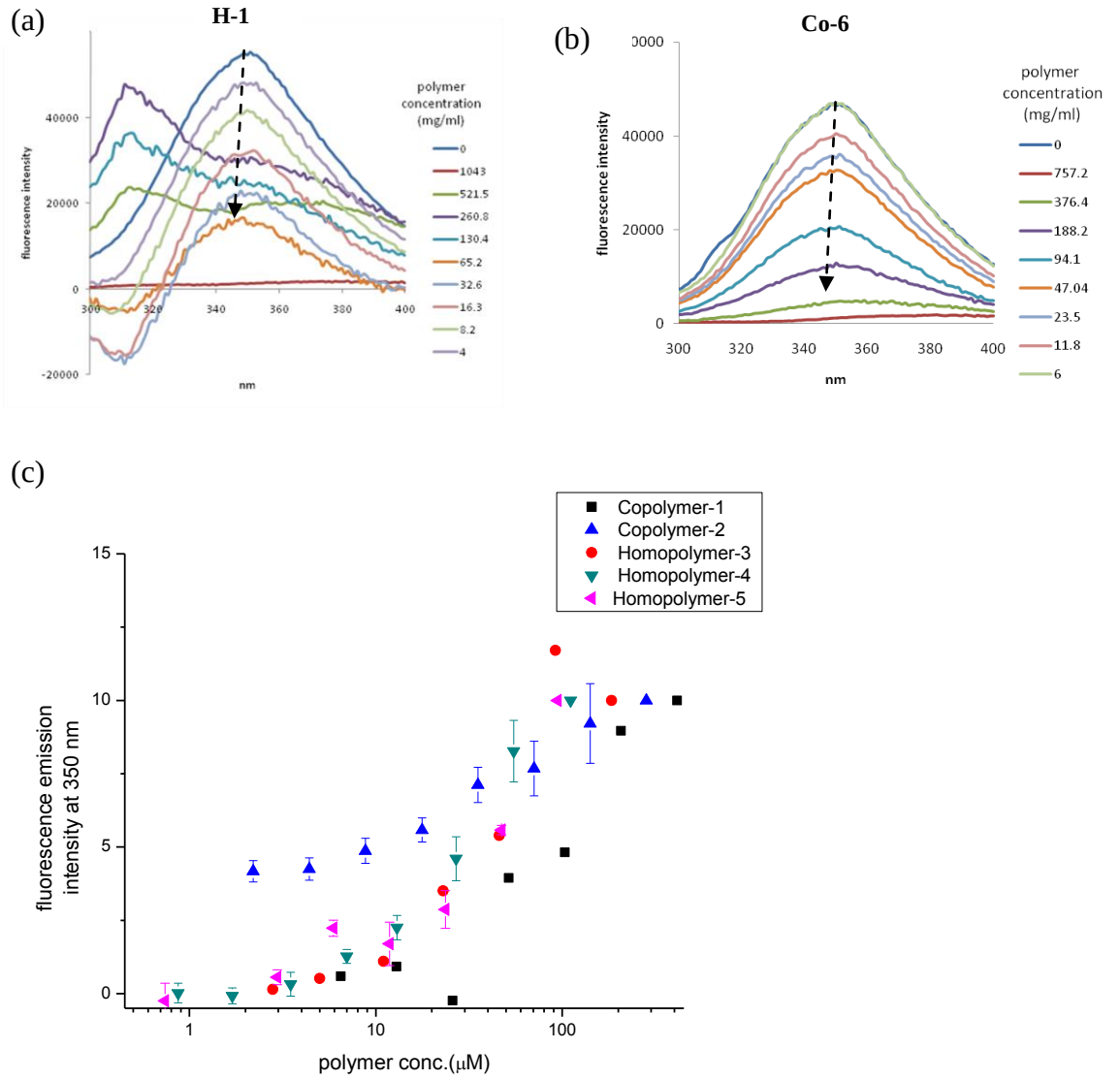

Figure 3-1. Fluorescence titration assay: (a) Homopolymer-**1**, (b) Homopolymer-**6**, (c) fluorescence intensity of glycopolymers at 350 nm. Emission intensity is normalized to 10.

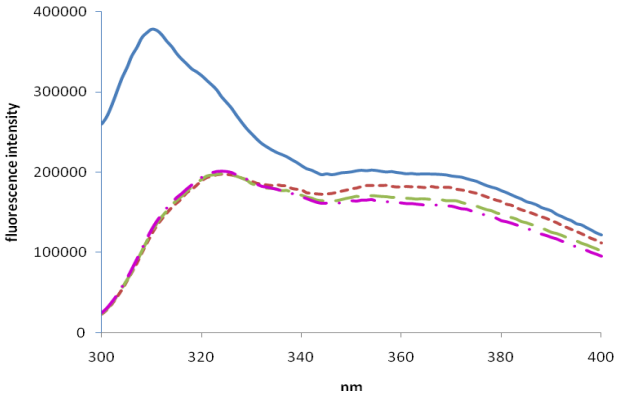

Figure 3-2. Fluorescence spectra of Homopolymer-3 (166μM) in presence of cut-off filter and DMSO. Polymer only (—), polymer/cut-off filter (···), polymer/cut-off filter/5% DMSO (- - -), polymer/cut-off filter/10% DMSO (-·-·-)

In addition, we tested how residual catalyst affected fluorescence even though a very small amount of catalyst was left from polymerization process. Since catalyst and polymer showed similar λ_{max} (246 nm) in UV spectra, catalyst may fluorescent. However, the emission intensity of catalyst was relatively low (~5%) compared to that of polymers.

Excitation and emission spectra of polymers were screened to find optimal wavelength in which emission of polymer is reduced and protein can be excited at the edge of absorbance of tryptophan. However, changing excitation wavelengths did not eliminate absorbance around 360 nm in emission spectrum (Figure 3-3 and 3-4). In addition, this phenomenon was more problematic with longer polymers

a)

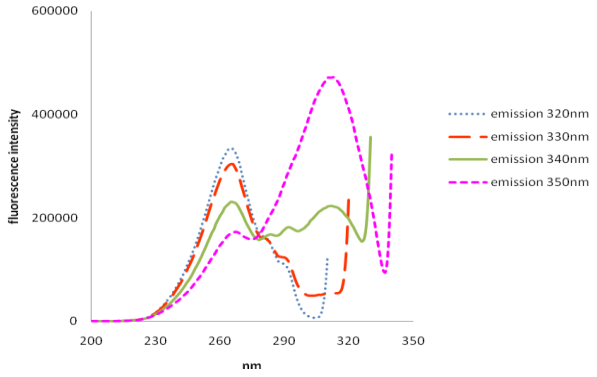

b)

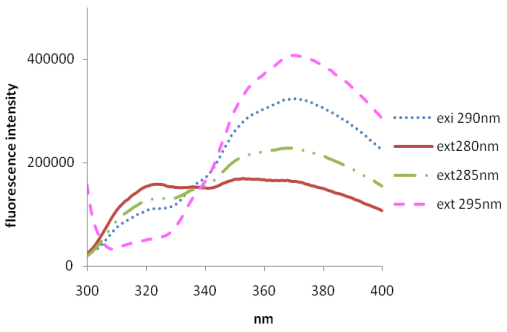

Figure 3-3. Fluorescence spectra of Homopolymer-**3** (166 µM). (a) Excitation spectra with emission wavelength from wavelength 320 nm to 350 nm, (b) Emission spectra with excitation wavelength from 280 nm- 295 nm.

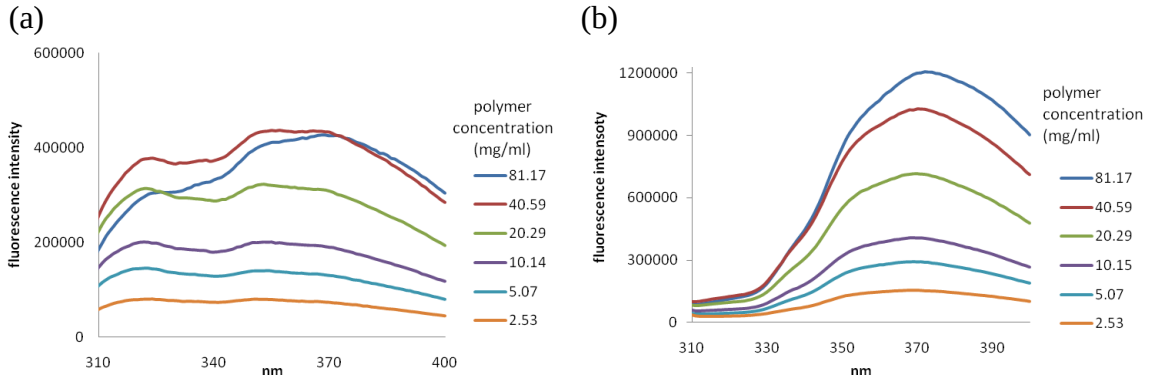

Figure 3-4. Fluorescence spectra of Homopolymer-**4**. (a) Emission spectrum with excitation at 280nm, (b) Emission spectrum with excitation at 295nm

Since fluorescence titration assay was not efficient even though conditions were changed such as cut-off filters, buffer and addition of organic solvents, a higher concentration of protein (2.5 µM) was employed to increase the protein signal relative to the polymer signal. Fluorescence spectra of glycopolymers resulted in better signal for binding. (Figure 3-4). The changes in emission at 350 nm in the presence of homopolymers (Homopolymer-3, 4- and -5) and triblock copolymers (Copolymer-1 and -2) are summarized in Figure 3-5.

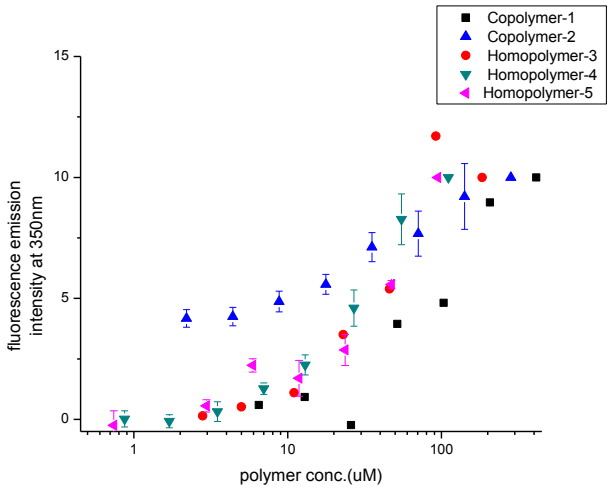

Figure 3-5. Fluorescence titration assay with glycopolymers in the presence of 2.5µM CT B_5 excitation at 295 nm

ELISA

ELISA was carried out for evaluation of interactions of glycopolymers with CT B_5. For this study, CT B_5 was expressed in *E.coli* following procedures in literature.[133] The well-known method for screening inhibitors of CT B_5 is enzyme-linked lectin assay (ELLA) in which commercial CT B_5-HRP was used. With CT B_5 in hands, the assay method was modified where rabbit anti-cholera toxin-HRP was used to detect CT B_5.

Microtiter plates were coated with 2 μg/ml of GM1. Various concentrations of glycopolymers were preincubated with 4 ng/ml of CT B_5. The polymer-CT B_5 solutions were transferred to the GM1 coated plates and incubated for 30 min. In this step, free CT B_5 – which does not bind to the polymers was bound to GM1 in plate wells and GM1- CT B_5 complexes were detected by adding antibody. The development of color by 3,3',5,5'-tetramethylbenzidine (TMB) solution was inversely proportional to binding efficiency of polymers. Homopolymers and Copolymer-3 showed similar behavior (Figure 3-6 (a)-(d)). Generally, the binding efficiencies increased as a function of polymer concentration. Interestingly, moderate binding efficiencies were observed at low concentration of polymers. Copolymer-1 and -2 showed similar results like homopolymers (Figure 3-6 (e) and (f)). From biphasic pattern of ELISA results, we supposed that different structures of glycopolymers might involve in CT B_5 binding. Cyclobutene-based polymers (Copolymer-4 and -5) exhibited different behaviors than other glycopolymers. The binding of those glycopolymers to CT B_5 increased as polymer concentration increased. However, no significant binding was detected at low polymer concentrations (Figure 3-5 (g) and (h)).

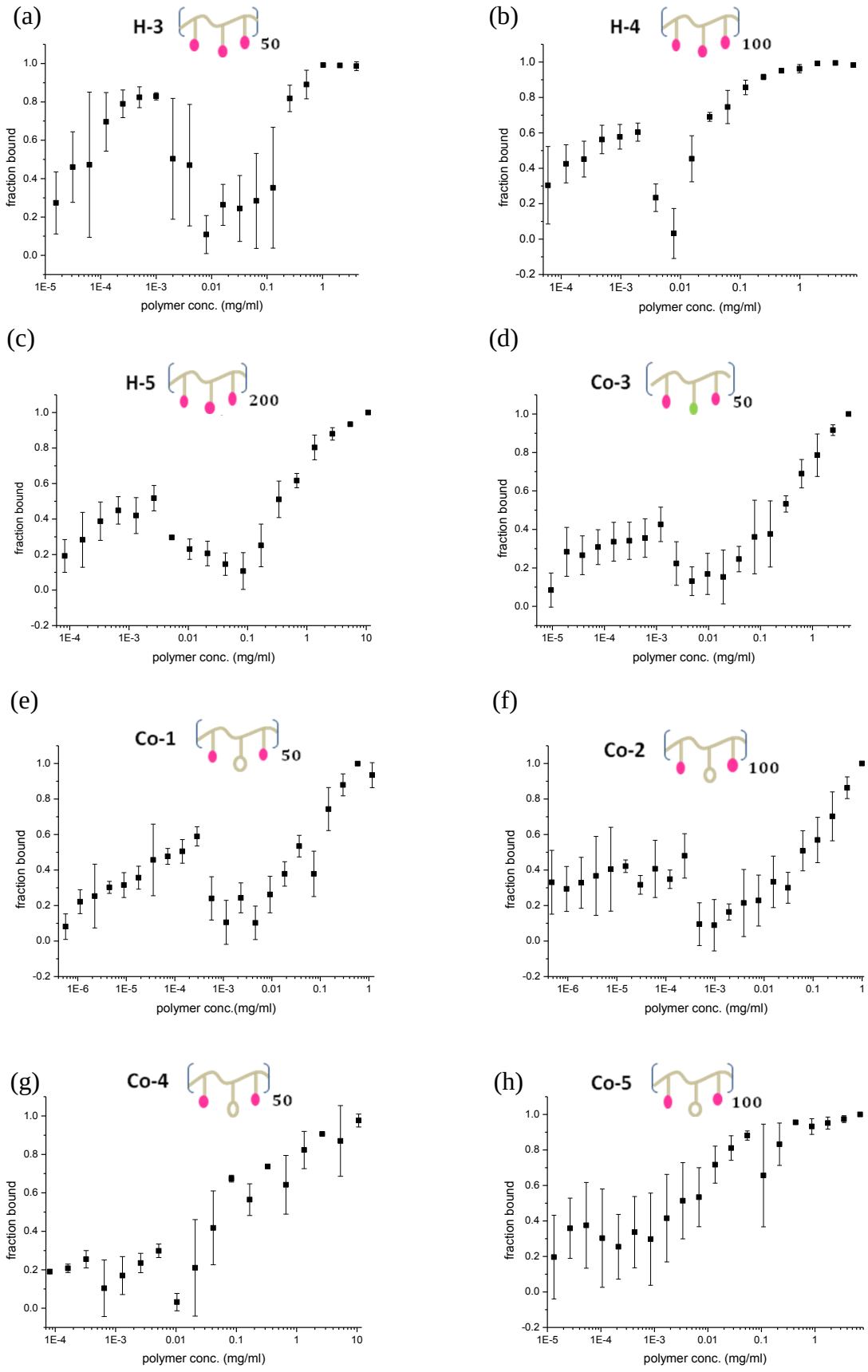
(a)
H-3
50
fraction bound
polymer conc. (mg/ml)
(b)
H-4
100
fraction bound
polymer conc. (mg/ml)
(c)
H-5
200
fraction bound
polymer conc. (mg/ml)
(d)
Co-3
50
fraction bound
polymer conc. (mg/ml)
(e)
Co-1
50
fraction bound
polymer conc.(mg/ml)
(f)
Co-2
100
fraction bound
polymer conc. (mg/ml)
(g)
Co-4
50
fraction bound
polymer conc. (mg/ml)
(h)
Co-5
100
fraction bound
polymer conc. (mg/ml)

Figure 3-6. ELISA results for glycopolymers. (a) Homopolymer-3, (b) Homopolymer-4, (c) Homopolymer-5, (d) Copolymer-3, (e) Copolymer-1, (f) Copolymer-2, (g) Copolymer-4, (h) Copolymer-5.

1D ^{1}H NMR study of glycopolymers-CT B_5 complexes

Since the binding of cholera toxin B subunits to oligosaccharides of GM1 happened near the tryptophan residue, NMR experiment was performed to monitor the interactions of CT B_5 with glycopolymers, especially in the aromatic region of aromatic group. Homopolymer-2 was mixed with CT B_5 in D_2O at 298K. Homopolymer has one terminal phenyl group which normally appeared as a small peak in D_2O, allowing resonances of aromatic groups in CT B_5 to be distinguished from that of polymers. The spectrum of the protein in the presence of polymers showed changes of resonance as polymer bound to the protein between 6.0 to 9.0 ppm (Figure 3-7). Signals for the indole ring of tryptophan reside around to 6.8 ppm and 7.18 ppm. The peaks of the protein become broaden and shifted between 6.5 and 8.0 ppm and a new peak appeared at 8.66 ppm. The NMR study confirmed Homopolymer-4 bound to CT B_5 which cause changes of environment of binding sites of CT B_5.

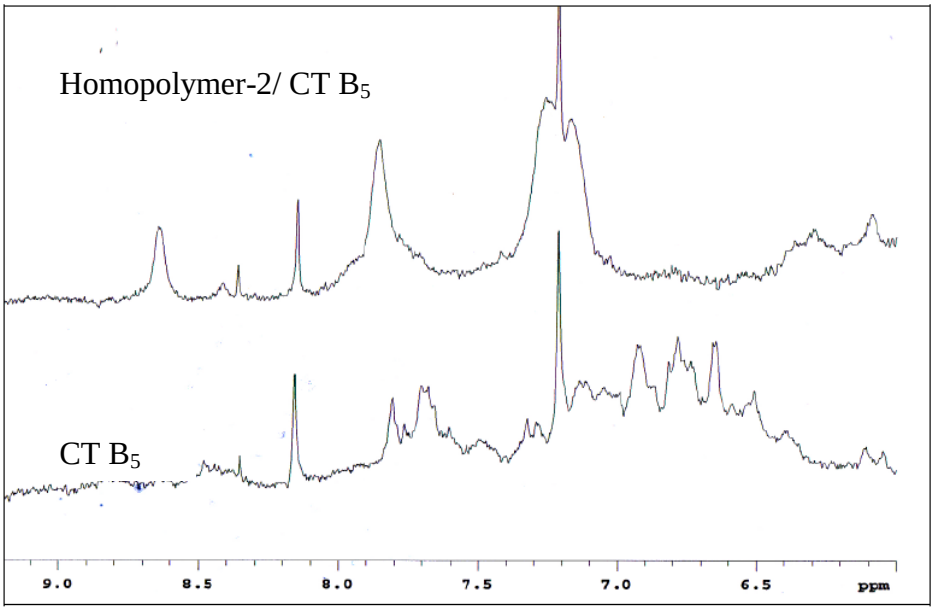

Figure 3-7. ^{1}H NMR of Homopolymer-4 / CT B_5 complexes (top) and free CT B_5 (bottom).

III. Discussion

The binding of glycopolymers was evaluated using fluorescence titration assay, ELISA and 1D ^{1}H NMR. In this study, the main goal was to identify how the differences in structural features of glycopolymers affect the CT B_5 binding efficiencies.

Fluorescence titration assay

Glycopolymers containing galactose bind to CT B_5 which causes changes in the fluorescence spectrum of Trp 88 in CT B_5 binding sites. As galactose moieties stack around the indole ring of Trp 88, the environment for the indole ring becomes more hydrophobic, resulting in a decrease in intensity of the emission spectrum with a blue shift of emission maximum.[123,134] Fluorescence titration assay was monitored between 300 nm and 400 nm

with an excitation of 280nm. The emission intensity of CT B_5 decreased as a function of polymer concentration. However, norborene-based glycopolymers showed UV absorbance around 280 nm and high intensity in emission spectrum around 320 nm and 350 nm.

Several issues were considered to explain this phenomenon such as polymer aggregates, terminal phenyl group of polymers and polymer-protein aggregates. Terminal phenyl group was not likely to affect emission spectrum because intensity of emission spectrum of polymers increased as molecular weight of polymers increase. The more likely explanation is that polymeric aggregates were involved in this experiment. DMSO increased solubility of the aggregates which lead to reduce emission intensity around 300-320 nm. However, DMSO was not sufficient to reduce emission intensity around 350-360 nm. It is more likely that the spectrum arise from $\pi \rightarrow \pi^*$ or $n \rightarrow \pi$ transition within backbone of polymers because the backbones of glycopolymers are composed of repeating olefin groups and many copies of carbonyl groups. In addition, the polymer structures also affected the transition because cyclobutene-based polymers did not show any UV absorbance or fluorescence. Higher concentrations of CT B_5 gave better inhibition pattern in emission spectrum because relative amount of protein signal increased. However, experimental difficulties resulted from high emission intensity of polymers made titration assay inaccurate. Thus another method was required to probe binding of polymers to CT B_5.

ELISA

To pursue the main goals of exploring the effects of polymer structures in the process of polymer-protein binding events, the binding efficiencies of glycopolymers were evaluated by

ELISA. Glycopolymers containing structural diversity in the presence of CT B_5 resulted in variable differences in enhanced binding affinity.

Homopolymers, -3,-4 and -5 and Copolymer-3 showed similar binding patterns. Binding affinities reached moderate values at low polymer concentration and dropped to a minimum value. Then the binding of the polymers increased as function of polymer concentration. It was suggested that polymeric aggregates were involved in polymer-CT B_5 interactions. This phenomenon is also comparable with the result of fluorescence titration assay. At low polymer concentrations, polymers reside mainly as unimers in which a small portion of polymer is bound to the protein. When the concentration of polymer is high enough to form a micelle, the polymeric micelle interacts with CT B_5, resulting that binding efficiencies of polymers were achieved as polymer concentration increase.

The ELISA results of Copolymer 1- and -2 resulted in plots similar to those for homopolymers. In a later study (Chapter 4), the structural features of those polymers are discussed as they did not form micelles, which do not explain ELISA results of the polymers to CT B_5. It was suggested binding affinity at low polymer concentration was likely due to favorable electrostatic interactions with CT B_5. It was reported that the main amino acids nearby receptor binding sites of CT B_5 are positively charged and neutral residues.[109] Copolymer-1 and -2 were composed of mainly negatively charged residues which lead more favorable polymer-protein interactions.

The results of ELISA for Copolymer 4- and -5 were different from those of other polymers. It was found that the binding efficiencies of the polymers increased depending on polymer concentration. However, binding of the polymers at low concentration was not detected. It was confirmed in fluorescence titration assay, the spectra of Copolymer-4 and 5

were not the same as those of other polymers. In addition, CMC values of those polymers (Chapter 4) are higher than for other polymers. This further supports the importance of micelles. It is implied that Copolymer-4 and -5 behave differently in the binding events which arise from difference structures in backbone and side chain structure.

1D ^{1}H NMR study of glycopolymers-CT B_5 complexes

The NMR study was carried out to measure differences in resonance of CT B_5 in presence of Homopolymer-4. The receptor binding sites of CT B_5 have a tryptophan residue, thus NMR spectrum of the protein in aromatic region exhibited resonance changes as polymer bound to the protein. This method might be a direct method to monitor interactions between polymers and protein. There are no significant peaks of polymers in aromatic region, thus NMR spectrum of polymer-protein complexes was distinguishable from that of free CT B_5. The result of NMR study revealed that protein peaks appeared/disappeared obtained upon addition of polymers. However, signals in NMR spectrum of the protein were broad and aromatic residues other than Trp reside in the protein. Thus this experiment supported that polymers bound CT B_5, but cannot provide conformational detail or quantitative analysis for the binding events of glycopolymers.

Chapter IV

Characterization of glycopolymers: Self-assembly

I. Introduction

II. Results

III. Discussion

I. Introduction

Numerous types of block polymers have been developed and applied in the biomedical and biomaterial arenas. Natural molecules, lipids, proteins, amino acids, nucleic acids and carbohydrates have been incorporated into synthetic blocks as hydrophilic components.[135-137] The activity of synthetic block copolymers has been extensively investigated to generate self-assembled structures. Self-assembled block copolymers form various shapes in micelles, ellipsoids, disks, cylinders, vesicles, or lamellae depending on the structure of macromolecules, concentration, solvent environment and non-covalent interactions such as hydrogen bonding and π-π interactions.[86,138,139]

The self-assembly of glycopolymers has been reported for block copolymers containing hydrophobic alkyl chain block and a hydrophilic terminal sugar block.[140-144] Rarely, has it been reported that homo-glycopolymers can self-assemble into aggregated structures.[145-147] Although homo-glycopolymers cannot phase separate like structures for block copolymers are, hydrophilic saccharide moieties and hydrophobic backbones can associate through the hydrophobic effect and hydrogen bonding to form aggregates.

(a) (b)

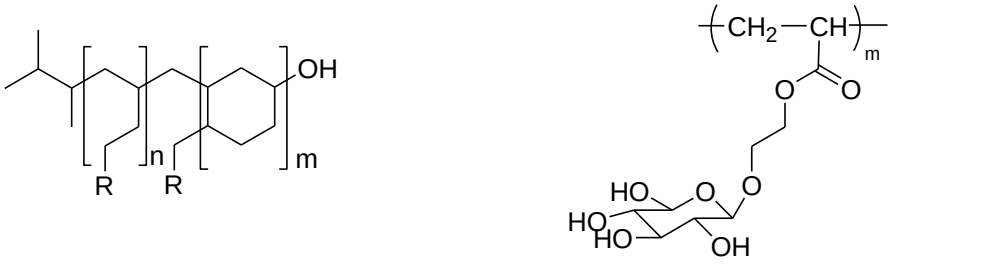

Figure 4-1. Examples of self-assembled glycopolymers: (a) Hydrophilically modified 1,2-polybutadienes block copolymer (R=glucose)[14] (b) Poly[2-β- D-glucosyloxy]ethyl acrylate.[13]

In addition, self-assembled structures of multivalent ligands showed enhanced binding efficiency for their receptors. Glycodendrimers were self-assembled into noncovalent nanoparticles in the presence of receptor.[148] The dendrimer particles behave like polyvalent ligands, which efficiently inhibit polyvalent processes both in vitro and in vivo. Multivalency of two different structures of multivalent ligands were compared.[149] Dendritic peptides and micellar peptides resulted in enhanced binding efficiency. However, self-assembled structure showed slightly higher affinities.

The formation of a micelle is a cooperative process.[150] Micelles are thermodynamically stable. The critical micelle concentration (CMC) is an important parameter for self-assembled structures. Self-assembly into a micelle is driven by hydrophobic interactions between alkyl chains of self-assembled molecules. When amphiphilic molecules are immersed into water, energetically less favorable interactions between water and hydrophobic chain are eliminated to minimize their free energy. Therefore, hydrophobic chains go into the micelle core, and hydrophilic chains remain on the surface of micelle. Some surfactants form bilayer structures, vesicles which are spherical and can be unilamellar or multilamellar. Unlike micelles, vesicles may not be thermodynamically stable. Another difference between vesicles and micelles is that vesicles have some aqueous phase inside.

There are several ways to measure CMC values such as tensiometry, conductivity fluorimetery, and calorimetery. Spectral methods using dye molecules are also used to determine CMC values. Pyrene is a widely used fluorescence probe because its emission characteristics are sensitive to the local environment, which allows measurement of the CMC of amphiphilic molecules. The solvent shifts of pyrene are observed in the emission spectrum between 370 and 410 nm in which there are five emissions peaks at 373, 379, 383, 389 and

392 nm. [151,152] Other fluorescence dyes to measure CMC are N-phenyl-1-napthylamine (PNA) and 1, 6-diphenyl-1, 3, 5-hexatriene (DPH).[153,154] PNA is a charged fluorescence dye. If detergents or amphiphilic molecules have opposite charges, measurements of CMC do not work.[155] DPH is a neutral probe which can be avoid charge effects in CMC measurement assays.[154]

II. Results

CMC value

Aqueous solutions of glycopolymers were mixed with pyrene (benzo[def]phenanthrene) and incubated for 17 hours to reach equilibrium. Emission spectra of pyrene were obtained between 350 and 450 nm with excitation at 335 nm. The intensity of emission increased as a function of polymer concentration (Figure 4-2a). The change in intensity of the first peak at 371 nm was plotted against polymer concentration (Figure 4-2b). Homopolymers,-3, -4, -5 and Copolymer-3 showed sharp transitions in emission intensity as concentration of polymer increased, consistent with the formation of micelles. This transition reflects that the glycopolymers form a hydrophobic core in which pyrene resides. However, the emission spectra of Copolymer-1 and -2 containing carboxyl groups and did not show changes typical of micelle formation. CMC values were determined by plotting the change in intensity of first peak (I_I) of pyrene against polymer concentration.[156,157]

To confirm self-assembly of glycopolymers, CMC measurements of Homopolymers and Copolymer-1 and -2 were performed in phosphate buffer with a second probe, 1, 6-diphenyl-1, 3, 5-hexatriene (DPH). Emission intensity of DPH at 428 nm decreased as polymer concentration increased (Figure 4-3). CMC values were determined by plotting the change in

emission maxima of florescence dye against polymer concentration. Copolymer-1 and -2 was not able to measure CMC in water. However, CMC of Copolymer-1 and -2 in phosphate buffer was determined with DPH, indicating that Copolymer-1 and -2 self-assemble into polymeric aggregates in phosphate buffer.

Titration of pyrene with Copolymer -4 and -5 indicated that their behavior were different than other polymers. Their aggregation behavior was tested with second probes, N-phenyl-1-napthylamine (PNA) and 1, 6-diphenyl-1, 3, 5-hexatriene (DPH). PNA is a hydrophobic probe which strongly emits in nonpolar solvents, while it is quenched in polar solvents.[153,158] The change of environment of PNA was detected as the resulting intensity of emission increased as a function of polymer concentration. In addition, the emission maximum of PNA showed blueshift from 460 nm to 438 nm (Figure 4-4). 1, 6-diphenyl-1, 3, 5-hexatriene (DPH) was used to confirm self-assembly of Copolymer-**4** and -**5**. Emission intensity of DPH at 428 nm decreased as a function of polymer concentration (Figure 4-5). The CMC values for all glycopolymers were determined from the transition point between the two lines of different slopes and are summarized in Table 4-1.

Table 4-1. Characterization of a series of glycopolymers

	CMC (mg/ml)	Diameter (nm)
Homopolymer-3	0.026[a] (0.039)[c]	311[d] (316)[e]
Homopolymer-4	0.033[a] (0.064)[c]	303[d] (236)[e]
Homopolymer-5	0.022[a] (0.094)[c]	322[d] (433)[e]
Copolymer-1	0.148[c]	394[d] (260)[e]
Copolymer-2	0.171[c]	894[d] (385)[e]
Copolymer-3	0.085[a]	205[d]
Copolymer-4	0.026[b] (0.13)[c]	221[d] (261)[e]
Copolymer-5	0.013[b] (0.0067)[c]	347[d] (370)[e]

[a]determined with fluorecence probe, pyrene
[b]determined with fluorecence probe, PNA
[c]determined with fluorecence probe, DPH
[d]measured by DLS in water
[e]measured by DLS in phosphate-buffered saline (pH 7.2) containing 150 mM NaCl

(a)

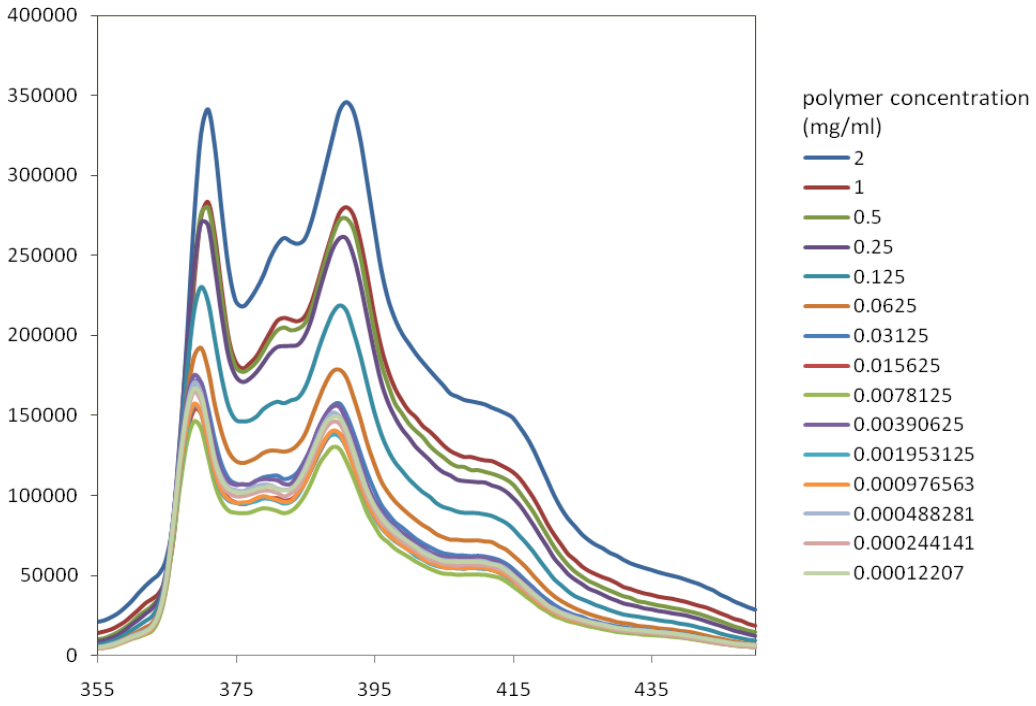

(b)

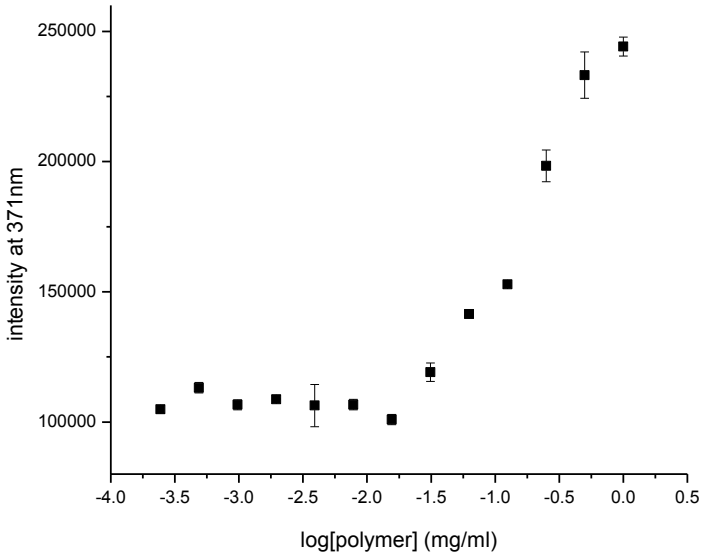

Figure 4-2. Fluorescence intensity of pyrene in the presence of Homopolymer-**3**. (a) Emission spectra with excitation 334nm wavelengthas function of polymer concentration (b) Emission intensity at 371nm as a fucntion of polymer concentration to determine CMC. [pyrene]=1×10 $^{-7}$ M, polymer solutions were preapered in water. All measurements were performed at 24℃.

(a)

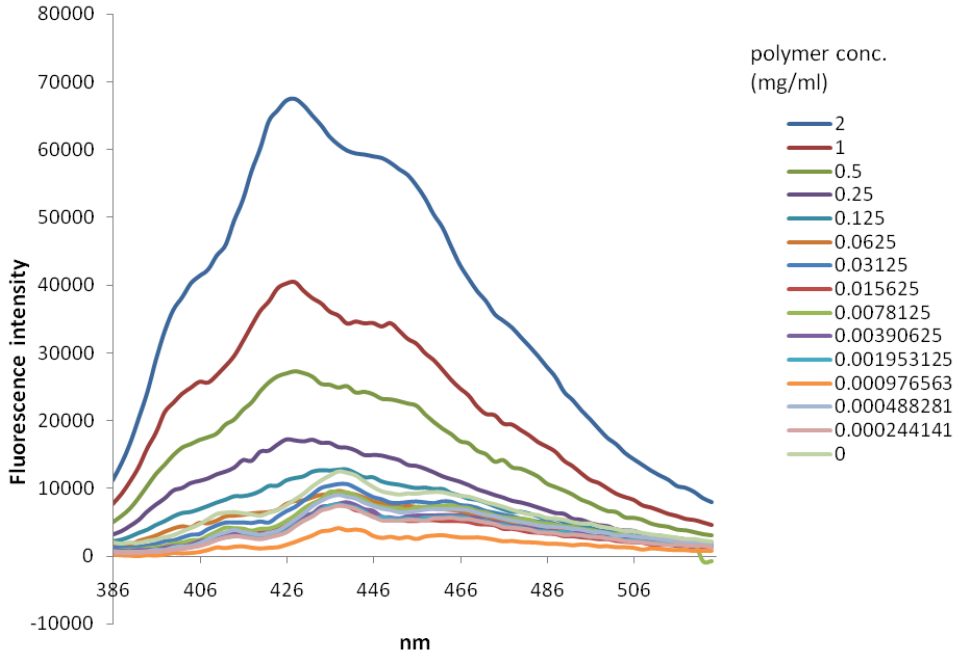

(b)

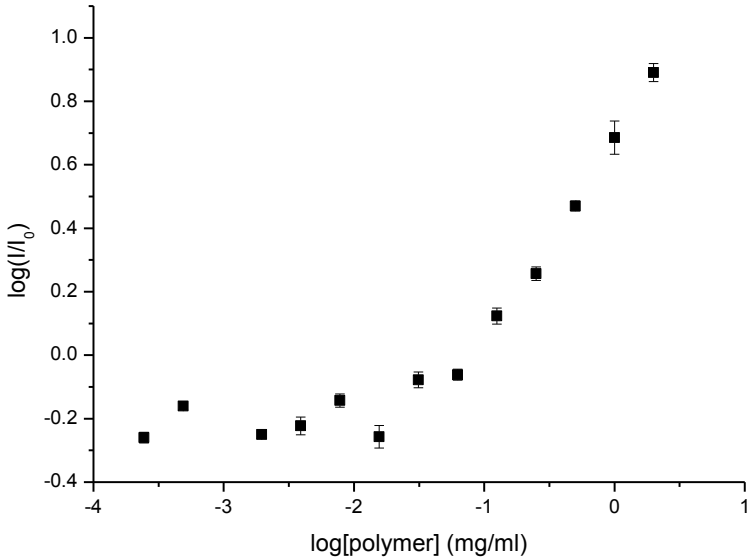

Figure 4-3. (a) Fluorescence intensity of DPH in the presence of Homopolymer-**3**. (a) Emission spectra with excitation 358 nm wavelengthas function of polymer concentration (b) Emission intensity at 428 nm as a fucntion of polymer concentration to determine CMC. [DPH]= 0.5×10^{-6} M, polymer solutions were preapered in phosphate buffer (pH=7.2). All measurements were performed at 24℃.

(a)

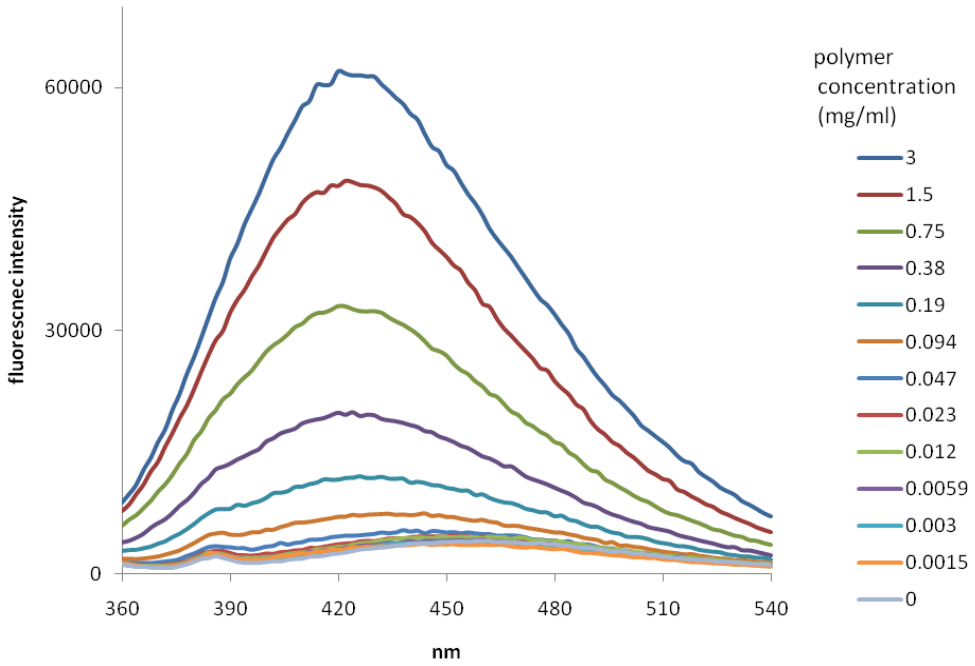

(b)

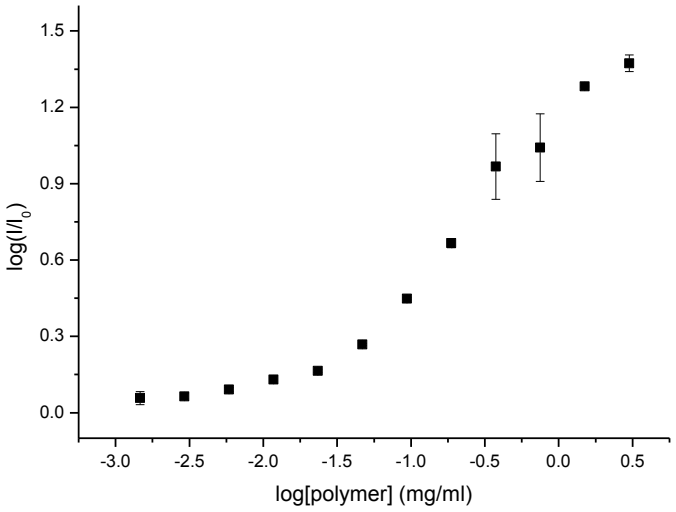

Figure 4-4. (a) Fluorescence intensity of PNA in the presence of Copolymer-**4**. (a) Emission spectra with excitation 340 nm wavelength as function of polymer concentration (b) Emission intensity at 420 nm as a function of polymer concentration to determine CMC. [PNA]= 6×10^{-6} M, polymer solutions were prepaered in water. All measurements were performed at 24℃.

(a)

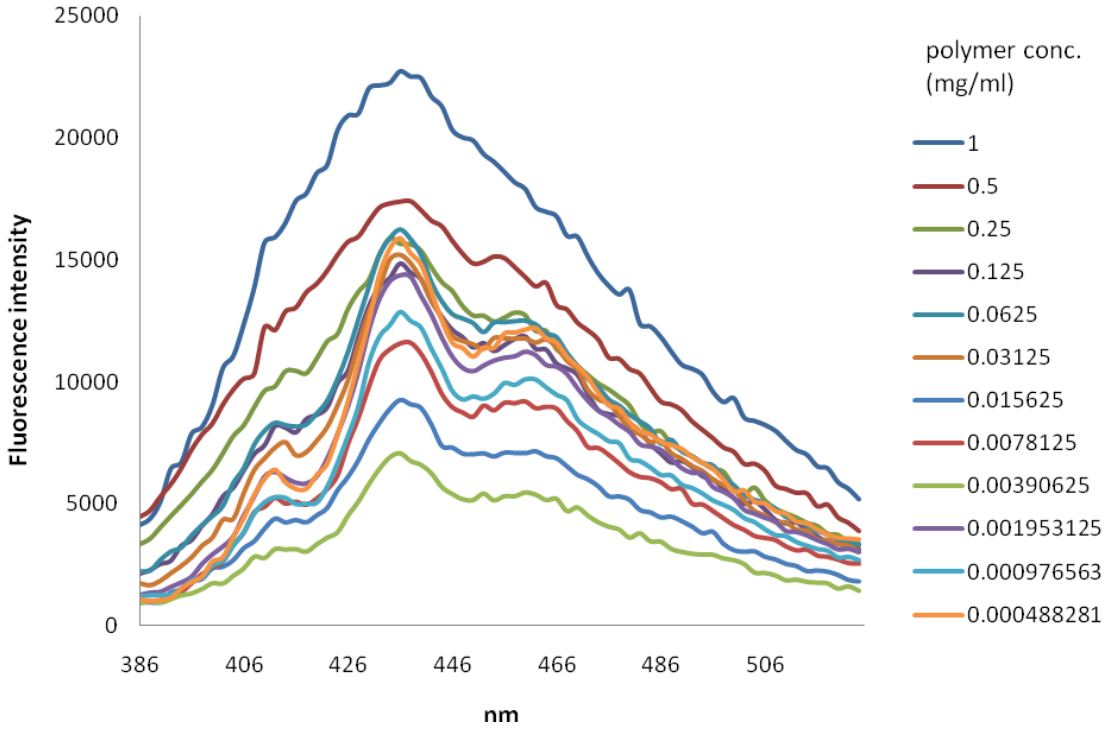

(b)

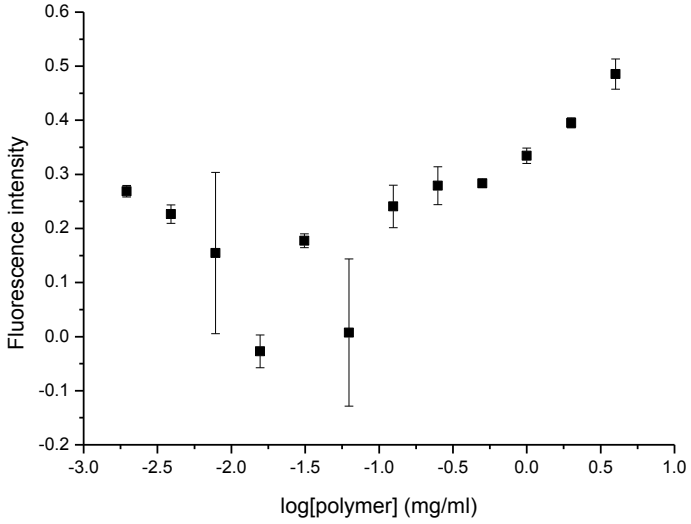

Figure 4-5. (a) Fluorescence intensity of DPH in the presence of Copolymer-**4**. (a) Emission spectra with excitation 358 nm wavelengthas function of polymer concentration (b) Emission intensity at 430 nm as a fucntion of polymer concentration to determine CMC. [DPH]= 0.5×10^{-6} M, polymer solutions were preapered in phosphate buffer (pH=7.2). All measurements were performed at 24℃.

Size and morphology

The sizes of glycopolymers were measured by dynamic light scattering (DLS) and are summarized in Table 4-1. For measuring diameters of glycopolymers, all polymer solutions were prepared in water and phosphate buffer at 1 mg/ml. Particle size of glycopolymers did not show big difference both in water and in phosphate buffer except for Copolymer -1 and -2.

Particle-size displayed multimodal distributions for all glycopolymers. For homopolymers (Homopolymer-3, -4 and -5), polymeric particles showed two discrete distributions around 100 nm and 400-500 nm, suggesting that homopolymers form micelles and aggregates of micelles. In intensity distribution, dominant peaks are large aggregates around 300-400 nm because large aggregates exhibit stronger scattering than small particles (Figure 4-6). To remove large aggregates, polymer solutions were filtered using a 0.45 µm filter. The size of polymers after filtration resulted in small micelles and their aggregates, suggesting that filtration breaks up or separates large particles (Figure 4-7).

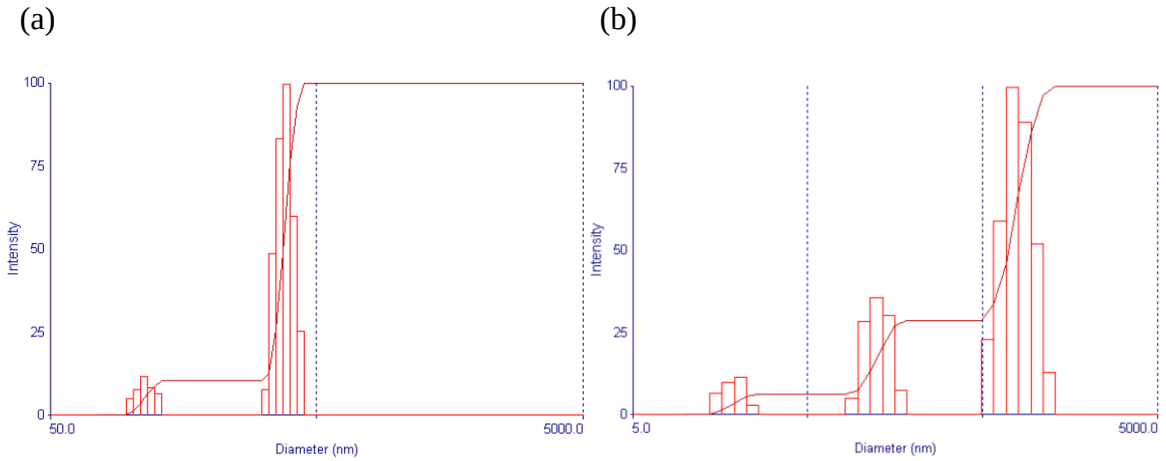

Figure 4-6. Size distribution for Homopolymer-**3** (a) and -**5** (b) by DLS. Polymer solutions were prepared in water (1 mg/ml).

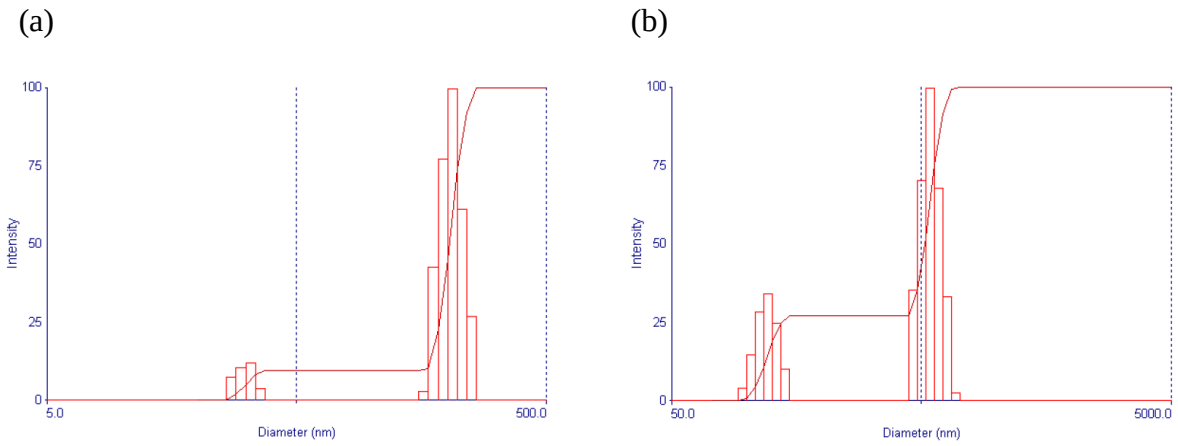

Figure 4-7. Size distribution for Homopolymer-**4** by DLS before 0.45 µm filtration (a) and after 0.45 µm filtration (b). Polymer solutions were prepared in water (1 mg/ml).

The particle size of Copolymer-3 was relatively smaller than homopolymers. It was found that Copolymer-1 and -2 have the biggest diameter among the glycopolymers, 394 nm and 894 nm in water, respectively. However, diameter of Copolymer-1 and -2 in buffer was smaller than in water, 260 nm and 385 nm, respectively. The average size distribution of Copolymer-4 and -5 was 221 and 347 nm. A high amount of small particles less than 40 nm were found in the polymer solutions (Figure 4-8).

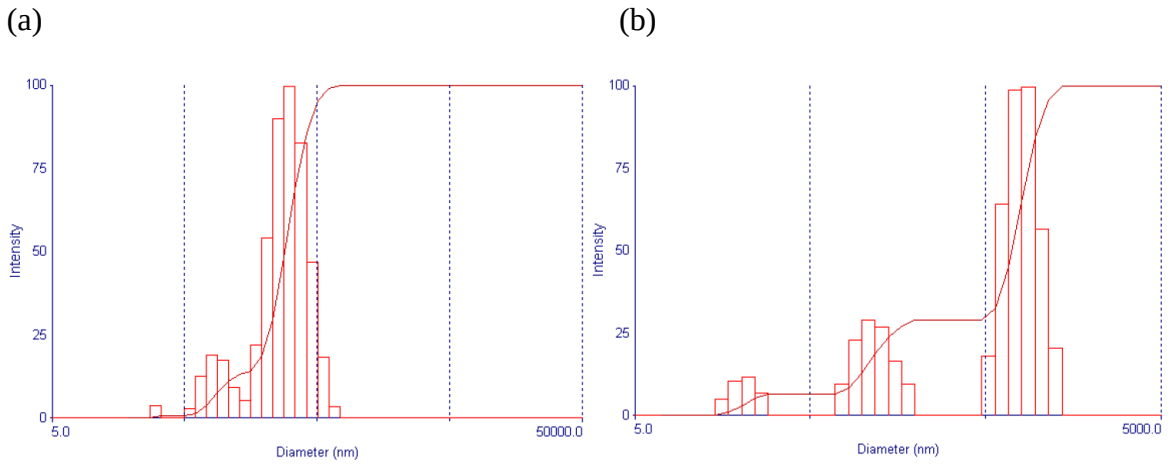

Figure 4-8. Size distribution for Copolymer-**4** (a) and Copolymer-**5** (b) by DLS. Polymer solutions were prepared in water (1 mg/ml).

Size determined by DLS correlated with the CMC value determined by fluorescence intensity (Figure 4-9). Polymer aggregates were detected by DLS above the CMC, but no significant particles existed in solution below the CMC.

In addition, a significant increase in diameter was not observed in polymer-protein complexes compared to polymer alone, the protein did not induce further aggregation (Figure 4-8).

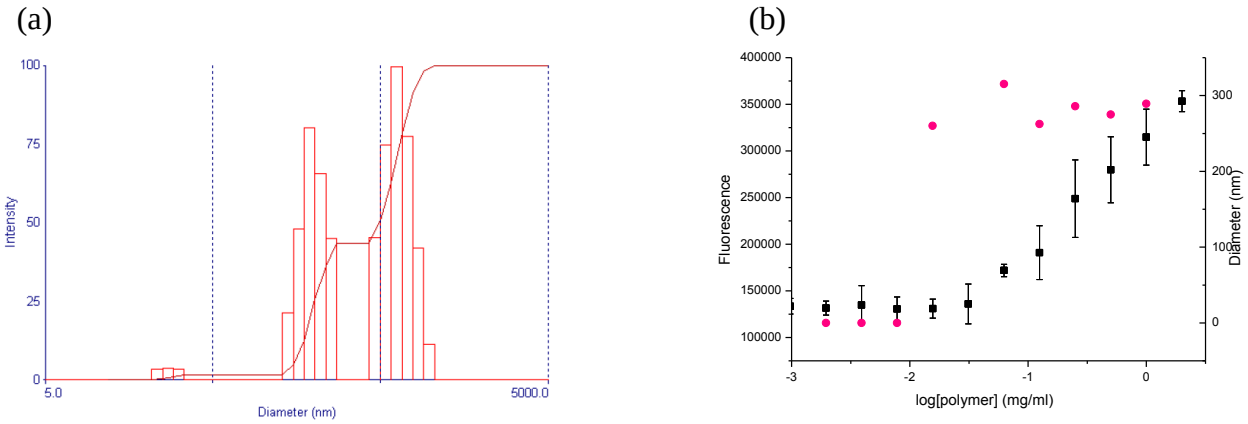

Figure 4-9. (a) Diameter distribution of Homopolymer-**4**/ CT B_5 complexes (b) Pyrene fluorescence intensity as a function of polymer concentration was used to determine CMC value. The particle diameter is measured by DLS concomitantly with the change of fluorescence intensity change. Polymer solutions were prepared in water (1 mg/ml). (■) Fluorescence intensity (●) Diameter measured by DLS.

TEM

Glycopolymers morphology was determined by transmission electron microscopy (TEM). Homopolymer-3 and -4 and Copolymer-1, -4, -5 were used for TEM analyses. The spherical polymeric aggregates of Homopolymer -3, -4 and Copolymer-4, -5 were observed in the TEM images (Figure 4-10). Negative staining with uranyl acetate was used to detect polymer samples. The hydrophilic periphery of the micelle stains, whereas the hydrophobic interior is unstained. The size of the glycopolymer particles was heterogeneous, but consistent with DLS

results. The diameters of Homopolymer-4 and Copolymer-4 were similar. A higher density of spherical shape of polymeric aggregates was observed in Homopolymer-4 than Copolymer-4. However, the spherical polymeric aggregates were not found in TEM image of Copolymer-1.

(a) (b)

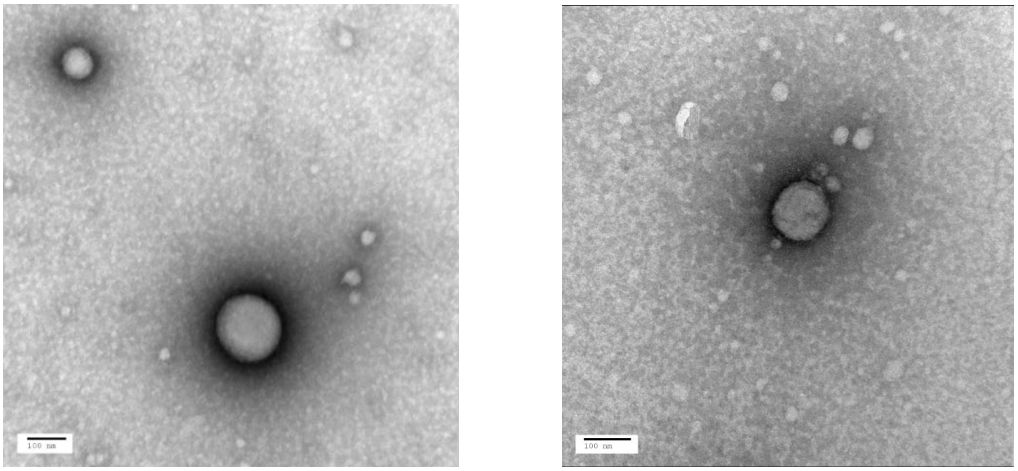

Figure 4-10. Self-assembled structures of Homopolymer-**4** (a) and Copolymer-**4** (b). TEM image shows the spherical polymeric aggregates in aqueous solution (5 mg/ml). Scale bar is 100 nm. Samples were deposited onto Formvar coated 400 mesh copper grids and were counter stained with aqueous 2% uranyl acetate. TEM was performed at a 120 kV accelerating voltage

2D-^{1}H,^{1}H- NOESY- NMR spectroscopy

Further study to confirm the self-assembled structure of glycopolymers was conducted using 2D-^{1}H,^{1}H- NOESY-NMR spectroscopy (Figure 4-11). NMR study of Homopolymer-3 is representative of self-assembled polymeric structure. The polymer solution was prepared in 1 % (w/v) solution in DMSO-d^{6}. The signals for galactose units reside at δ ~4.78, 3.92-4.01 and 3.10-3.15. Olefin protons in the polymer backbone appeared at δ ~5.2-5.4. Cross peaks between galactose moieties and olefin protons in the polymer backbone appeared for the linkers to the sugar moieties. There were no cross peaks between backbone protons and

galactose protons. The galactose cross peaks only appeared in the region of galactose itself. The results indicate that the hydrophobic backbone only interacted with backbone and linker residues. The absence of cross peaks of sugar moieties with protons of backbones also reflected that there is only hydrogen bonding interactions between hydrophilic segments.

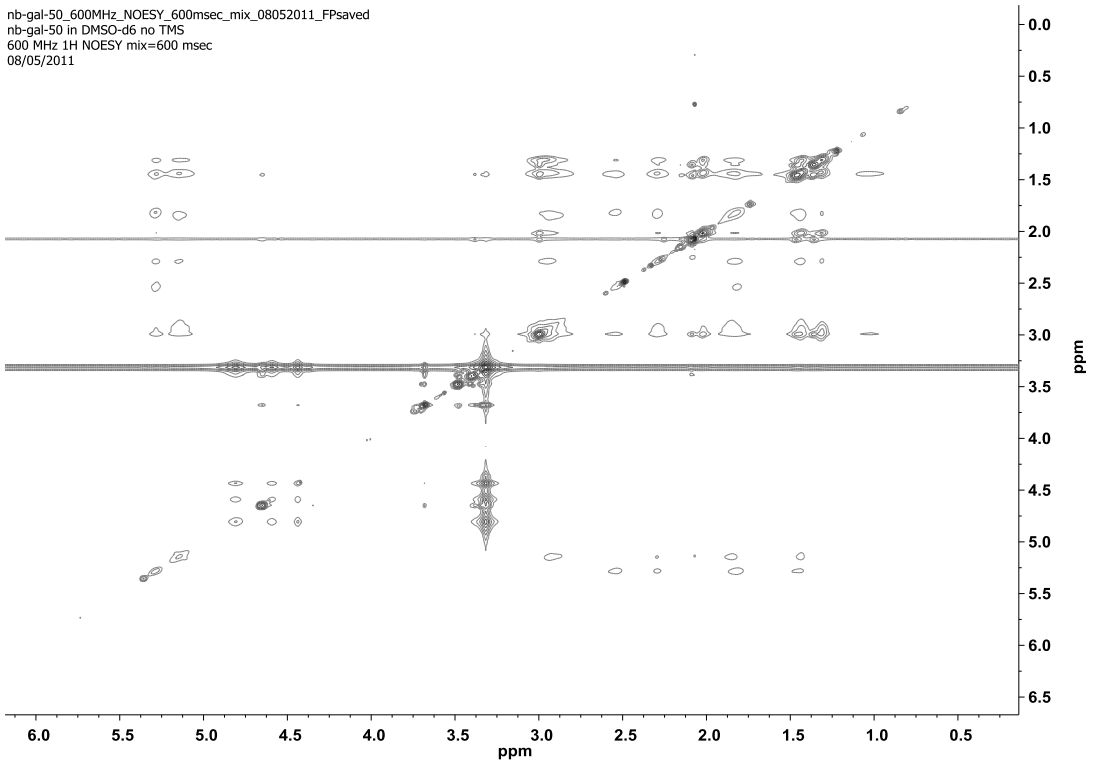

Figure 4-11. 2D-^{1}H,^{1}H- NOESY- NMR of Homopolymer-**3** (600MHz, mixing time : 600 ms at room temperature). 1 % (w/v) Homopolymer-1 was prepared in DMSO-d6.

III. Discussion

In order to identify morphology and behavior of synthetic glycopolymers in aqueous solution, we performed characterization of glycopolymers by measuring CMC values, diameter and morphology. Glycopolymers exhibited different structural features depending on composition of polymer chains.

Comparing CMC values for homopolymers (Homopolymer-**3**, -**4** and -**5**), no significant difference was found between them for values determined with pyrene in water. However, CMCs determined with DPH in phosphate buffer showed that glycopolymers with a higher number of repeating units have higher CMC values. These polymers have the same molecular structures with different numbers of repeating units. Diameters in both water and phosphate buffer measured by DLS resulted in similar size for those polymers. It demonstrates that the length of polymers did not influence the supramolecular structure of the polymeric micelles.

The effects of valency as well as composition of glycopolymers were critical for polymeric micelle formation. Comparing the same length, Homopolymer-**3** and Copolymer-**3**, Homopolymer-**3** has a lower CMC value. Homopolymer-3 has a galactose moiety as a repeating unit. Copolymer-**3** has mannose moieties as a spacer and shorter linkers to the sugar than Homopolymer-**3**. The lower CMC results from different intra-/ inter-molecular interactions of linker and sugar moieties in the polymers.

Regarding Copolymer-**3** and Copolymer-**4**, the dependence of architecture on polymer composition was revealed. Copolymer-**3** and Copolymer-**4** have the same length, but different backbones, norbornene and cyclobutene, respectively. The monomer repeat of these polymers have similar hydrophobicities (ClogP of copolymer-3: -0.498 and ClogP of copolymer-4:

0.643). In addition, the size of those polymeric particles measured by DLS are similar, 205 nm for Copolymer-3 and 221 nm for Copolymer-**4**. However, we found that Copolymer-**4** was different from Copolymer-3 based on the results of CMC value. CMC value of Copolymer-4 and -5 was not determined by pyrene probe. Second fluorescence dyes, PNA and DPH enabled to measure CMC of Copolymer -**4** and -**5**. It was not explained the reason pyrene do not work. However, it is supposed that the differences in polymer behavior in aqueous solution are due to the cyclobutene backbone which is less rigid than the norbornene backbone. Sugar molecules also affected the structure of the polymers because Copolymer-**4** has many copies of hydroxyl groups instead of sugar molecules.

Homopolymer-**3** and Copolymer-**1** (or Homopolymer-**4** and Copolymer-**2**) have same length of polymer chain and similar monomer hydrphobicities (ClogP of monomer for Homopolymer-**3**: -2.045 and ClogP of monomer for Copolymer-**1**: -2.183). However, Copolymer-**1** and -**2** form polymeric aggregates in phosphate buffer, not in water. Those copolymers possess negatively charged side chains. It is supposed that strong repulsion of negative charged residues interfere with formation of polymeric aggregates in water, whereas the electrostatic shielding of saltings allows polymers to aggregate.

The diameter and morphology of glycopolymers were measured by DLS and TEM. Spherical aggregates of homo-glycopolymers were exhibited in TEM images. Negative staining method using uranyl acetate clearly showed that spherical polymeric micelles have hydrophobic interior and hydrophilic periphery. The sizes were consistent with the value measured by DLS.

Triblock copolymer having mannose as a spacer (Copolymer-**3**) had a smaller diameter (205 nm) than homopolymers. Copolymer-**3** has shorter linkers between sugar and backbone

than those in homopolymers, which might result in smaller size of polymeric aggregates. Copolymer -**1** and -**2** exhibited bigger size in water. However, polymer solution of Copolymer -**1** and -**2** in phosphate buffer showed diameters of those polymers were smaller than in water. TEM image of Copolymer-**4** and -**5** exhibited spherical polymeric aggregates. Average diameters of copolymers are similar to homopolymers.

CMC result is consistent with the diameters determined by DLS. From the study of Homopolymer-**3**, the polymeric particles of were observed above CMC in which diameters were constant around 300 nm. Polymeric unimers mainly reside below CMC, which were not detected by DLS. Additionally, similar sizes of polymeric aggregates were found at a higher concentration of CMC, indicating that polymeric aggregates are stable during dilution processes.

In 2D-^{1}H,^{1}H- NOESY- NMR spectrum, a nuclear overhauser effect (NOE) was not detected between galactose protons and olefin protons in polymer backbones. It indicated that hydrophobic segment composed of backbones of polymers did not contact with hydrophilic sugar segments.

Based on CMC results, DLS and TEM, the glycopolymers except for Copolymer-**1** and -**2** form spherical micelles. In their aggregates, hydrophilic sugar moieties are located on the surface and hydrophobic backbones are inside of micelles (Figure 4-12a). It is supposed that two different structure of glycopolymers, spherical polymeric aggregates and linear shape are involved in the binding to CT B_5 (Figure 4-12b).

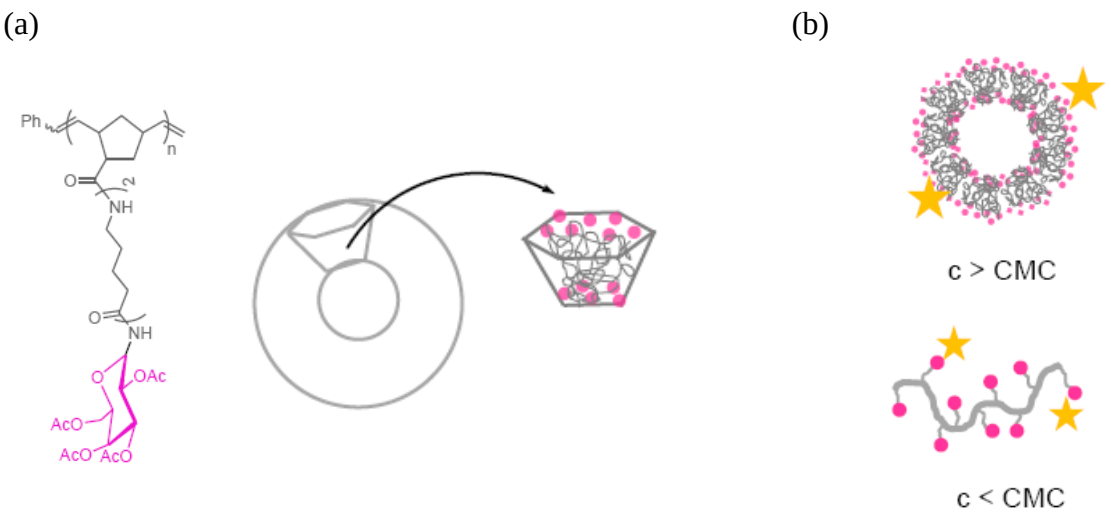

Figure 4-12. (a) Proposed structure of self-assembled glycopolymers and (b) Proposed structure of glycopolymer/ CT B_5(★)complexes for self-assembled glycopolymers (top) and linear glycopolymers (bottom).

Table 4-2. Summary of characterization of a series of glycopolymers

Polymer name	Polymer random-coil (Å)	Random-coil distances between spacers (Å)	$IC50_1$[a] mg/ml (μM)	$IC50_2$[a] mg/ml (μM)	CMC (mg/ml)	Diameter (nm)
Homopolymer-3	38.2	-	1.66×10^{-5} (0.0007)	0.1458 (5.83)	0.026[b] (0.039)[d]	311[e] (316)[f]
Homopolymer-4	54.0	-	$<6.02\times10^{-5}$* (0.0006)	0.011 (0.22)	0.033[b] (0.064)[d]	303[e] (236)[f]
Homopolymer-5	76.4	-	<0.0002* (0.0017)	0.59 (5.9)	0.022[b] (0.094)[d]	322[e] (433)[f]
Copolymer-1	38.2	36.6	7.04×10^{-6} (0.0007)	0.1 (9.4)	0.148[d]	394[e] (260)[f]

Copolymer-2	54	52.9	$<1.51\times10^{-5*}$ (0.0007)	0.084 (3.8)	0.171[d]	894[e] (385)[f]
Copolymer-3	38.2	37.4	$<1.88\times10^{-5*}$ (0.0005)	0.4407 (12.53)	0.085[b]	205[e]
Copolymer-4	31.6	31	0.052 (6.75)		0.026[c] (0.013)[d]	221[e] (261)[f]
Copolymer-5	44.7	44.2	0.004 (0.27)		0.013[c] (0.0067)[d]	347[e] (370)[f]

[a]determined by ELISA
[b]determined with fluorecence probe, pyrene
[c]determined with fluorecence probe, PNA
[d]determined with fluorecence probe, DPH
[e]measured by DLS in water
[f]measured by DLS in phosphate-buffered saline (pH 7.2) containing 150 mM NaCl
* estimate value from ELISA

Chapter V

Experimental Methods

I. Synthesis of monomers and polymers

II. Analysis of glycopolymer binding to cholera toxin B subunit

III. Characterization of self-assembled structures

I. Synthesis of monomers and polymers

Materials and methods. 1-Ethyl-3-(3-dimethylaminopropyl)carbodiimide hydrochloride (EDC•HCl) and N-hydroxybenzotriazole (HOBt) purchased from Advanced Chem Tech (Louisville, KY). Solvent and reagents were purchased from Fisher Scientific, Inc (Sprinfield, NJ). $(H_2IMes)(PCy)_2Cl_2Ru$=CHPh was purchased from Sigma-Aldrich (Milwaukee, WI). 3rd generation Grubbs Catalyst, $(H_2IMes)(BrPyr)_2Cl_2Ru$=CHPh **23** was prepared according to the literature.[159] All solvents were dried under N_2 before use. For analytical thin layer chromatography (TLC), pre-coated silica gel plates ($60F_{254}$) were used. TLC spots were detected by UV light and by staining with phosphomolybdic acid (PMA) or ninhydrin. Molecular weight was determined by gel permeation chromatography (Phenogel 5μM MXL) eluting with THF using UV/VIS detector. Mass spectra were acquired on an Agilent 1100LC (API-ES)/MSD-VL. NMR spectra were recorded on Varian 400, 500 and 600 MHz spectrometers.

5-norbornene-exo-carboxylic acid.[50] Dicyclopentadiene (6 g, 0.05 mol) was heated to produce cyclopentadiene. The desired product was collected in an acetone-dry ice bath (5 g, 0.07 mol). Cyclopentadiene and methyl acrylate (7.2 g, 0.08 mol) were dissolved in dry

CH_2Cl_2. The mixture was maintained at reflux for 10 h. After removing the solvent under reduced pressure, the crude product was dissolved in $NaOCH_3$/MeOH (3 g $NaOCH_3$ in 20 mL MeOH). The reaction mixture was maintained at reflux for 5 h, and then the solvent was evaporated. The crude product was dissolved in H_2O (20 mL) and the solution was maintained at reflux until the methyl ester was transformed into the acid (about 8 h). The reaction mixture was cooled to rt, and then extracted with Et_2O (3×20 mL). The aqueous phases were acidified to pH 2 with 30% H_2SO_4, and extracted with Et_2O (3×20 mL). The combined ether phase was washed with cold H_2O (3×20 mL), dried over Na_2SO_4, and then evaporated. The resulting acid mixture was dissolved in a solution of $NaHCO_3$ (8.2 g, 0.09 mol) in H_2O (135 mL). A solution of I_2 (8.2 g, 0.03 mol) and KI (16.2 g, 0.09 mol) in H_2O (125 mL) was added dropwise via an addition funnel until a dark brown color persisted. 10% $Na_2S_2O_3$ solution was added to the aqueous phase to decolorize the solution. The resulting solution was acidified to pH 2 with 1N H_2SO_4, and then extracted with Et_2O (4 × 30 mL). The aqueous phase was readjusted to pH 2, extracted with Et_2O (20 mL), and the combined ether phases dried over anhydrous Na_2SO_4. The combined ether phases were evaporated to give pale yellow oil. The resulting oil was precipitated form cold pentane (-78 °C) to yield pure exo acid (4.1 g, 40%) as pale yellow solid. ^{1}H NMR (400 MHz, D_2O) δ 6.11 (dd, *J* = 5.5 Hz, 3.0 Hz, 2H), 3.13 (br s, 1H), 2.90 (br s, 1H), 2.22 (dd, *J* = 9.5 Hz, 5.0 Hz, 1H), 1.92 (dt, *J* = 12.0 Hz, 4.0 Hz, 1H), 1.31-1.50 (m, 3H). All ^{1}H NMR data were consistent with literature.[50]

Cyclobutene-1-carboxylic acid.[160] KOH (6 g, 107 mmol) was dissolved in toluene (90 mL) by heating to 130℃. After the mixture cooled to rt, ethyl 1-bromocyclobutanecarboxylate (4.90 g, 23.7 mmol) was added dropwise to the solution. The reaction mixture was heated at

reflux for 1 h. After it cooled to rt, cold H_2O (60 mL) was added, and the aqueous phase was washed with pentane (2 x 40 mL). After the pH of aqueous phase was adjusted to 2.5 with 30% aq H_2SO_4, the product was extracted with Et_2O (4 x 40 mL). The combined ether extracts were dried over anhydrous Na_2SO_4 and the Et_2O was evaporated. The resulting product was dissolved in pentane (50 mL). The upper phase was separated and was stirred for 20 min in an acetone-dry ice bath. The white precipitate was filtered and dried (1.1 g, 47%). The final product was stored at -20 ℃. ^{1}H NMR (400 MHz, D_2O) δ 6.94 (t, *J* = 1.2 Hz, 1H), 2.76 (t, *J* = 3.2 Hz, 2H), 2.51 (td, *J* = 3.2 Hz, 1.2 Hz, 2H). All ^{1}H NMR data were consistent with the literature.[160]

Pentaacetyl-D-galactose, 1.[112] Acetic anhydride (31.5 mL, 333 mmol) was slowly added to a solution of D-galactose (3 g, 16.65 mmol) in dry pyridine (33 mL) at 0 ℃ under N_2. The reaction mixture was stirred at 0 ℃ for 1 h before a catalytic amount of DMAP (200 mg, 1.67 mmol) was added. As the reaction mixture was allowed to reach rt, the reaction became slightly exothermic. After 6 h, the clear yellow mixture was slowly poured into 500 mL of fast stirring ice-water, giving a sticky solid. After EtOAc extraction (75 mL), evaporation of the solvent, and coevaporations with dry toluene, **1** was obtained as an clear oil (5.77 g, 89 %). ^{1}H NMR (600 MHz, $CDCl_3$) δ 6.39 (br s, 1H), 5.52 (br s, 1H), 5.35 (br s, 2H), 4.35 - 4.37 (m, 1H), 4.08 - 4.15 (m, 2H), 2.14 - 2.17 (br s, 6H), 2.02 - 2.11 (br s, 9H). All ^{1}H NMR data were consistent with literature.[112]

1-β-Bromo-2,3,4,6-tetraacetyl-D-galactose, 2.[112] Compound **1** (5.77 g, 14.7 mmol) was dissolved in 20 mL of a solution of HBr in acetic acid (30% w/w, 14.7 mmol). After 1 h, all

the acetic acid was evaporated and coevaporated with dry toluene. **2** was obtained as a brown oil (5.69 g, 94%). Due to instability, no further purification was undertaken. ^{1}H NMR (500 MHz, $CDCl_3$) δ 7.19 - 7.27 (m, 2H), 6.71 - 6.72 (br s, 1H), 5.54 (br s, 1H), 5.42 (dd, *J* = 7.0 Hz, 3.5 Hz, 1H), 5.01 (dd, *J* = 7.0 Hz, 3.5 Hz, 1H), 4.51 (t, *J* = 6.0 Hz, 1H), 4.11 - 4.23 (m, 2H), 2.17 (s, 3H), 2.13 (s, 3H), 2.08 (s, 3H), 2.03 (s, 3H). All ^{1}H NMR data were consistent with the literature.[112]

1-β-Azido-2,3,4,6-tetraacetyl-D-galactose, 3.[112] NaN_3 (4.5 g, 69.1 mmol), tetrabutylammonium hydrogen sulfate (4.7 g, 13.8 mmol) and 57 mL of a saturated solution of $NaHCO_3$ was added to a solution of **2** (5.69 g, 13.8 mmol) in CH_2Cl_2 (57 mL) at rt. The reaction mixture was stirred vigorously at rt for 3 h and diluted with EtOAc (500 mL). The organic layer was washed with 200 mL of a saturated solution of $NaHCO_3$ and evaporated under reduced pressure. Crude **3** was obtained as a pale yellow solid (5.02 g, 97%). Recrystallization from MeOH yielded **3** as white crystals.^{1}H NMR (600 MHz, $CDCl_3$) δ 5.44 (d, *J* = 3.0 Hz, 1H), 5.17 (m, 1H), 5.05 (dd, *J* = 8.1 Hz, 4.2 Hz, 1H), 4.61 (d, *J* = 10.2 Hz, 1H), 4.19 (m, 2H), 4.04 (m, 1H), 2.19 (s, 3H), 2.11 (s, 3H), 2.08 (s, 3H), 2.01 (s, 3H). All ^{1}H NMR data were consistent with the literature.[112]

Pentaacetyl-D-mannose, 4.[113] Pentaacetyl-D-mannose was prepared according to the procedure as Liptak et al with minor modification.[113] Acetic anhydride (21 mL, 222 mmol) was slowly added to a solution of D-mannose (2 g, 11.1 mmol) in dry pyridine (33 mL) at 0 ℃ under N_2. The reaction mixture was stirred at 0 ℃ for 1 h before a catalytic amount of DMAP (133mg, 1.1 mmol) was added. As the reaction mixture was allowed to reach rt, the

reaction became slightly exothermic. After 6 h, the clear yellow mixture was slowly poured into 500 mL of fast stirring ice-water, giving a sticky solid. After EtOAc extraction (75 mL), evaporation of the solvent, and coevaporation with dry toluene, **4** was obtained as a clear oil (3.89 g, 90%). ^{1}H NMR (600 MHz, $CDCl_3$) δ 6.06 (br s, 1H), 5.31 (br s, 1H), 5.24 (br s, 2H), 4.26 (m, 1H), 4.03 - 4.09 (m, 2H), 2.14 - 2.32 (br s, 6H), 2.06 (br s, 3H), 1.98 (br s, 3H), 1.69 (br s, 3H).

Pentaacetyl-D-mannose-Cl, 6.[114] Pentaacetyl-D-mannose-Cl was prepared according to the procedure as Kleinert et al with minor modification.[114] Hydrazine acetate (0.37 g, 4.03 mmol) was slowly added to a solution of **4** (1.31 g, 3.36 mmol) in dried DMF under N_2. The reaction mixture was stirred at 40 - 50 ^{o}C for 3 h. After pouring EtOAc (50 mL) to the reaction mixture, the organic layer was washed with H_2O and brine, dried over $MgSO_4$, and concentrated under vacuum to afford tetraacetyl-D-mannose-OH as an oil (1.11 g, 95%). To a solution of the crude mannose-OH (1.11 g, 3.21 mmol) in dried CH_2Cl_2 (18 mL) was added trichloroacetonitrile, CCl_3CN (3.17 mL, 0.03 mol) and 1,8-diazabicyclo[5.4.0]undec-7-ene (DBU) (48 mg, 0.32 mmol) at rt under N_2. The reaction mixture became brown after 30 min, and then was stirred a further 3.5 h. The reaction mixture was diluted with EtOAc. The organic layer was washed with a saturated solution of $NaHCO_3$, dried over $MgSO_4$, filtered, and evaporated under reduced pressure. Purification by flash chromatography (n-hexane/EtOAc, 7/3) gave crude **5** as a pale yellow gel (0.92 g, 56% for 2 steps). To a solution of **5** (0.92 g, 1.87 mmol) and 2-chloroethanol (751.6 mg, 9.34 mmol) in dried CH_2Cl_2 (18 mL) was added $BF_3.OEt_2$ (42.5 mg, 0.37 mmol) at -78 ^{o}C under N_2. The reaction mixture was stirred for 3 h at -60 to -70 ^{o}C and then allowed to warm to rt. The reaction mixture was

diluted with CH_2Cl_2 (85 mL) and then washed with 1N-HCl, 5% $NaHCO_3$, and H_2O. The organic layer was dried over $MgSO_4$ and concentrated under vacuum. Purification by flash chromatography (n-hexane/EtOAc, 5/5) gave **6** (537 mg, 70%) as a pale yellow gel. ^{1}H NMR (600 MHz, $CDCl_3$) δ 8.78 (s, 1H), 6.28 (br s, 1H), 5.47 (br s, 1H), 5.39 - 5.40 (m, 2H), 4.26 - 4.29 (m, 1H), 4.15 - 4.19 (m, 3H), 2.19 (s, 3H), 2.07 (s, 3H), 2.06 (, 3H), 2.00 (s, 3H).

α-Azido-2,3,4,6-tetraacetyl-D-mannose, 7.[115] α-Azido-2,3,4,6-tetraacetyl-D-mannose was prepared according to the procedure as Sun et al with minor modification.[115] The mannose-Cl, **6** (0.75 g, 1.83 mmol) and NaN_3 (1.19 g, 18.3 mmol) were dissolved in a mixture of DMSO (25 mL) and H_2O (5 mL). The reaction mixture was stirred for 3 days at 60 - 70 ^oC under N_2. The orange colored solution was diluted with EtOAc and then subsequently washed with 1N-HCl, 5% $NaHCO_3$, and H_2O. The organic layer was dried over $MgSO_4$ and concentrated under vacuum to afford **7** (452 mg, 61%) as a pale yellow gel. ^{1}H NMR (600 MHz, $CDCl_3$) δ 5.27 - 5.37 (m, 3H), 4.86 (s, 1H), 4.27 - 4.30 (m, 1H), 4.11 - 4.14 (m, 2H), 3.80 (m, 1H), 3.48 (m, 1H), 3.46 - 3.48 (m, 2H), 2.61 (s, 1H), 2.15 (s, 3H), 2.14 (s, 3H), 2.08 (s, 3H), 1.99 (s, 3H).

5-Benzyloxycarbonyl-aminopentanoic acid, 8. 5-aminovaleric acid (0.5 g, 4.3 mmol) was dissolved in a 2N aqueous sodium hydroxide solution (0.6 mL) and the solution was cooled in an ice bath to 0 °C. Under vigorous stirring, benzyl chloroformate (736 μL, 5.2 mmol) and a 2N aqueous NaOH solution (0.6 mL) were simultaneously added within 2 min. The mixture was stirred for 30 min at rt and washed with Et_2O (20 mL). The aqueous phase was separated and acidified with conc. HCl to pH 2. The resulting emulsion was extracted with EtOAc (5

mL). The organic phases were combined, washed with brine, and dried over Na_2SO_4. Concentration in vacuo gave **8** (1.1 g, 99%) as white needles. ^{1}H NMR (400 MHz, $CDCl_3$) δ 7.28 - 7.36 (m, 5H), 7.22 (br s, 1H), 4.99 (s, 2H), 2.97 (dt, *J* = 6.6 Hz, 5.4 Hz, 2H), 2.17 (m, 2H), 1.39 - 1.47 (m, 4H).

Methyl 5-aminopentanoate, 9.[161] Conc. HCl (2.1 mL) was added to a vigorously stirring a solution of 5-aminovaleric acid (0.5 g, 4.3 mmol) in 2,2-dimethoxypropane (16 mL, 128 mmol). The mixture was stirred for 24 h at rt. The dark red solution was concentrated under reduced pressure and the resulting brown solution was extracted with Et_2O. The precipitated solid was filtered, washed with Et_2O and recrystallized from EtOH/EtOAc (10 mL, v/v 95/5) to afford **9** (0.4 g, 70%) as white crystalline solid. All ^{1}H NMR data were consistent with the literature.[161] ^{1}H NMR (400 MHz, $CDCl_3$) δ 8.23 (s, 3H), 3.67 (s, 3H), 2.99 - 3.11 (m, 2H), 2.35 - 2.40 (m, 2H), 1.73- 1.86 (m, 4H).

Compound 11.

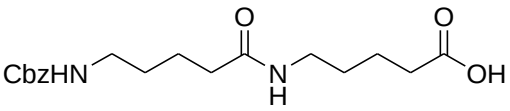

A mixture of **8** (0.4 g, 3.1 mmol), HOBt (0.4 g, 3.1 mmol), and EDC (0.6 g, 3.1 mmol) were dissolved in CH_2Cl_2 (20 mL), and **9** (0.3 g,2.6 mmol) and DIEA (513 μL, 3.1mmol) was added. The solution was stirred for 16 h at rt under N_2. The reaction mixture was washed with 5% $NaHCO_3$ and 1N HCl. The combined organic phases were dried over $MgSO_4$, filtered, and concentrated. Purification by flash chromatography (CH_2Cl_2/acetone, 7/3) gave **10** (0.95 g,

85 %) as white solid. ^{1}H NMR (400 MHz, $CDCl_3$) δ 7.27 - 7.34 (m, 5H), 7.23 (br s, 1H), 5.05 (s, 2H), 3.61 (s, 3H), 3.15 - 3.23 (m, 4H), 2.13 (m, 2H), 2.16 (m, 2H), 1.45 - 1.67 (m, 8H). **10** (0.5 g, 1.4 mmol) was dissolved in 9 mL THF/H_2O (1/3). The solution was cooled in an ice bath to 0 °C and NaOH (0.6 g, 14 mmol) was added. The reaction was monitored by TLC analysis. After 5 h, the solvent was concentrated and the solution as diluted with H_2O. Then the aqueous phase was acidified with conc.HCl to pH 2. The resulting emulsion was extracted with EtOAc. The combined organic phases were dried over $MgSO_4$, filtered, and concentrated, yielding **11** (0.4 g, 83%) as white solid. ^{1}H NMR (400 MHz, DMSO-d_6) δ 7.69 (br s, 1H), 7.25 - 7.31 (m, 5H), 7.17 (br s, 1H), 4.95 (s, 2H), 2.90 - 2.98 (m, 4H), 2.15 (m, 2H), 1.98 (m, 2H), 1.29 - 1.44 (m, 8H).

Compound 13.

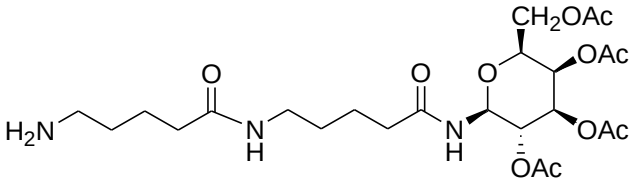

A solution of **11** (845 mg, 2.4 mmol), 1-β-azido-2,3,4,6-tetraacetyl-D-galactose, **3** (0.5 g, 1.34 mmol), and HOBt (344 mg, 2.5 mmol) in dry THF (66 mL) under nitrogen was cooled to 0 ℃. Then DIC (397 μL, 2.5 mmol) was added and the solution was stirred for 10 min, followed by the addition of tri-n-butylphosphine (402 μL, 1.6 mmol) and stirring for 1 h at 0 ℃. Then the reaction mixture was stirred for 16 h at rt, diluted with H_2O (50 mL) and extracted with EtOAc. The combined organic phases were washed with brine, dried over $MgSO_4$ and the mixture was filtered and concentrated under reduced pressure. Purification by

flash chromatography (CH_2Cl_2/acetone, 7/3) gave **12** (136 mg, 83%) as pale yellow oil. ^{1}H NMR (600 MHz, $CDCl_3$) δ 7.26 - 7.33 (m, 5H), 6.51 - 6.53 (m, 1H), 5.95 (br s, 1H), 5.40 (s, 1H), 5.21 (br s, 1H), 5.06 - 5.11 (m, 4H), 4.07 (m, 2H), 3.98 (m, 1H), 3.18 - 3.22 (m, 4H), 1.97 - 2.22 (m, 16H), 1.38 - 1.60 (m, 8H). **12** (0.1 g, 0.15 mmol) was suspended in 6 mL MeOH/HCO_2H (v/v 95/5) in the presence of 10% Pd/C (80 mg, 0.75). After 3 h, Pd/C was removed by filtration over Celite, and the filtrate was concentrated to afford **13** (25.5 mg, 90%) as pale yellow solid. ^{1}H NMR (600 MHz, $CDCl_3$) δ 6.60 (br s, 1H), 6.00 - 6.16 (m, 3H), 5.42 (s, 1H), 5.22 (m, 1H), 5.10 (m, 1H), 4.08 (d, *J* = 6.6 Hz, 2H), 4.01 (m, 1H), 3.21 - 3.25 (m, 4H), 2.94 (br s, 1H), 2.86 - 2.89 (m, 2H), 1.97 - 2.22 (m, 16H), 1.49 - 1.67 (m, 8H). ESI mass spectrum: Calcd (MH^+) 546.0, Found: 546.0.

Compound 14.

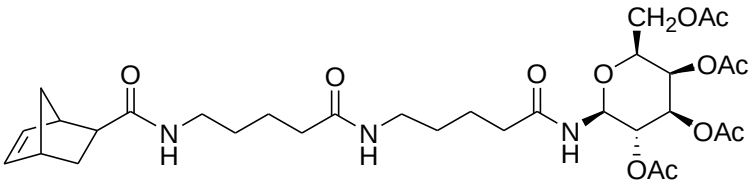

5-norbornene-exo-carboxylic acid (37 mg, 0.27 mmol), EDC (52 mg, 0.27 mmol), and HOBt (36 mmg, 0.27 mmol) were dissolved in CH_2Cl_2/DMF (2 mL, 1/1) and **13** (100 mg, 0.18 mmol) and DIEA (45 μL, 0.27 mmol) were added. After stirring for 20 h at rt, the solvent was concentrated and washed with 5% $NaHCO_3$ and 1N HCl. The combined organic phases were dried over $MgSO_4$, filtered, and concentrated. Purification by flash chromatography (CH_2Cl_2/acetone, 8/2) gave **14** (60 mg, 50%) as pale yellow solid. ^{1}H NMR (600 MHz, $CDCl_3$) δ 6.50 (br s, 1H), 6.49 (m, 1H), 6.11-6.14 (m, 3H), 5.43 (br s, 1H), 5.07 (m, 2H), 5.15

(m, 1H), 4.00 - 4.10 (m, 3H), 3.19 - 3.31 (m, 4H), 2.92 (br s, 1H), 2.27 - 1.98 (m, 17H), 1.8 - 1.90 (m, 1H), 1.48 - 1.71 (m, 8H). ESI mass spectrum: Calcd (MH^+) 666.4, Found: 666.0.

Compound 15.

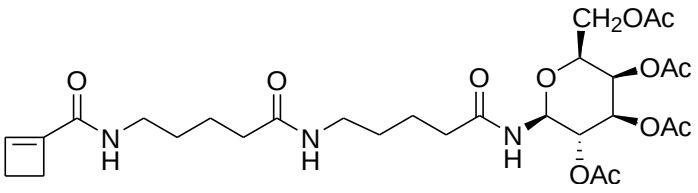

Cyclobutene-1-carboxylic acid (60 mg, 0.3 mmol), EDC (58 mg, 0.3 mmol), and HOBt (40.5 mg, 0.3 mmol) were dissolved in DMF/CH_2Cl_2 (4 mL, 1/1) and **13** (89 mg, 0.2 mmol) and DIEA (49.7 μL, 0.3 mmol) were added. After stirring for 20 h at rt, the solvent was concentrated and washed with 5% $NaHCO_3$ and 1N HCl. The combined organic phases were dried over $MgSO_4$, filtered, and concentrated. Purification by flash chromatography (CH_2Cl_2/acetone, 7/3) gave **15** (60 mg, 48%) as a brown oil. ^{1}H NMR (600 MHz, $CDCl_3$) δ 6.59 (br s, 1H), 6.10-6.53 (m, 1H), 5.94-6.02 (m, 2H), 5.43 (br s, 1H), 5.23 (t, *J* = 9.0 Hz, 1H), 5.09-5.12 (m, 2H), 4.10-4.09 (m, 3H), 3.23-3.32 (m, 4H), 2.67(t, *J* = 3.0 Hz, 2H), 2.43 (br s, 2H), 1.98-2.24 (m, 16H), 1.48-1.70 (m, 8H). ESI mass spectrum: Calcd (MH^+) 626.4, Found: 626.3.

2-Acetyloxyethylamine hydrochloride, 16.[117] To 2-hydroxyethylamine hydrochloride (1 g, 0.01 mmol) was added 0.75 mL of AcOH and 3 mL of acetyl chloride. The reaction mixture was stirred in ice-water for 30 min, and then stirred for 20 h at rt. The excess acetyl chloride and acetic acid were removed under vacuum. The product was crystallized from absolute EtOH, and crystals were collected (1.2 g, yield 84%). ^{1}H NMR (300 MHz, DMSO-d6) δ 8.34

(s, 3H), 4.20 (t, J = 5.2 Hz, 2 H), 3.03 (t, J = 5.3 Hz, 2 H), 2.04 (s, 3H). All ^{1}H NMR data were consistent with the literature.[117]

Compound 17.

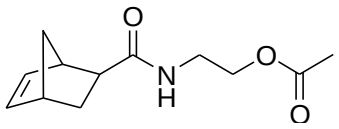

5-norbornene-exo-carboxylic acid (100 mg, 0.72 mmol), and EDC (138.6 mg, 0.72 mmol) were dissolved in dry CH_2Cl_2. 2-acetyloxyethylamine hydrochloride (77.1 mg, 0.48 mmol) and DIEA (318.1 μL, 1.92 mmol) were added to the reaction mixture. After stirring for 20 h at rt The reaction mixture was washed with 5% $NaHCO_3$ and 1N HCl. The combined organic phases were dried over $MgSO_4$, filtered, and concentrated. Purification by flash chromatography (CH_2Cl_2 / EtOAc, 7/3) gave **17** (51 mg, 47 %) as a clear gel. ^{1}H NMR (600 MHz, $CDCl_3$) δ 6.09 - 6.15 (m, 2H), 5.81 (br s, 1H), 4.17 (t, *J* = 5.1 Hz, 2H), 3.52 - 3.54 (m, 2H), 2.91 (br s, 2H), 2.07 (s, 3H), 1.89 - 2.01 (m, 2H), 1.53 -1.60 (m, 1H), 1.31 - 1.37 (m, 2H).

Compound 18.

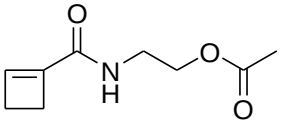

Cyclobutene-1-carboxylic acid (70.9 mg, 0.72 mmol), and EDC (138.6 mg, 0.72 mmol) were dissolved in dry CH_2Cl_2. 2-acetyloxyethylamine hydrochloride (77 mg, 0.48 mmol) and DIEA (45 μL, 0.27 mmol) were added to the reaction mixture. After stirring for 20 h at rt, he

reaction mixture was washed with 5% $NaHCO_3$ and 1N HCl. The combined organic phases were dried over $MgSO_4$, filtered, and concentrated. Purification by flash chromatography (CH_2Cl_2/EtOAc, 7/3) gave **18** (73 mg, 55%) as a clear gel. ^{1}H NMR (600 MHz, $CDCl_3$) δ 6.14 (dd, *J* = 3.9 Hz, 2.4 Hz, 1H), 6.11 (dd, *J* = 4.2 Hz, 3.0 Hz, 1H), 6.1 (br s, 1H), 4.06 (dd, *J* = 6.9 Hz, 5.4 Hz, 2H), 3.76 (s, 3H), 2.97 (br s, 1H), 2.92 (br s, 1H), 2.07 - 2.09 (m, 1H), 1.91 - 1.94 (m, 1H), 1.64 - 1.69 (m, 2H), 1.32 - 1.36 (m, 2H). ^{13}C NMR (100 MHz, $CDCl_3$) δ 176.0, 170.9, 138.5, 133.2, 52.5, 47.3, 46.5, 41.5, 30.6.

Compound 19.

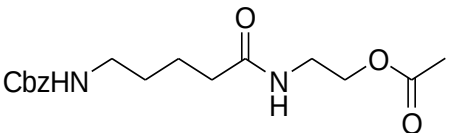

Compound **8** (532 mg, 2.2 mmol) and EDC (414 mg, 2.2 mmol) were dissolved in dry CH_2Cl_2 added under N_2. **16** (200 mg, 1.4 mmol) and DIEA (953 µL, 5.7 mmol) were added to the reaction mixture. After stirring for 20 h at rt, the solvent was concentrated and washed with 5% $NaHCO_3$ and 1N HCl. The combined organic phases were dried over $MgSO_4$, filtered, and concentrated. Purification by flash chromatography (CH_2Cl_2 /EtOAc, 7/3) gave **19** (330 mg, 62%) as white solid. ^{1}H NMR (600 MHz, $CDCl_3$) δ 7.31 - 7.34 (m, 5H), 5.93 (br s, 1H), 5.08 (br s, 1H), 4.94 (br s, 1H), 4.14 (t, *J* = 5.4 Hz, 2H), 3.49 (m, 2H), 3.19 (br s, 2H), 2.19 - 2.22 (m, 2H), 2.05 (br s, 3H), 1.62 (dd, *J* = 11.1 Hz, 7.2 Hz, 2H), 1.52 - 1.54 (m, 2H).

Compound 20.

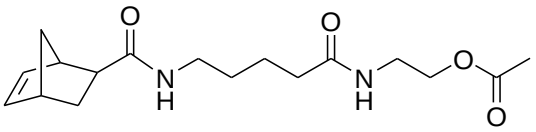

To a solution of **19** (34.2 mg, 0.09 mmol) in 6 mL MeOH/HCO_2H (v/v,95/5) was added 10% Pd/C (1.9 mg, 0.018 mmol). After 3 h, 10% Pd/C was removed by filtration over Celite, and the filtrate was concentrated to afford Cbz-deprotected **19** (17 mg, 90 %) as a pale yellow gel. 5-norbornene-exo-carboxylic acid (17 mg, 0.12 mmol), and EDC (23.0 mg, 0.12mmol) were dissolved in dry CH_2Cl_2 and the deprotected **19** (16.8 mg, 0.08 mmol), and DIEA (33 μL, 0.2 mmol) were added. After stirring for 20 h at rt, the reaction mixture was washed with 5% $NaHCO_3$ and 1N HCl.. The combined organic phases were dried over $MgSO_4$, filtered, and concentrated. Purification by flash chromatography (CH_2Cl_2/acetone, 7/3) gave **20** (12 mg, 48%) as clear gel. ^{1}H NMR (600 MHz, $CDCl_3$) δ 6.07-6.13 (m, 2H), 5.78 (br s, 1H), 5.75 (br s, 1H), 4.15 (t, *J* = 5.4 Hz, 2H), 3.50 - 3.52 (m, 2H), 3.28 (m, 2H), 2.91 (br s, 2H), 2.25 - 2.28 (m, 2H), 2.08 (br s, 3H), 1.89 - 2.01 (m, 2H), 1.51 - 1.73 (m, 5H), 1.31 - 1.37 (m, 2H).

Compound 21.

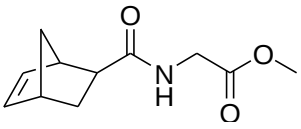

To a solution of 5-norbornene-exo-carboxylic acid (37 mg, 0.27 mmol) and EDC (52 mg, 0.27 mmol) in dry CH_2Cl_2 (2 mL) was added L-glycine•HCl (100 mg, 0.18 mmol) and DIEA (44.7 μL, 0.27 mmol). After stirring for 20 h at rt, The reaction mixture was washed with 5% $NaHCO_3$ and 1N HCl. The combined organic phases were dried over $MgSO_4$, filtered, and

concentrated. Purification by flash chromatography (CH_2Cl_2/acetone, 8/2) gave **21** (60 mg, 50 %) as a pale yellow solid. ^{1}H NMR (600 MHz, $CDCl_3$) δ 6.07 - 6.13 (m, 2H), 4.03 (m, 2H), 3.73 (br s, 3H), 2.89 - 2.95 (m, 2H), 2.07 (m, 1H), 1.89 (m, 1H), 1.65 (m, 1H), 1.30 (m, 2H).

Compound 22.

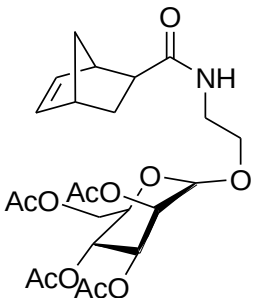

To a solution of 5-norbornene-exo-carboxylic acid (37 mg, 0.27 mmol), EDC (52 mg, 0.27 mmol) in dry CH_2Cl_2 (2 mL) was added 1-β-Azido-2,3,4,6-tetraacetyl-D-mannose in CH_2Cl_2/DMF. After stirring for 16 h at rt, the solvent was concentrated and washed with 5% $NaHCO_3$ and 1N HCl. The combined organic phases were dried over $MgSO_4$, filtered, and concentrated. Purification by flash chromatography (CH_2Cl_2/acetone, 8/2) gave **22** (60 mg, 50%) as a pale yellow gel. ^{1}H NMR (600 MHz, $CDCl_3$) δ 6.11 - 6.13 (m, 2H), 5.94 (br s, 1H), 4.81 (s, 1H), 4.22 - 4.23 (m, 1H), 4.10 (m, 1H), 3.96 (m, 1H), 3.78 (m, 1H), 3.53 - 3.55 (m, 3H), 2.91 (br s, 2H), 2.15 (s, 3H), 2.08 (s, 3H), 2.03 (s, 3H), 1.99 (s, 3H), 1.80-1.85 (m, 3H), 1.69 (m, 1H), 1.33 (m, 2H).

Ring opening metathesis polymerization (ROMP)

The general procedure for ROMP is described for Homopolymer-**3**. Details about scale, yield, and spectroscopic characterization for each polymer are presented individually for each polymer.

Homopolymer-3. Monomer **14** (96 mg, 0.14 mmol) was dissolved in dry CH_2Cl_2 (1.5 mL). **23** (2.8 mg, 0.0028 mmol) was dissolved in dry CH_2Cl_2 (0.5 mL). The catalyst solution was added to a solution of **14** and stirred for 1 h at 25 ℃. Ethyl vinyl ether (0.5 mL) was added to the mixture and stirred for an additional 40 min to quench the reaction. After removing the solvent, the residue was triturated in cold Et_2O to yield a pale yellow solid. The solid product was dissolved in MeOH (3 mL) and treated with 0.3M NaOMe in MeOH (0.4 mL). The solution was stirred for 2 h. Amberlite IR-120 resin (H^+ form) was added, filtered and the filtrate was concentrated under vacuum. The product was dialyzed and lyophilized to afford Homopolymer-**3** (86 mg, 90%) as yellowish-white solid. ^{1}H NMR (600 MHz, $CDCl_3$) δ 5.10 - 5.39 (m), 4.80 - 4.81 (m), 4.64 - 4.65 (br s), 3.89 (br s), 3.54 -3.66 (m), 3.01 - 3.09 (br s), 2.25 - 2.35 (m), 1.43 - 1.52 (m).

Homopolymer-1. Monomer **14** (100 mg, 0.15 mmol) and **23** (10 mg, 0.015 mmol) in dry CH_2Cl_2 (1.5 mL) afforded Homopolymer-**1** (80 mg, 80%) as a brownish gel. ^{1}H NMR (600 MHz, $CDCl_3$) δ 5.24 - 5.40 (m), 4.87 (br s), 4.64 - 4.65 (br s), 3.94 (br s), 3.55 -3.79 (m), 3.39 - 3.45 (br s), 3.17 - 3.35 (m), 2.16 -2.35 (m), 1.53 - 1.68 (m).

Homopolymer-2. Monomer **14** (100 mg, 0.15 mmol) and **23** (5 mg, 0.003 mmol) in dry CH_2Cl_2 (1.5 mL) afforded Homopolymer-2 (82 mg, 82%) as a brownish gel. ^{1}H NMR (600 MHz, $CDCl_3$) δ 5.20 - 5.36 (m), 4.83 (br s), 3.89 (br s), 3.52 -3.71 (m), 3.30 - 3.34 (br s), 3.17 (br s), 2.14 -2.39 (m), 1.48 - 1.63 (m).

Homopolymer-4. Monomer **14** (100 mg, 0.15 mmol) and **23** (2.5 mg, 0.0015 mmol) in dry CH_2Cl_2 (1.5 mL) afforded Homopolymer-4 (84 mg, 84%) as a yellowish-white solid. ^{1}H NMR (600 MHz, $CDCl_3$) δ 5.07 - 5.37 (m), 4.80 (m), 4.64 - 4.65 (br s), 3.89 (br s), 3.54-3.66 (m), 3.25 (br s), 2.97 - 3.12 (br s), 2.12 - 2.53 (m), 1.33 - 1.52 (m).

Homopolymer-5. Monomer **14** (94 mg, 0.14 mmol) and **23** (0.63 mg, 0.007 mmol) in dry CH_2Cl_2 (1.5 mL) afforded Homopolymer-**5** (79 mg, 84%) as a yellowish-white solid. ^{1}H NMR (600 MHz, $CDCl_3$) δ 7.63 -7.97 (m), 5.05 - 5.47 (m), 4.82 (m), 4.66 (br s), 3.91 (m), 3.57 - 3.64 (m), 3.09 (br s), 2.14 - 2.27 (m), 1.45 - 1.55 (m).

Homopolymer-6. Monomer **14** (213 mg, 0.34 mmol) and **23** (30 mg, 0.034 mmol) in dry CH_2Cl_2 (1.5 mL) afforded Homopolymer-**6** (181 mg, 85%) as a brownish gel. ^{1}H NMR (600 MHz, $CDCl_3$) δ 6.08 - 6.12 (m), 4.82 (br s), 4.64 - 4.81 (br s), 3.89 (m), 3.62 - 3.66 (m), 3.08 (br s), 2.83 (br s), 2.62 (br s), 2.24 (br s), 1.28 - 1.53 (m).

Copolymer-1. Monomer **15** (224 mg, 0.035 mmol) and **23** (9.18 mg, 0.01 mmol) in dry CH_2Cl_2 (2 mL) was stirred for 30 min. Monomer **21** (100 mg, 0.47 mmol) in dry CH_2Cl_2 (6 mL) was added to the reaction mixture and stirred for 1 h. Monomer **15** (12.7 mg, 0.02 mmol) in dry CH_2Cl_2 (2 mL) was added to the reaction mixture and was stirred for 30 min. Ethyl vinyl ether (0.5 mL) was added to the mixture and stirred for an additional 40 min to quench the reaction. After removing the solvent, the residue was triturated in cold Et_2O to give pale yellow solid. The solid product was dissolved in MeOH (0.3 mL) and treated with 0.3 M NaOMe in MeOH (0.3 mL). The solution was stirred for 1 h. Amberlite IR-120 resin (H^+ form) was added, filtered and the filtrate was concentrated under vacuum. The product was

dialyzed against H_2O and lyophilized to afford Copolymer-**1** (112 mg, 90%) as a yellowish-white solid. ^{1}H NMR (600 MHz, $CDCl_3$) δ 5.11 - 5.55 (m), 4.64 - 4.66 (m), 3.53 - 3.93 (m), 2.39 - 3.17 (m), 1.35 - 2.01 (m), 0.95 - 1.21 (m).

Copolymer-2 was synthesized following the same procedure as described for Copolymer-**1** from monomer **15** and monomer **21:** (90 mg, 90%, yellowish-white solid). ^{1}H NMR (600 MHz, $CDCl_3$) δ 5.20 - 5.38 (m), 4.62 - 4.69 (m), 3.51 - 3.87 (m), 2.41 - 3.15 (m), 1.40 - 2.10 (m), 0.98 - 1.24 (m).

Copolymer-3 was synthesized following the same procedure as described for Copolymer-**1** from monomer **15** and monomer **22** (112 mg, 87%, yellowish-white solid). ^{1}H NMR (600 MHz, $CDCl_3$) δ 5.08 - 5.35 (m), 4.79 - 4.90 (br s), 3.82 -4.36 (m), 3.42 - 3.78 (m), 2.92 - 3.10 (br s), 2.53 - 2.72 (br s), 1.99 - 2.44 (m).

Copolymer-4 was synthesized following the same procedure as described for Copolymer-**1** from monomer **15** and monomer **18** (64 mg, 85%, yellowish-white solid).^{1}H NMR (600 MHz, $CDCl_3$) δ 6.03 - 6.10 (br s), 4.53 - 4.63 (br s), 2.96 - 3.76 (m), 1.44 - 2.61 (m).

Copolymer-4 was synthesized following the same procedure as described for Copolymer-**1** from monomer **15** and monomer **18**. (70 mg, 87%, yellowish-white solid) ^{1}H NMR (600 MHz, $CDCl_3$) δ 6.06 - 6.13 (br s), 4.63 - 4.65 (br s), 2.98 - 3.80 (m), 1.48 - 2.45 (m).

II. Analysis of glycopolymer binding to Cholera toxin B subunit

Materials and methods. pAE-ctxB was kindly provided by Dr.Paulo Lee Ho (Centro de Biotecnologia, Instituto Butantan). For the expression of protein recombinant CT B_5, BL21-AI™ competent cells (Invitrogen) were used. Talon metal affinity resin was purchased from Clontech Laboratories, Inc. Chemicals were purchased from Fisher Scientific, Inc (Springfield, NJ). GM1 was obtained from Sigma-Aldrich (St. Louis, MO). Costar 3590 96-well plate was purchased from Corning Inc. Centricon30 was purchased from Millipore (Billerica, MA). SureBlue TMB was purchased from KPL, Inc. (Gaithersburg, Maryland). Rabbit anti-cholera toxin-HRP was purchased from AbD Serotec (Raleigh, NC). Microplate reader (Synergy™ 2, BioTek) was used for ELISA. Fluorescence spectra were taken on a PTI spectrofluorimeter (QM-4/ 2005-SE) (Photon Technology International, Inc, Lawrenceceville, NJ).

Expression CT B_5. CT B_5 was expressed following the procedure in literature.[133] Briefly, BL21-AI competent cells were transformed with the pAE-ctxB plasmid and grown overnight at 37 °C. The colonies were inoculated in 10 mL LB-amp and grown overnight at 37 °C. BL21 AI carrying the plasmid from an overnight culture was diluted 20-fold in LB-amp broth. When A_{600} =0.6, L-arabinose was added to the medium at a final concentration of 0.02 % (w/v). After 17 h, cells were harvested by centrifugation (5000 rpm, 30 min). The recombinant CT B_5 was expressed in an insoluble form as inclusion bodies. The cells were resuspended in 50 mL lysis buffer, pH 8.0 (300 mM NaCl, 100 mM Tris-Cl, 0.1 % Triton X-100) and lysed by French press. Cellular lysates were centrifuged at 26,000 g for 15 min. Inclusion bodies were washed twice with 10 mL of binding buffer (50 mM Tris-Cl, 500 mM NaCl) containing 10 mM β-mercaptoethanol and 2 M urea. Then, the inclusion bodies were

dissolved in 10 mL binding buffer containing 10 mM β-mercaptoethanol and 8 M urea. The solubilized pellet was slowly diluted in 2 L of binding buffer containing 5 mM imidazole for CTB refolding and incubated for 24 h at rt.

Purification of CT B_5. The refolded protein was centrifuged (5,000 rpm, 15 min) and the supernatant was loaded onto a Talon resin column. The resin was washed with 5 bed volumes of wash buffer (50 mM sodium phosphate, 300 mM NaCl, pH 8.0) containing 5 mM imidazole. CT B_5 was eluted with 10 bed volumes of elution buffer (50 mM sodium phosphate, 300 mM NaCl, 150 mM imidazole, pH 8.0). After analyzing fractions by 15 % SDS–PAGE, combined fractions were dialyzed in two steps. First, the equilibrium was established using 2 L solution containing 2 mM Tris, 20 mM NaCl, 0.1% glycine, and 10 mM EDTA, to eliminate imidazole. In the second step, the same buffer was used, without EDTA. Then purified CT B_5 was subject to an additional purification using Centricon30, to separate the monomeric and active pentameric forms. The sample was centrifuged for 15 min at 3,000 g and retentate CT B_5 was analyzed by 15 % SDS–PAGE.

Fluorescence titration assay. All spectra were recorded between 300 - 400 nm, using an excitation wavelength of 280 nm or 295 nm at 23 °C. CT B_5 was incubated with polymer solutions for 10 min prior to recording each spectrum. For all spectra, a reference spectrum with the same amount of sugar or polymer but no protein was acquired and subtracted from the sample spectrum in which the CT B_5 was present.

ELISA. Microtiter plates were incubated at rt for 16 h with 100 µL of 2 µg/mL GM1 dissolved per well in phosphate-buffered saline (pH 7.2) containing 150 mM NaCl and 10 mM potassium phosphate (PBS). Unattached ganglioside was removed by washing the wells three times with 10 mM PBS (pH 7.4, 0.05% Tween 20). Additional binding sites on the plate surface were blocked by incubating the wells with 200 µL of a 1% (w/v) bovine serum albumin (BSA)-PBS solution for 30 min at 37 ℃ and then washing them 3 times with 10 mM PBS (pH 7.4, 0.05% Tween 20). Various concentrations of polymer solutions were prepared in 0.1% BSA-0.05% Tween 20-PBS and preincubated with CT B_5 for 2 h. Preincubated samples (100 µL) were added to each well and incubated for 30 min at rt. Unbound toxin was removed by washing three times with 0.05 % Tween 20-PBS. Rabbit anti-cholera toxin-HRP (100 µL, diluted 1:1000) was added to each well, and then incubated for 1 h at rt. Toxin bound to GM1 was then revealed by addition of 100 µL of TMB solution for 15 min followed by 100 µL of 0.5N M HCl and the absorbance recorded at 450 nm on a Synergy^{TM} 2 (BioTek) ELISA microtiter plate reader.

NMR analysis. NMR analysis was performed at 298K in D_2O with a Varian 600 MHz spectrometer. Protein was exchanged into 50 mM sodium phosphate buffer (pH 7.6), then subjected to freeze-drying. The samples were dissolved in D_2O, and transferred to the NMR tube to a final concentration of 85.4 µM for protein and 1.3 mM for polymer.

III. Characterization of self-assembled structures

Materials and methods. Solvent and reagents were purchased from Fisher Scientific, Inc (Springfield, NJ). Fluorescence spectra were acquired on a PTI spectrofluorimeter (QM-4/ 2005-SE) (Photon Technology International, Inc, Lawrenceville, NJ). The mean diameter of glycopolymer was determined on a 90Plus-MAS (Brookhaven Instruments Corporation). TEM was performed with a FEI Tecnai12 BioTwinG2 transmission electron microscope at a 120 kV accelerating voltage and digital images were acquired with an AMT XR-60 CCD Digital Camera System. 2D-^{1}H,^{1}H-NOESY- NMR spectra were recorded on a Varian 600 MHz spectrometer.

CMC values. CMC values were evaluated with fluorescence dyes, pyrene, N-phenyl-1-naphthylamine (PNA) and 1,6-diphenyl-1,3,5-hexatriene (DPH). Fluorescence spectroscopy using pyrene was used to determine the CMC of glycopolymers. 10 µL of pyrene acetone solution (6×10^{-5} M) were added to vials and left for 1 h to evaporate the acetone. Various concentrations of glycopolymers solutions in distilled H_2O were added to the pyrene vials and allow to equilibrate for 20 h. The final concentration of pyrene was 6×10^{-7} M. The emission spectra of pyrene were measured from 350 nm to 450 nm at an excitation wavelength of 335 nm. The CMC was estimated from a plot of intensity of first peak at 371 nm against polymer concentration.

For fluorescence measurements with PNA, 10 µL of PNA acetone stock solution (6×10^{-5}M) was added to each of a series of vials and the acetone was removed. Various concentrations of glycopolymer solutions in distilled H_2O were added to the PNA vials and then heated at 45 ℃ for 3 h to equilibrate the PNA and the polymer solutions, and subsequently allowed to cool to rt and kept at rt for 17h. The emission spectra were measured

from 360 nm to 500 nm at an excitation wavelength of 340 nm. The CMC was estimated from plot of log (I/I_0) against polymer concentration.

For fluorescence measurements with DPH, DPH was dissolved in THF to produce a 0.5 mM DPH solution. Various concentrations of glycopolymer solutions were prepared in phosphate-buffered saline (pH 7.2) containing 150 mM NaCl and 10 mM potassium phosphate. 10 µL of DPH solution was added to polymer solutions and allowed to equilibrate for 10 min. The emission spectra were measured from 386 nm to 525 nm at an excitation wavelength of 358 nm. The CMC was estimated from a plot of intensity at 430 nm against polymer concentration.

Dynamic Light Scattering. Polymer solutions (1 mg/mL) were prepared in distilled H_2O and phosphate-buffered saline (pH 7.2) containing 150 mM NaCl and 10 mM potassium phosphate. Size was measured with or without 0.45 µM filtration. Measurements were performed at 25 ℃ with 90° scattering angle. Average diameters were obtained for 5 runs of size measurement.

TEM. Solutions of glycopolymers were prepared in distilled H_2O (5 mg/mL). Samples were deposited onto Formvar coated 400 mesh copper grids and were counter stained with aqueous 2% uranyl acetate.

NMR analysis. 2D-^{1}H,^{1}H- NOESY- NMR analyses were performed at 24℃ with a Varian 600 MHz spectrometer. 1% (w/v) Homopolymer-1 was prepared in DMSO-d_6. NMR spectra were recorded with scans and mixing times of 600 ms.

Bibliography

1 Dwek, R. A. Glycobiology: Toward understanding the function of sugars. *Chem Rev* **96**, 683-720 (1996).

2 Sharon, N. & Lis, H. Carbohydrates in Cell Recognition. *Sci Am* **268**, 82-89 (1993).

3 Bertozzi, C. R. & Kiessling, L. L. Chemical glycobiology. *Science (New York, N.Y.)* **291**, 2357-2364 (2001).

4 Lee, Y. C. & Lee, R. T. Carbohydrate-Protein Interactions - Basis of Glycobiology. *Accounts Chem Res* **28**, 321-327 (1995).

5 Flanagan, P. A. Evaluation of Protein-N-(2-Hydroxypropyl)Methacrylamide Copolymer Conjugates as Targetable Drug-Carriers .2. Body Distribution of Conjugates Containing Transferrin, Antitransferrin Receptor Antibody or Anti-Thy 1.2 Antibody and Effectiveness of Transferrin-Containing Daunomycin Conjugates against Mouse L1210 Leukemia Invivo. *J Control Release* **18**, 25-37 (1992).

6 Kodama, M. Polyacrylamide containing sugar residues: synthesis, characterization and cell compatibility studies. *Carbohyd Polym* **37**, 71-78 (1998).

7 Roy, R. Chemical modification of chitosan: Preparation and lectin binding properties of alpha-galactosyl-chitosan conjugates. Potential inhibitors in acute rejection following xenotransplantation. *Biomacromolecules* **1**, 303-305, doi:Doi 10.1021/Bm005536r (2000).

8 Yoshida, T. Synthesis of polymethacrylate derivatives having sulfated maltoheptaose side chains with anti-HIV activities. *J Polym Sci Pol Chem* **37**, 789-800 (1999).

9 Okada, M. Molecular design and syntheses of glycopolymers. *Progress in Polymer Science* **26**, 67-104, doi:10.1016/s0079-6700(00)00038-1 (2001).

10 Ladmiral, V., Melia, E. & Haddleton, D. M. Synthetic glycopolymers: an overview. *European Polymer Journal* **40**, 431-449, doi:10.1016/j.eurpolymj.2003.10.019 (2004).

11 Ohno, K., Fukuda, T. & Kitano, H. Free radical polymerization of a sugar residue-carrying styryl monomer with a lipophilic alkoxyamine initiator: synthesis of a well-defined novel glycolipid. *Macromol Chem Physic* **199**, 2193-2197 (1998).

12 Chen, Y. M. & Wulff, G. Synthesis of poly(styryl sugar)s by TEMPO mediated free radical polymerization. *Macromol Chem Physic* **202**, 3426-3431 (2001).

13 Chen, Y. M. & Wulff, G. Amphiphilic block copolymers with pendent sugar as hydrophilic segments and their surface properties. *Macromol Chem Physic* **202**, 3273-3278 (2001).
14 Godula, K. & Bertozzi, C. R. Synthesis of Glycopolymers for Microarray Applications via Ligation of Reducing Sugars to a Poly(acryloyl hydrazide) Scaffold. *J Am Chem Soc* **132**, 9963-9965, doi:Doi 10.1021/Ja103009d (2010).
15 Liu, L., Zhang, J. C., Lv, W. H., Luo, Y. & Wang, X. J. Well-Defined pH-Sensitive Block Glycopolymers via Reversible Addition-Fragmentation Chain Transfer Radical Polymerization: Synthesis, Characterization, and Recognition with Lectin. *J Polym Sci Pol Chem* **48**, 3350-3361, doi:Doi 10.1002/Pola.24119 (2010).
16 Ohno, K., Tsujii, Y. & Fukuda, T. Synthesis of a well-defined glycopolymer by atom transfer radical polymerization. *J Polym Sci Pol Chem* **36**, 2473-2481 (1998).
17 Matyjaszewski, K. & Tsarevsky, N. V. Nanostructured functional materials prepared by atom transfer radical polymerization. *Nat Chem* **1**, 276-288, doi:Doi 10.1038/Nchem.257 (2009).
18 Zhang, M. F. & Muller, A. H. E. Cylindrical polymer brushes. *J Polym Sci Pol Chem* **43**, 3461-3481, doi:Doi 10.1002/Pola.20900 (2005).
19 You, L. C., Lu, F. Z., Li, Z. C., Zhang, W. & Li, F. M. Glucose-sensitive aggregates formed by poly(ethylene oxide)-block-poly(2-glucosyl-oxyethyl acrylate) with coneanavalin A in dilute aqueous medium. *Macromolecules* **36**, 1-4, doi:Doi 10.1021/Ma025641o (2003).
20 Ladmiral, V. Synthesis of neoglycopolymers by a combination of "click chemistry" and living radical polymerization. *J Am Chem Soc* **128**, 4823-4830, doi:Doi 10.1021/Ja058364k (2006).
21 Beers, K. L., Gaynor, S. G., Matyjaszewski, K., Sheiko, S. S. & Moller, M. The synthesis of densely grafted copolymers by atom transfer radical polymerization. *Macromolecules* **31**, 9413-9415 (1998).
22 Cheng, G. L., Boker, A., Zhang, M. F., Krausch, G. & Muller, A. H. E. Amphiphilic cylindrical core-shell brushes via a "grafting from" process using ATRP. *Macromolecules* **34**, 6883-6888, doi:Doi 10.1021/Ma0013962 (2001).
23 Zhang, M. F., Breiner, T., Mori, H. & Muller, A. H. E. Amphiphilic cylindrical brushes with poly(acrylic acid) core and poly(n-butyl acrylate) shell and narrow length distribution. *Polymer* **44**, 1449-1458 (2003).
24 Dupayage, L., Nouvel, C. & Six, J. L. Protected Versus Unprotected Dextran Macroinitiators for ATRP Synthesis of Dex-g-PMMA. *J Polym Sci Pol Chem* **49**, 35-46, doi:Doi 10.1002/Pola.24409 (2011).
25 Muthukrishnan, S., Erhard, D. P., Mori, H. & Muller, A. H. E. Synthesis and characterization of surface-grafted hyperbranched glycomethacrylates. *Macromolecules* **39**, 2743-2750, doi:Doi 10.1021/Ma052575s (2006).
26 Pfaff, A. Glycopolymer-Grafted Polystyrene Nanospheres. *Macromol Biosci* **11**, 199-210, doi:DOI 10.1002/mabi.201000324 (2011).
27 Yang, Q. & Ulbricht, M. Cylindrical Membrane Pores with Well-Defined Grafted Linear and Comblike Glycopolymer Layers for Lectin Binding. *Macromolecules* **44**, 1303-1310, doi:Doi 10.1021/Ma1025972 (2011).

28 Gao, C. Linear and hyperbranched glycopolymer-functionalized carbon nanotubes: Synthesis, kinetics, and characterization. *Macromolecules* **40**, 1803-1815, doi:Doi 10.1021/Ma062238z (2007).
29 Bielawski, C. W. & Grubbs, R. H. Living ring-opening metathesis polymerization. *Prog Polym Sci* **32**, 1-29, doi:DOI 10.1016/j.progpolymsci.2006.08.006 (2007).
30 Lynn, D. M., Mohr, B., Grubbs, R. H., Henling, L. M. & Day, M. W. Water-soluble ruthenium alkylidenes: Synthesis, characterization, and application to olefin metathesis in protic solvents. *J Am Chem Soc* **122**, 6601-6609, doi:Doi 10.1021/Ja0003167 (2000).
31 Lynn, D. M. & Grubbs, R. H. Novel reactivity of ruthenium alkylidenes in protic solvents: Degenerate alkylidene proton exchange. *J Am Chem Soc* **123**, 3187-3193 (2001).
32 Gallivan, J. P., Jordan, J. P. & Grubbs, R. H. A neutral, water-soluble olefin metathesis catalyst based on an N-heterocyclic carbene ligand. *Tetrahedron Lett* **46**, 2577-2580, doi:DOI 10.1016/j.tetlet.2005.02.096 (2005).
33 Hong, S. H. & Grubbs, R. H. Highly active water-soluble olefin metathesis catalyst. *J Am Chem Soc* **128**, 3508-3509, doi:Doi 10.1021/Ja058451c (2006).
34 Fraser, C. & Grubbs, R. H. Synthesis of Glycopolymers of Controlled Molecular-Weight by Ring-Opening Metathesis Polymerization Using Well-Defined Functional-Group Tolerant Ruthenium Carbene Catalysts. *Macromolecules* **28**, 7248-7255 (1995).
35 Mortell, K. H., Gingras, M. & Kiessling, L. L. Synthesis of Cell Agglutination Inhibitors by Aqueous Ring-Opening Metathesis Polymerization. *J Am Chem Soc* **116**, 12053-12054 (1994).
36 Mortell, K. H., Weatherman, R. V. & Kiessling, L. L. Recognition specificity of neoglycopolymers prepared by ring-opening metathesis polymerization. *J Am Chem Soc* **118**, 2297-2298 (1996).
37 Schuster, M. C., Mortell, K. H., Hegeman, A. D. & Kiessling, L. L. Neoglycopolymers produced by aqueous ring-opening metathesis polymerization: Decreasing saccharide density increases activity. *J Mol Catal a-Chem* **116**, 209-216 (1997).
38 Kanai, M., Mortell, K. H. & Kiessling, L. L. Varying the size of multivalent ligands: The dependence of concanavalin a binding on neoglycopolymer length. *J Am Chem Soc* **119**, 9931-9932 (1997).
39 Sanders, W. J. Inhibition of L-selectin-mediated leukocyte rolling by synthetic glycoprotein mimics. *J Biol Chem* **274**, 5271-5278 (1999).
40 Nomura, K. & Schrock, R. R. Preparation of "sugar-coated" homopolymers and multiblock ROMP copolymers. *Macromolecules* **29**, 540-545 (1996).
41 Sutthasupa, S., Shiotsuki, M. & Sanda, F. Recent advances in ring-opening metathesis polymerization, and application to synthesis of functional materials. *Polym J* **42**, 905-915, doi:Doi 10.1038/Pj.2010.94 (2010).
42 Benson, S. W. Additivity Rules for Estimation of Thermochemical Properties. *Chem Rev* **69**, 279-& (1969).
43 Cairo, C. W., Gestwicki, J. E., Kanai, M. & Kiessling, L. L. Control of multivalent interactions by binding epitope density. *J Am Chem Soc* **124**, 1615-1619, doi:Doi 10.1021/Ja016727k (2002).

44 Brooks, P. C., Clark, R. A. F. & Cheresh, D. A. Requirement of Vascular Integrin Alpha(V)Beta(3) for Angiogenesis. *Science* **264**, 569-571 (1994).
45 Owen, R. M. *et al.* Bifunctional ligands that target cells displaying the alpha(v)beta(3) integrin. *ChemBioChem* **8**, 68-82 (2007).
46 Kiessling, L. L., Gestwicki, J. E. & Strong, L. E. Synthetic multivalent ligands as probes of signal transduction. *Angew Chem Int Edit* **45**, 2348-2368 (2006).
47 Levy, D., Bluzat, A., Seigneuret, M. & Rigaud, J. L. A Systematic Study of Liposome and Proteoliposome Reconstitution Involving Bio-Bead-Mediated Triton-X-100 Removal. *Biochim Biophys Acta* **1025**, 179-190 (1990).
48 Spaltenstein, A. & Whitesides, G. M. Polyacrylamides Bearing Pendant Alpha-Sialoside Groups Strongly Inhibit Agglutination of Erythrocytes by Influenza-Virus. *J Am Chem Soc* **113**, 686-687 (1991).
49 Lee, Y. & Sampson, N. S. Romping the cellular landscape: linear scaffolds for molecular recognition. *Curr Opin Struc Biol* **16**, 544-550 (2006).
50 Strong, L. E. & Kiessling, L. L. A general synthetic route to defined, biologically active multivalent arrays. *J Am Chem Soc* **121**, 6193-6196 (1999).
51 Choi, T. L., Rutenberg, I. M. & Grubbs, R. H. Synthesis of A,B-alternating copolymers by ring-opening-insertion-metathesis polymerization. *Angew Chem Int Edit* **41**, 3839-3841 (2002).
52 Kitov, P. I. Shiga-like toxins are neutralized by tailored multivalent carbohydrate ligands. *Nature* **403**, 669-672 (2000).
53 Kitov, P. I., Shimizu, H., Homans, S. W. & Bundle, D. R. Optimization of tether length in nonglycosidically linked bivalent ligands that target sites 2 and 1 of a Shiga-like toxin. *J Am Chem Soc* **125**, 3284-3294 (2003).
54 Mourez, M. Designing a polyvalent inhibitor of anthrax toxin. *Nat Biotechnol* **19**, 958-961 (2001).
55 Joshi, A., Saraph, A., Poon, V., Mogridge, J. & Kane, R. S. Synthesis of potent inhibitors of anthrax toxin based on poly-L-glutamic acid. *Bioconjugate Chem* **17**, 1265-1269 (2006).
56 Gujraty, K. V. Synthesis of polyvalent inhibitors of controlled molecular weight: Structure-activity relationship for inhibitors of anthrax toxin. *Biomacromolecules* **7**, 2082-2085 (2006).
57 Wolfenden, M. L. & Cloninger, M. J. Carbohydrate-functionalized dendrimers to investigate the predictable tunability of multivalent interactions. *Bioconjugate Chem* **17**, 958-966 (2006).
58 Benito, J. M. Optimizing saccharide-directed molecular delivery to biological receptors: Design, synthesis, and biological evaluation of glycodendrimer - Cyclodextrin conjugates. *J Am Chem Soc* **126**, 10355-10363 (2004).
59 Polizzotti, B. D. & Kiick, K. L. Effects of polymer structure on the inhibition of cholera toxin by linear polypeptide-based glycopolymers. *Biomacromolecules* **7**, 483-490, doi:Doi 10.1021/Bm050672n (2006).
60 Zhang, Z. S., Pickens, J. C., Hol, W. G. J. & Fan, E. K. Solution- and solid-phase syntheses of guanidine-bridged, water-soluble linkers for multivalent ligand design. *Org Lett* **6**, 1377-1380, doi:Doi 10.1021/Ol049835v (2004).

61 Merritt, E. A. Characterization and crystal structure of a high-affinity pentavalent receptor-binding inhibitor for cholera toxin and E-coli heat-labile enterotoxin. *J Am Chem Soc* **124**, 8818-8824, doi:Unsp Ja0202560 Doi 10.1021/Ja0202560 (2002).
62 Wang, Y. & Kiick, K. L. Monodisperse protein-based glycopolymers via a combined biosynthetic and chemical approach. *J Am Chem Soc* **127**, 16392-16393 (2005).
63 Zhang, Z. S., Liu, J. Y., Verlinde, C. L. M. J., Hol, W. G. J. & Fan, E. K. Large cyclic peptides as cores of multivalent ligands: Application to inhibitors of receptor binding by cholera toxin. *J Org Chem* **69**, 7737-7740, doi:Doi 10.1021/Jo0489770 (2004).
64 Pickens, J. C. Nonspanning bivalent ligands as improved surface receptor binding inhibitors of the cholera toxin B pentamer. *Chem Biol* **11**, 1205-1215, doi:DOI 10.1016/j.chembiol.2004.06.008 (2004).
65 Baessler, K. A., Lee, Y., Roberts, K. S., Facompre, N. & Sampson, N. S. Multivalent fertilin beta oligopeptides: The dependence of fertilization inhibition on length and density. *Chem Biol* **13**, 251-259 (2006).
66 Mammen, M., Dahmann, G. & Whitesides, G. M. Effective Inhibitors of Hemagglutination by Influenza-Virus Synthesized from Polymers Having Active Ester Groups - Insight into Mechanism of Inhibition. *J Med Chem* **38**, 4179-4190 (1995).
67 Reuter, J. D. Inhibition of viral adhesion and infection by sialic-acid-conjugated dendritic polymers. *Bioconjugate Chem* **10**, 271-278 (1999).
68 Sanders, W. J., Katsumoto, T. R., Bertozzi, C. R., Rosen, S. D. & Kiessling, L. L. L-selectin-carbohydrate interactions: Relevant modifications of the Lewis x trisaccharide. *Biochemistry-US* **35**, 14862-14867 (1996).
69 Carlson, C. B., Mowery, P., Owen, R. M., Dykhuizen, E. C. & Kiessling, L. L. Selective tumor cell targeting using low-affinity, multivalent interactions. *ACS Chem Biol* **2**, 119-127 (2007).
70 Gestwicki, J. E. & Kiessling, L. L. Inter-receptor communication through arrays of bacterial chemoreceptors. *Nature* **415**, 81-84 (2002).
71 Jones, D. S. *et al.* Multivalent thioether-peptide conjugates: B cell tolerance of an anti-peptide immune response. *Bioconjugate Chem* **10**, 480-488 (1999).
72 Spencer, D. M., Wandless, T. J., Schreiber, S. L. & Crabtree, G. R. Controlling Signal-Transduction with Synthetic Ligands. *Science* **262**, 1019-1024 (1993).
73 Rabinowitz, J. D. Formation of a highly peptide-receptive state of class II MHC. *Immunity* **9**, 699-709 (1998).
74 Owen, R. M., Gestwicki, J. E., Young, T. & Kiessling, L. L. Synthesis and applications of end-labeled neoglycopolymers. *Org Lett* **4**, 2293-2296, doi:Doi 10.1021/Ol0259239 (2002).
75 Mammen, M., Choi, S. K. & Whitesides, G. M. Polyvalent interactions in biological systems: Implications for design and use of multivalent ligands and inhibitors. *Angew Chem Int Edit* **37**, 2755-2794 (1998).
76 Kiessling, L. L., Gestwicki, J. E. & Strong, L. E. Synthetic multivalent ligands in the exploration of cell-surface interactions. *Curr Opin Chem Biol* **4**, 696-703 (2000).
77 Merritt, E. A. & Hol, W. G. J. AB5 toxins. *Curr Opin Struct Biol* **5**, 165-171, doi:10.1016/0959-440x(95)80071-9 (1995).
78 Minke, W. E., Roach, C., Hol, W. G. J. & Verlinde, C. L. M. J. Structure-based exploration of the ganglioside GM1 binding sites of Escherichia coli heat-labile

enterotoxin and cholera toxin for the discovery of receptor antagonists. *Biochemistry-US* **38**, 5684-5692 (1999).

79 Finkelstein, R. A., Boesman, M., Neoh, S. H., LaRue, M. K. & Delaney, R. Dissociation and recombination of the subunits of the cholera enterotoxin (choleragen). *Journal of immunology (Baltimore, Md. : 1950)* **113**, 145-150 (1974).

80 King, C. A. & Van Heyningen, W. E. Deactivation of cholera toxin by a sialidase-resistant monosialosylganglioside. *J Infect Dis* **127**, 639-647, doi:10.1093/infdis/127.6.639 (1973).

81 Kassis, S., Hagmann, J., Fishman, P. H., Chang, P. P. & Moss, J. Mechanism of action of cholera toxin on intact cells. Generation of A1 peptide and activation of adenylate cyclase. *J Biol Chem* **257**, 12148-12152 (1982).

82 Spangler, B. D. Structure and function of cholera toxin and the related Escherichia coli heat-labile enterotoxin. *Microbiological Reviews* **56**, 622-647 (1992).

83 Merritt, E. A. Crystal structure of cholera toxin B-pentamer bound to receptor GM1 pentasaccharide. *Protein Science* **3**, 166-175 (1994).

84 Merritt, E. A. The 1.25 angstrom resolution refinement of the cholera toxin B-pentamer: Evidence of peptide backbone strain at the receptor-binding site. *J Mol Biol* **282**, 1043-1059 (1998).

85 Sixma, T. K. Crystal-Structure of a Cholera Toxin-Related Heat-Labile Enterotoxin from Escherichia-Coli. *Nature* **351**, 371-377 (1991).

86 Discher, D. E. & Eisenberg, A. Polymer vesicles. *Science* **297**, 967-973 (2002).

87 Pfannemuller, B., Schmidt, M., Ziegast, G. & Matsuo, K. Properties of a Once-Broken Wormlike Chain Based on Amylose Tricarbanilate - Light-Scattering, Viscosity, and Dielectric-Relaxation. *Macromolecules* **17**, 710-716 (1984).

88 Muller, A. H. E. Micellar aggregates of amylose-block-polystyrene rod-coil block copolymers in water and THF. *Macromolecules* **38**, 873-879, doi:Doi 10.1021/Ma0345549 (2005).

89 Borsali, R., Lecommandoux, S., Pecora, R. & Benoit, H. Scattering properties of rod-coil and once-broken rod block copolymers. *Macromolecules* **34**, 4229-4234, doi:Doi 10.1021/Ma001760x (2001).

90 Lecommandoux, S. *et al.* Biomimetic Doxorubicin Loaded Polymersomes from Hyaluronan-block-Poly(gamma-benzyl glutamate) Copolymers. *Biomacromolecules* **10**, 2802-2808, doi:Doi 10.1021/Bm9006419 (2009).

91 Schlaad, H. & You, L. C. An easy way to sugar-containing polymer vesicles or glycosomes. *J Am Chem Soc* **128**, 13336-13337, doi:Doi 10.1021/Ja064569x (2006).

92 Schlaad, H. *et al.* Glycopolymer vesicles with an asymmetric membrane. *Chem Commun*, 1478-1480, doi:Doi 10.1039/B820887e (2009).

93 Nelson, A. Synthesis of a family of amphiphilic glycopolymers via controlled ring-opening polymerization of functionalized cyclic carbonates and their application in drug delivery. *Biomaterials* **31**, 2637-2645, doi:DOI 10.1016/j.biomaterials.2009.12.022 (2010).

94 Verlinde, C. L. M. J., Minke, W. E., Roach, C. & Hol, W. G. J. Structure-based exploration of the ganglioside GM1 binding sites of Escherichia coli heat-labile enterotoxin and cholera toxin for the discovery of receptor antagonists. *Biochemistry-US* **38**, 5684-5692 (1999).

95 Fan, E. K. Anchor-based design of improved cholera toxin and E-coli heat-labile enterotoxin receptor binding antagonists that display multiple binding modes. *Chem Biol* **9**, 215-224 (2002).
96 Bernardi, A. Mimics of ganglioside GM1 as cholera toxin ligands: replacement of the GalNAc residue. *Org Biomol Chem* **1**, 785-792, doi:Doi 10.1039/B210503a (2003).
97 Pukin, A. V. Strong inhibition of cholera toxin by multivalent GM1 derivatives. *ChemBioChem* **8**, 1500-1503, doi:DOI 10.1002/cbic.200700266 (2007).
98 Turnbull, W. B., Precious, B. L. & Homans, S. W. Dissecting the cholera toxin-ganglioside GM1 interaction by isothermal titration calorimetry. *J Am Chem Soc* **126**, 1047-1054, doi:Doi 10.1021/Ja0378207 (2004).
99 Cheshev, P. *et al.* Synthesis and Affinity Evaluation of a Small Library of Bidentate Cholera Toxin Ligands: Towards Nonhydrolyzable Ganglioside Mimics. *Chem-Eur J* **16**, 1951-1967, doi:DOI 10.1002/chem.200902469 (2010).
100 Merritt, E. A., Sarfaty, S., Feil, I. K. & Hol, W. G. J. Structural foundation for the design of receptor antagonists targeting Escherichia coli heat-labile enterotoxin. *Structure* **5**, 1485-1499 (1997).
101 Pickens, J. C. Anchor-based design of improved cholera toxin and E-coli heat-labile enterotoxin receptor binding antagonists that display multiple binding modes. *Chem Biol* **9**, 215-224 (2002).
102 Bernardi, A., Checchia, A., Brocca, P., Sonnino, S. & Zuccotto, F. Sugar mimics: An artificial receptor for cholera toxin. *J Am Chem Soc* **121**, 2032-2036 (1999).
103 Bernardi, A. Synthesis of a pseudo tetrasaccharide mimic of ganglioside GM1. *Eur J Org Chem*, 1311-1317 (1999).
104 Bernardi, A., Carrettoni, L., Ciponte, A. G., Monti, D. & Sonnino, S. Second generation mimics of ganglioside GM1 as artificial receptors for cholera toxin: Replacement of the sialic acid moiety. *Bioorg Med Chem Lett* **10**, 2197-2200 (2000).
105 Fan, E. K. *et al.* High-affinity pentavalent ligands of Escherichia coli heat-labile enterotoxin by modular structure-based design. *J Am Chem Soc* **122**, 2663-2664 (2000).
106 Vrasidas, I., de Mol, N. J., Liskamp, R. M. J. & Pieters, R. J. Synthesis of lactose dendrimers and multivalency effects in binding to the cholera toxin B subunit. *Eur J Org Chem*, 4685-4692 (2001).
107 Sisu, C. The Influence of Ligand Valency on Aggregation Mechanisms for Inhibiting Bacterial Toxins. *ChemBioChem* **10**, 329-337, doi:DOI 10.1002/cbic.200800550 (2009).
108 Polizzotti, B. D., Maheshwari, R., Vinkenborg, J. & Kiick, K. L. Effects of saccharide spacing and chain extension on toxin inhibition by glycopolypeptides of well-defined architecture. *Macromolecules* **40**, 7103-7110, doi:Doi 10.1021/Ma070725o (2007).
109 Maheshwari, R., Levenson, E. A. & Kiick, K. L. Manipulation of Electrostatic and Saccharide Linker Interactions in the Design of Efficient Glycopolypeptide-Based Cholera Toxin Inhibitors. *Macromol Biosci* **10**, 68-81, doi:DOI 10.1002/mabi.200900182 (2010).
110 Verlinde, C. L. M. J. Protein Crystallography and Infectious-Diseases. *Protein Sci* **3**, 1670-1686 (1994).
111 Minke, W. E., Hong, F., Verlinde, C. L. M. J., Hol, W. G. J. & Fan, E. Using a galactose library for exploration of a novel hydrophobic pocket in the receptor binding

site of the Escherichia coli heat-labile enterotoxin. *J Biol Chem* **274**, 33469-33473 (1999).
112 Maier, M. A. Synthesis of antisense oligonucleotides conjugated to a multivalent carbohydrate cluster for cellular targeting. *Bioconjugate Chem* **14**, 18-29, doi:Doi 10.1021/Bc020028v (2003).
113 Fekete, A., Gyergyoi, K., Kover, K. E., Bajza, I. & Liptak, A. Preparation of the pentasaccharide hapten of the GPL of Mycobacterium avium serovar 19 by achieving the glycosylation of a tertiary hydroxyl group. *Carbohyd Res* **341**, 1312-1321 (2006).
114 Kleinert, M., Rockendorf, N. & Lindhorst, T. K. Glyco-SAMs as glycocalyx mimetics: Synthesis of L-fucose- and D-mannose-terminated building blocks. *Eur J Org Chem*, 3931-3940, doi:DOI 10.1002/ejoc.200400239 (2004).
115 Gu, L. R. *et al.* Single-walled carbon nanotube as a unique scaffold for the multivalent display of sugars. *Biomacromolecules* **9**, 2408-2418, doi:Doi 10.1021/Bm800395e (2008).
116 Schierholt, A., Shaikh, H. A., Schmidt-Lassen, J. & Lindhorst, T. K. Utilizing Staudinger Ligation for the Synthesis of Glycoamino Acid Building Blocks and Other Glycomimetics. *Eur J Org Chem*, 3783-3789, doi:DOI 10.1002/ejoc.200900437 (2009).
117 Liu, J. Q., Kolar, C., Lawson, T. A. & Gmeiner, W. H. Targeted drug delivery to chemoresistant cells: Folic acid derivatization of FdUMP[10] enhances cytotoxicity toward 5-FU-resistant human colorectal tumor cells. *J Org Chem* **66**, 5655-5663, doi:Doi 10.1021/Jo005757n (2001).
118 Merritt, E. A. & Bacon, D. J. Raster3D: Photorealistic molecular graphics. *Method Enzymol* **277**, 505-524 (1997).
119 Krishnamurthy, V. M., Semetey, V., Bracher, P. J., Shen, N. & Whitesides, G. M. Dependence of effective molarity on linker length for an intramolecular protein-ligand system. *J Am Chem Soc* **129**, 1312-1320 (2007).
120 Crombie, A. L. Synthesis and biological evaluation of tricyclic anilinopyrimidines as IKK beta inhibitors. *Bioorg Med Chem Lett* **20**, 3821-3825, doi:DOI 10.1016/j.bmcl.2010.04.022 (2010).
121 Wang, H. S. *et al.* Discovery of (2E)-3-{2-Butyl-1[2-(diethylamino)ethyl]-1H-benzimidazol-5-yl}-N-hydroxyacrylamide (SB939), an Orally Active Histone Deacetylase Inhibitor with a Superior Preclinical Profile. *J Med Chem* **54**, 4694-4720, doi:Doi 10.1021/Jm2003552 (2011).
122 Ploemen, J. P. H. T. M. Use of physicochemical calculation of pKa and CLogP to predict phospholipidosis-inducing potential - A case study with structurally related piperazines. *Exp Toxicol Pathol* **55**, 347-355 (2004).
123 Mertz, J. A., McCann, J. A. & Picking, W. D. Fluorescence analysis of galactose, lactose, and fucose interaction with the cholera toxin B subunit. *Biochem Bioph Res Co* **226**, 140-144 (1996).
124 Svennerholm, A. M. & Holmgren, J. Identification of Escherichia-Coli Heat-Labile Enterotoxin by Means of a Ganglioside Immunosorbent Assay (Gm1-Elisa) Procedure. *Curr Microbiol* **1**, 19-23 (1978).
125 Lundquist, J. J. & Toone, E. J. The cluster glycoside effect. *Chem Rev* **102**, 555-578, doi:Doi 10.1021/Cr000418f (2002).

126 Sigurskjold, B. W., Berland, C. R. & Svensson, B. Thermodynamics of Inhibitor Binding to the Catalytic Site of Glucoamylase from Aspergillus-Niger Determined by Displacement Titration Calorimetry. *Biochemistry-US* **33**, 10191-10199 (1994).
127 Williams, B. A., Chervenak, M. C. & Toone, E. J. Energetics of Lectin-Carbohydrate Binding - a Microcalorimetric Investigation of Concanavalin a-Oligomannoside Complexation. *J Biol Chem* **267**, 22907-22911 (1992).
128 Chervenak, M. C. & Toone, E. J. A Direct Measure of the Contribution of Solvent Reorganization to the Enthalpy of Ligand-Binding. *J Am Chem Soc* **116**, 10533-10539 (1994).
129 Mayer, M. & Meyer, B. Characterization of ligand binding by saturation transfer difference NMR spectroscopy. *Angew Chem Int Edit* **38**, 1784-1788 (1999).
130 Liu, J. Y. *et al.* Multivalent drug design and inhibition of cholera toxin by specific and transient protein-ligand interactions. *Chem Biol Drug Des* **71**, 408-419, doi:DOI 10.1111/j.1747-0285.2008.00648.x (2008).
131 Bergstrom, M., Liu, S., Kiick, K. L. & Ohlson, S. Cholera Toxin Inhibitors Studied with High-Performance Liquid Affinity Chromatography: A Robust Method to Evaluate Receptor-Ligand Interactions. *Chem Biol Drug Des* **73**, 132-141, doi:DOI 10.1111/j.1747-0285.2008.00758.x (2009).
132 Pera, N. P. Rapid Screening of Lectins for Multivalency Effects with a Glycodendrimer Microarray. *ChemBioChem* **11**, 1896-1904, doi:DOI 10.1002/cbic.201000340 (2010).
133 Areas, A. P. D. Synthesis of cholera toxin B subunit gene: cloning and expression of a functional 6XHis-tagged protein in Escherichia coli. *Protein Expres Purif* **25**, 481-487 (2002).
134 Fishman, P. H., Moss, J. & Osborne, J. C. Interaction of Choleragen with Oligosaccharide of Ganglioside Gm1 - Evidence for Multiple Oligosaccharide Binding-Sites. *Biochemistry-US* **17**, 711-716 (1978).
135 Schlaad, H. & Antonietti, M. Block copolymers with amino acid sequences: Molecular chimeras of polypeptides and synthetic polymers. *Eur Phys J E* **10**, 17-23 (2003).
136 Turnbull, W. B., Pease, A. R. & Stoddart, J. F. Synthetic carbohydrate dendrimers, part 8 - Toward the synthesis of large oligosaccharide-based dendrimers. *ChemBioChem* **1**, 70-74 (2000).
137 Miura, Y. Synthesis and biological application of glycopolymers. *J Polym Sci Pol Chem* **45**, 5031-5036, doi:Doi 10.1002/Pola.22369 (2007).
138 Antonietti, M. & Forster, S. Vesicles and liposomes: A self-assembly principle beyond lipids. *Adv Mater* **15**, 1323-1333, doi:DOI 10.1002/adma.200300010 (2003).
139 Bates, F. S. & Jain, S. On the origins of morphological complexity in block copolymer surfactants. *Science* **300**, 460-464 (2003).
140 Hu, Z., Fan, X. & Zhang, G. Synthesis and characterization of glucose-grafted biodegradable amphiphilic glycopolymers P(AGE-glucose)-b-PLA. *Carbohydrate Polymers* **79**, 119-124, doi:10.1016/j.carbpol.2009.07.041 (2010).
141 Schatz, C. & Lecommandoux, S. Polysaccharide-containing block copolymers: synthesis, properties and applications of an emerging family of glycoconjugates. *Macromol Rap Comm* **31**, 1664-1684, doi:10.1002/marc.201000267 (2010).
142 Leon, O., Munoz-Bonilla, A., Bordege, V., Sanchez-Chaves, M. & Fernandez-Garcia, M. Amphiphilic block glycopolymers via atom transfer radical polymerization:

Synthesis, self-assembly and biomolecular recognition. *J Poly Sci, Part A: Polymer Chem* **49**, 2627-2635, doi:10.1002/pola.24694 (2011).
143 Nagasaki, Y., Yasugi, K., Yamamoto, Y., Harada, A. & Kataoka, K. Sugar-Installed Block Copolymer Micelles: Their Preparation and Specific Interaction with Lectin Molecules. *Biomacromolecules* **2**, 1067-1070, doi:10.1021/bm015574q (2001).
144 Houga, C. Micelles and Polymersomes Obtained by Self-Assembly of Dextran and Polystyrene Based Block Copolymers. *Biomacromolecules* **10**, 32-40, doi:10.1021/bm800778n (2009).
145 Liang, Y.-Z., Li, Z.-C. & Li, F.-M. Self-Association of Poly[2-(β-D-glucosyloxy)ethyl Acrylate] in Water. *J Coll Interf Sci* **224**, 84-90, doi:10.1006/jcis.1999.6644 (2000).
146 You, L.-C., Lu, F.-Z., Li, Z.-C., Zhang, W. & Li, F.-M. Glucose-Sensitive Aggregates Formed by Poly(ethylene oxide)-block-poly(2-glucosyloxyethyl acrylate) with Concanavalin A in Dilute Aqueous Medium. *Macromolecules* **36**, 1-4, doi:10.1021/ma025641o (2003).
147 Hordyjewicz-Baran, Z., You, L., Smarsly, B., Sigel, R. & Schlaad, H. Bioinspired Polymer Vesicles Based on Hydrophilically Modified Polybutadienes. *Macromolecules* **40**, 3901-3903, doi:10.1021/ma070347n (2007).
148 Thoma, G., Katopodis, A. G., Voelcker, N., Duthaler, R. O. & Streiff, M. B. Novel glycodendrimers self-assemble to nanoparticles which function as polyvalent ligands in vitro and in vivo. *Angew Chem Int Edit* **41**, 3195-+ (2002).
149 Welsh, D. J. & Smith, D. K. Comparing dendritic and self-assembly strategies to multivalency-RGD peptide-integrin interactions. *Org Biomol Chem* **9**, 4795-4801, doi:Doi 10.1039/C1ob05241a (2011).
150 Steed, J. W. & Atwood, J. L. *Supramolecular Chemistry: A Concise Introduction*. (2000).
151 Basu Ray, G., Chakraborty, I. & Moulik, S. P. Pyrene absorption can be a convenient method for probing critical micellar concentration (cmc) and indexing micellar polarity. *J Coll Interf Sci* **294**, 248-254, doi:10.1016/j.jcis.2005.07.006 (2006).
152 Kalyanasundaram, K. & Thomas, J. K. Environmental effects on vibronic band intensities in pyrene monomer fluorescence and their application in studies of micellar systems. *J Am Chem Soc* **99**, 2039-2044, doi:10.1021/ja00449a004 (1977).
153 Akiyoshi, K., Deguchi, S., Moriguchi, N., Yamaguchi, S. & Sunamoto, J. Self-Aggregates of Hydrophobized Polysaccharides in Water - Formation and Characteristics of Nanoparticles. *Macromolecules* **26**, 3062-3068 (1993).
154 Chattopadhyay, A. & London, E. Fluorimetric Determination of Critical Micelle Concentration Avoiding Interference from Detergent Charge. *Anal Biochem* **139**, 408-412 (1984).
155 Mast, R. C. & Haynes, L. V. Use of Fluorescent-Probes Perylene and Magnesium 8-Anilinonaphthalene-1-Sulfonate to Determine Critical Micelle Concentration of Surfactants in Aqueous-Solution. *J Colloid Interf Sci* **53**, 35-41 (1975).
156 Lee, E. S., Shin, H. J., Na, K. & Bae, Y. H. Poly(L-histidine)-PEG block copolymer micelles and pH-induced destabilization. *J Control Release* **90**, 363-374, doi:Doi 10.1016/S0168-3659(03)00205-0 (2003).
157 Hu, Z. G., Fan, X. S. & Zhang, G. S. Synthesis and characterization of glucose-grafted biodegradable amphiphilic glycopolymers P(AGE-glucose)-b-PLA. *Carbohyd Polym* **79**, 119-124, doi:DOI 10.1016/j.carbpol.2009.07.041 (2010).

158 Liang, Y. Z., Li, Z. C. & Li, F. M. Self-association of poly[2-(beta-D-glucosyloxy)ethyl acrylate] in water. *J Colloid Interf Sci* **224**, 84-90 (2000).
159 Love, J. A., Morgan, J. P., Trnka, T. M. & Grubbs, R. H. A practical and highly active ruthenium-based catalyst that effects the cross metathesis of acrylonitrile. *Angew Chem Int Edit* **41**, 4035-4037 (2002).
160 Yagi, H., Thakker, D. R., Lehr, R. E. & Jerina, D. M. Benzo-Ring Diol Epoxides of Benzo[E]Pyrene and Triphenylene. *J Org Chem* **44**, 3439-3442 (1979).
161 Schmuck, C., Rehm, T., Geiger, L. & Schafer, M. Synthesis and self-association properties of flexible guanidiniocarbonylpyrrole-carboxylate zwitterions in DMSO: Intra-versus intermolecular ion pairing. *J Org Chem* **72**, 6162-6170, doi:Doi 10.1021/Jo070641d (2007).

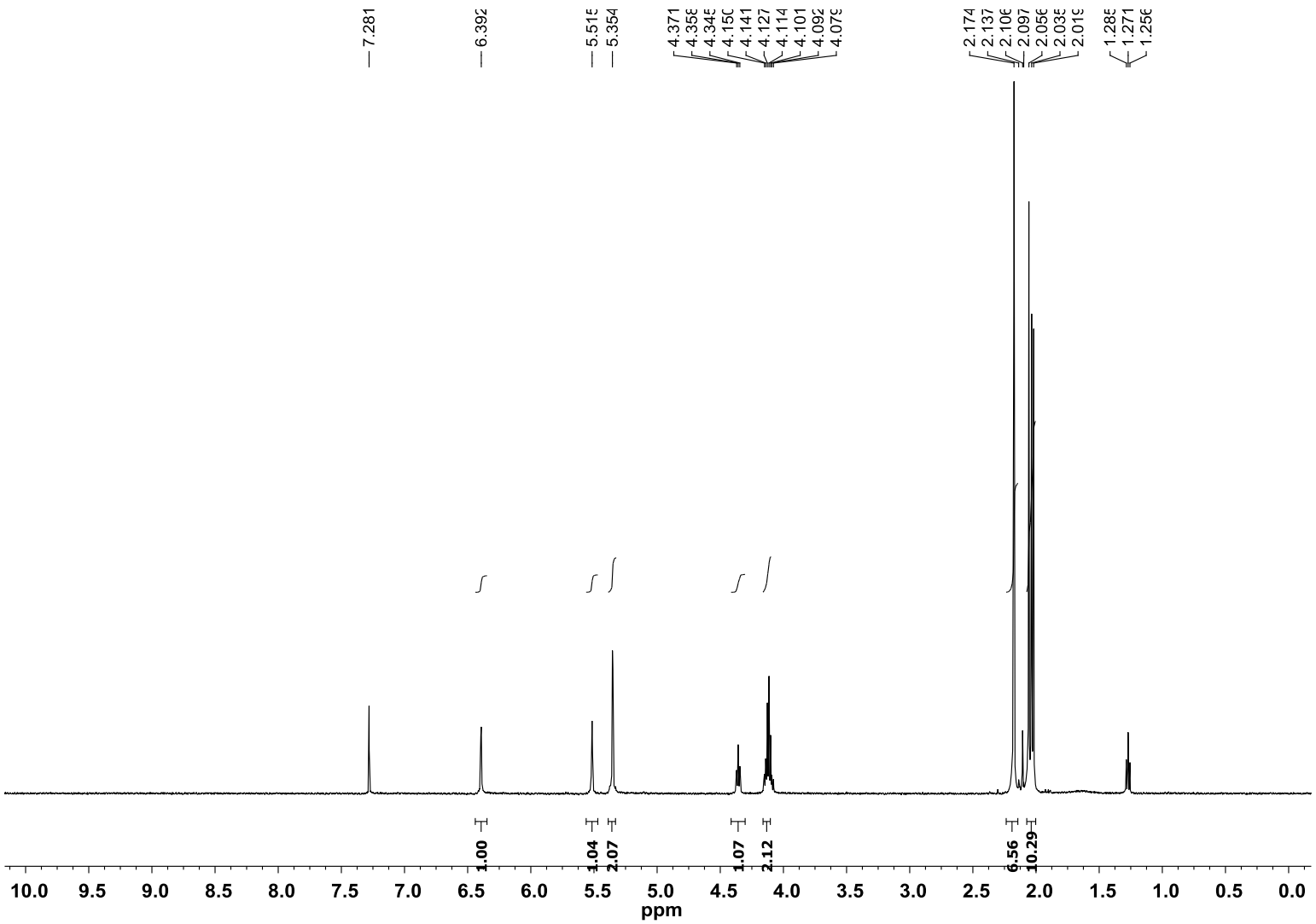

A-1: ^{1}H NMR spectrum of pentaacetyl-D-galactose, 1

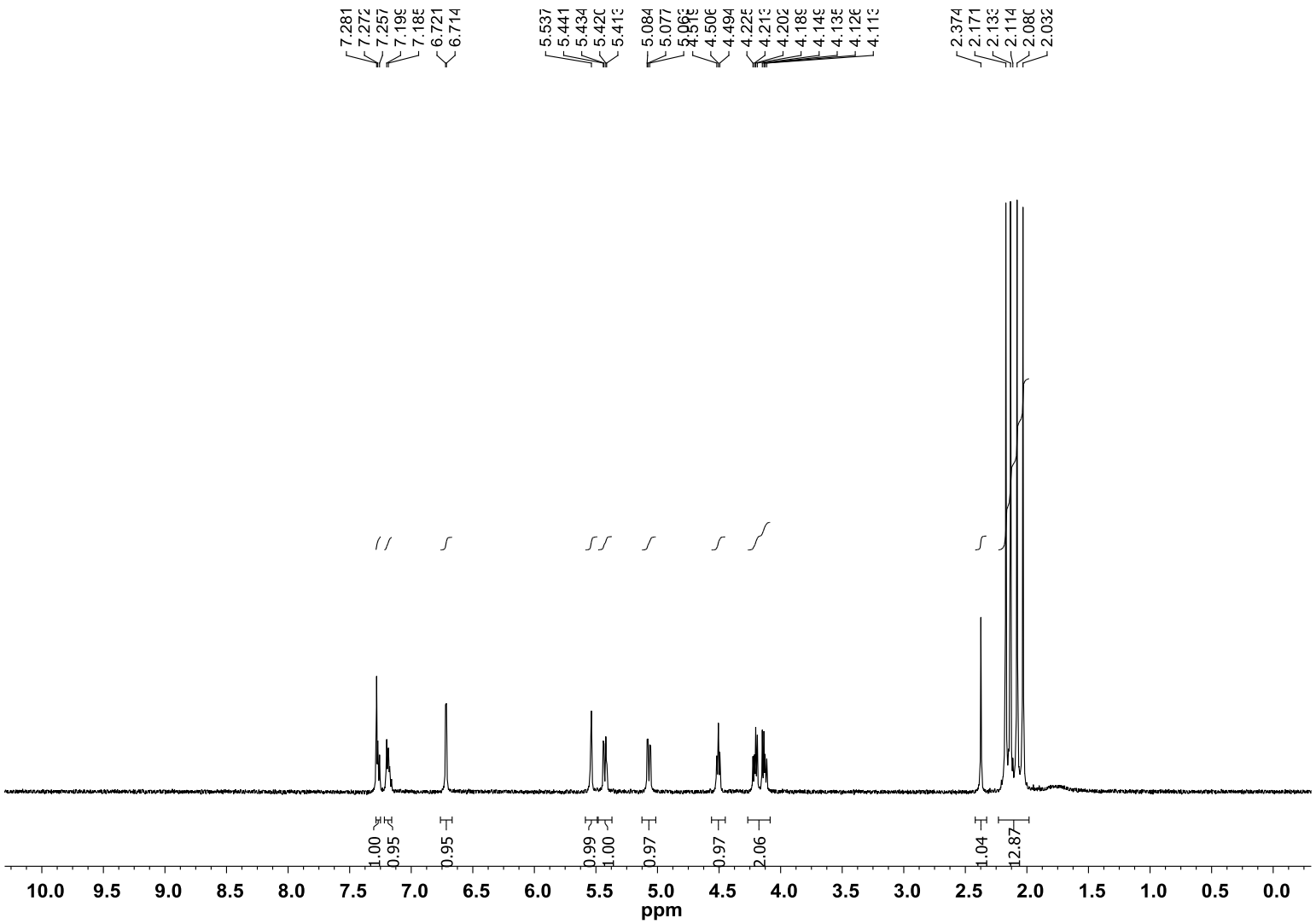

A-2: ^{1}H NMR spectrum of 1-β-bromo-2,3,4,6-tetraacetyl-D-galactose, 2

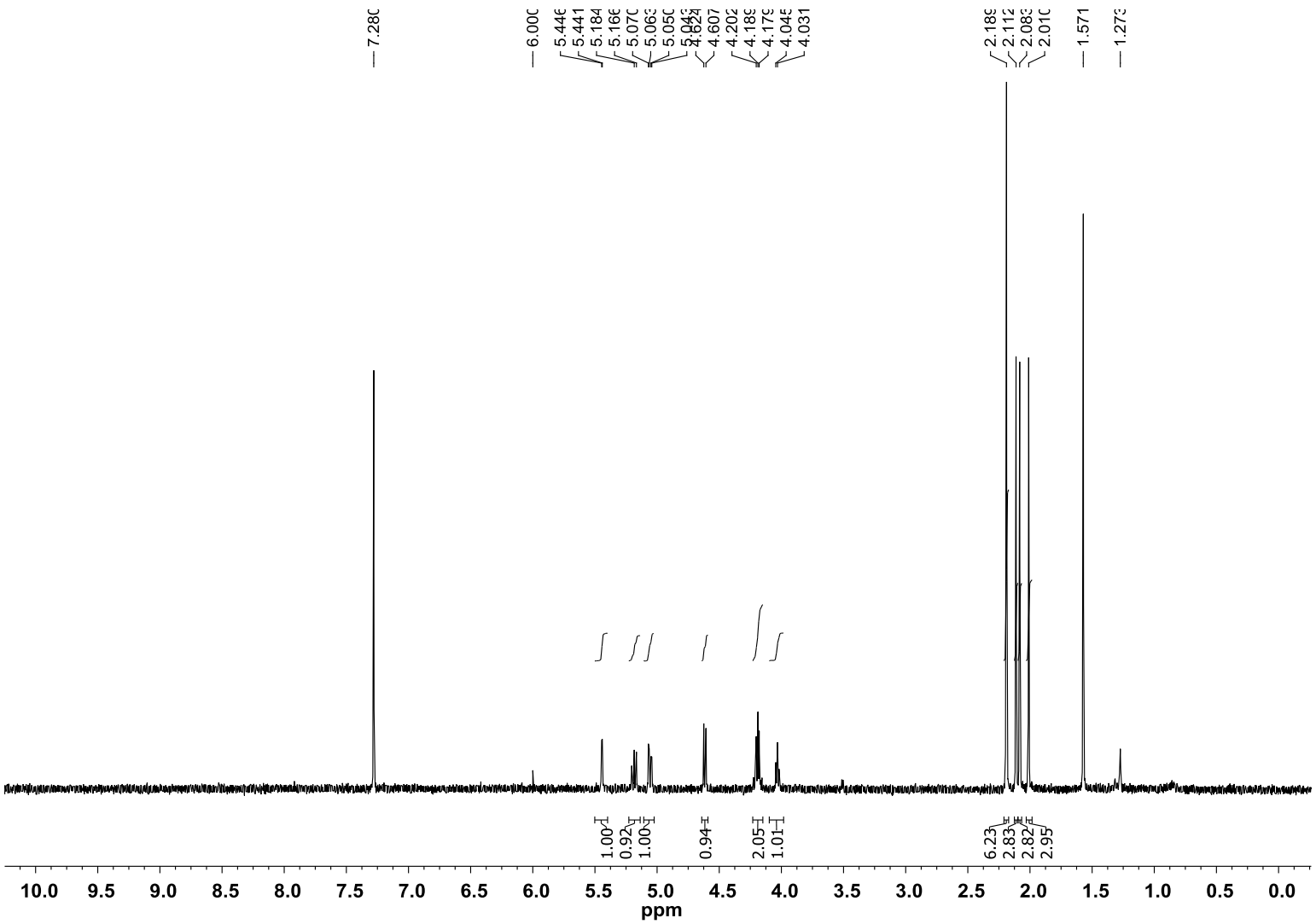

A-3: ^{1}H NMR spectrum of 1-β-azido-2,3,4,6-tetraacetyl-D-galactose, 3

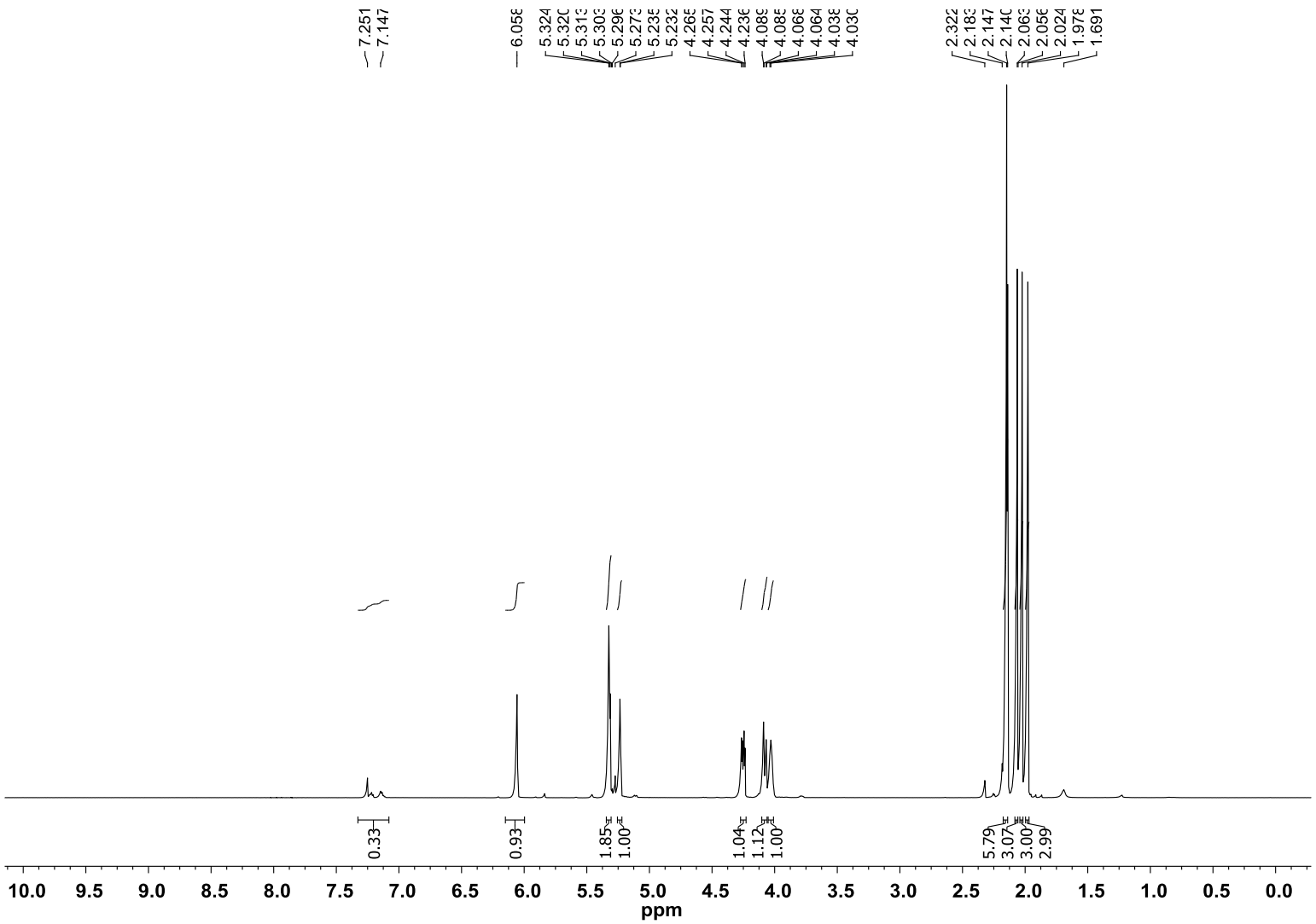

A-4: ^{1}H NMR spectrum of pentaacetyl-D-mannose, 4

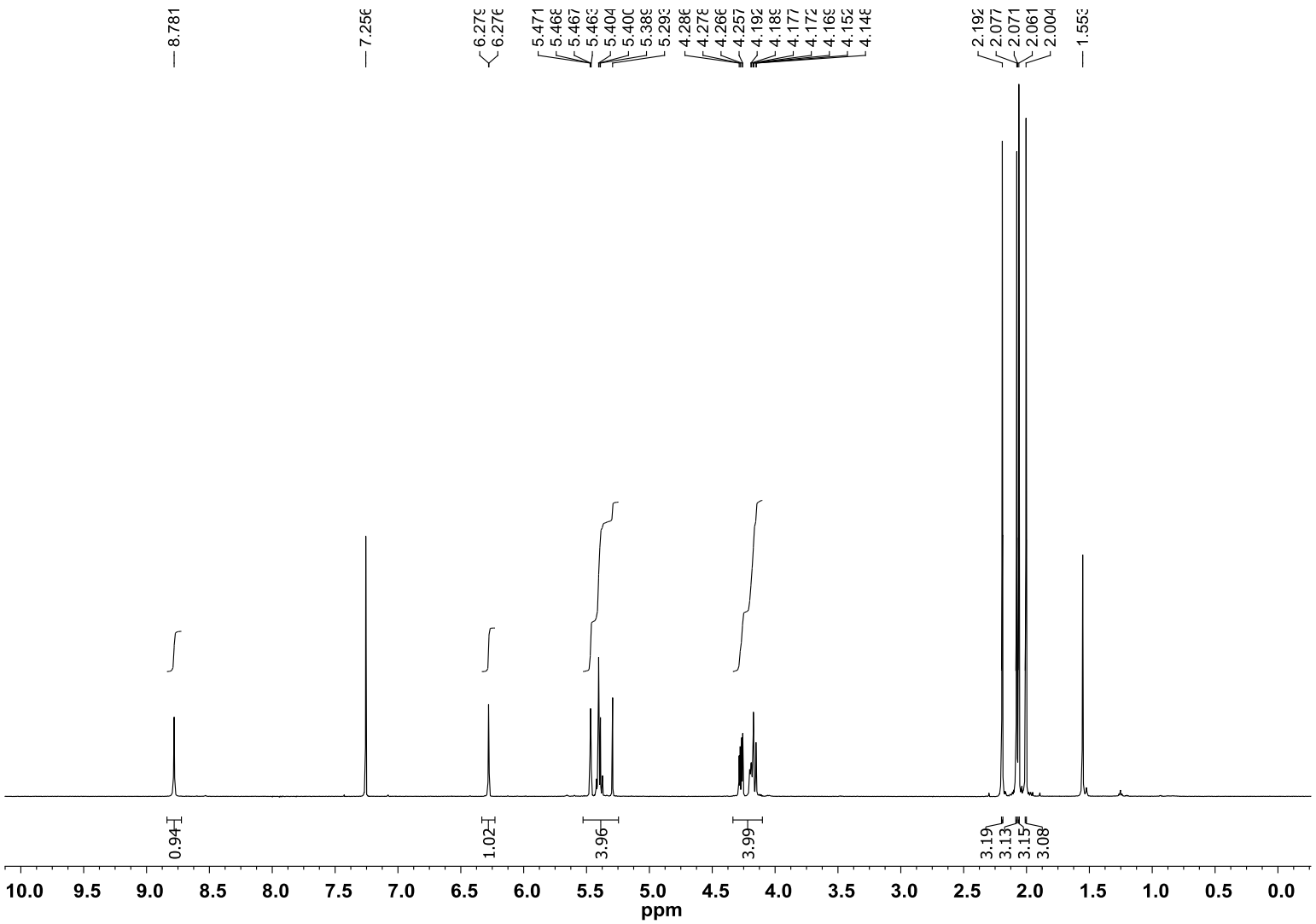

A-5: ^{1}H NMR spectrum of pentaacetyl-D-mannose-Cl, 6

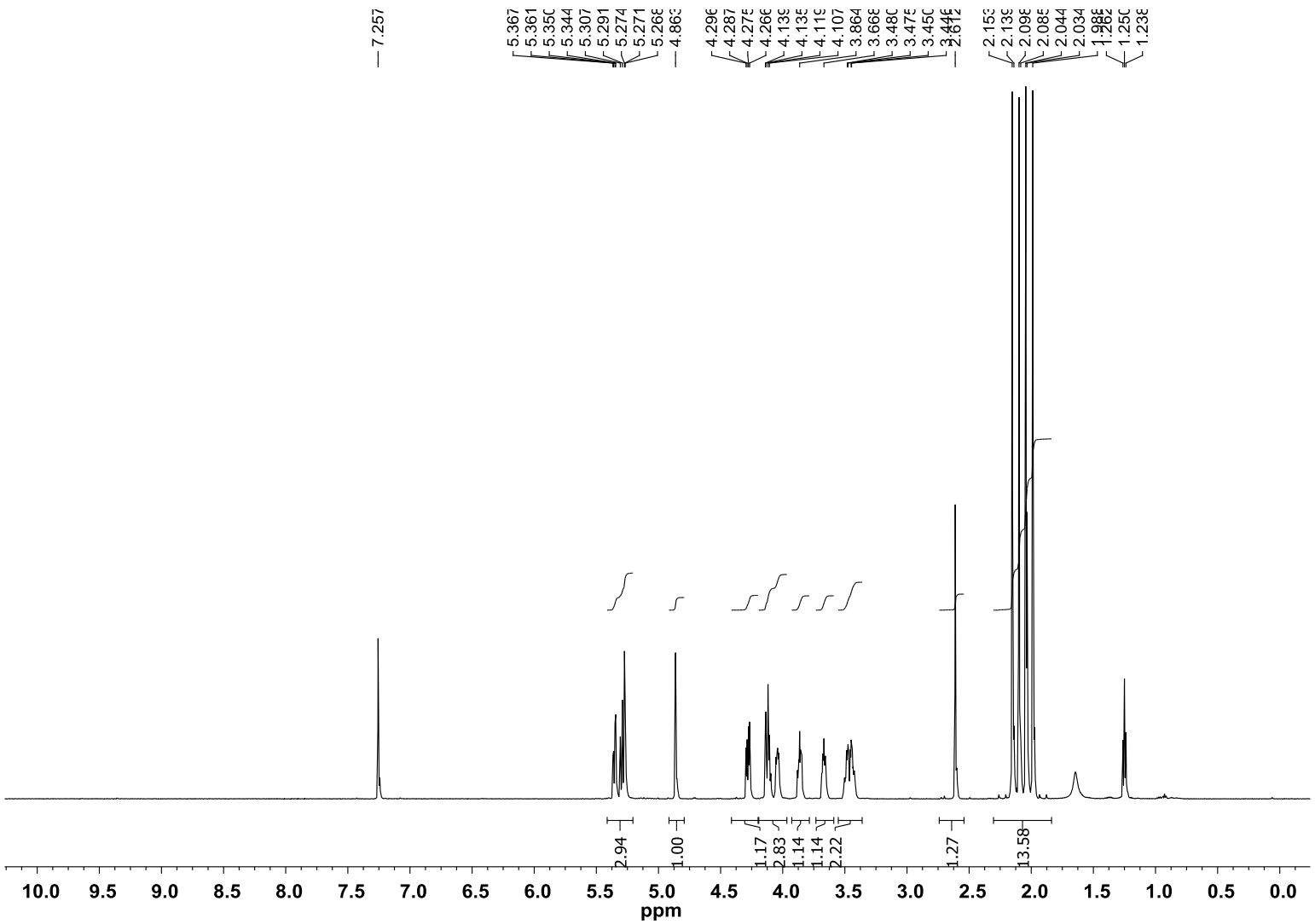

A-6: ^{1}H NMR spectrum of β-azido-2,3,4,6-tetraacetyl-D-mannose, 7

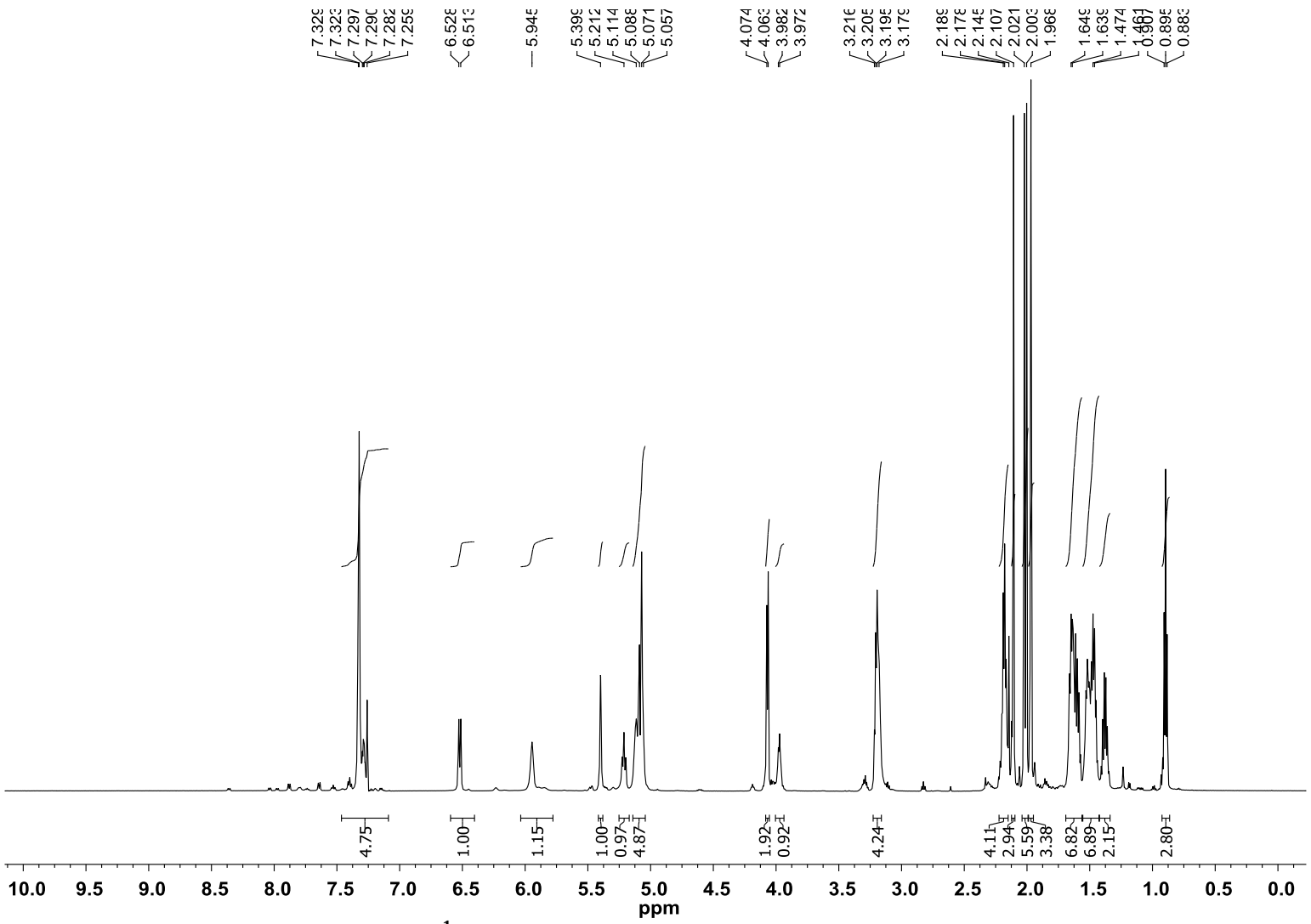

A-7: ^{1}H NMR spectrum of Z-(ava)$_2$-Ac$_y$-gal, 12

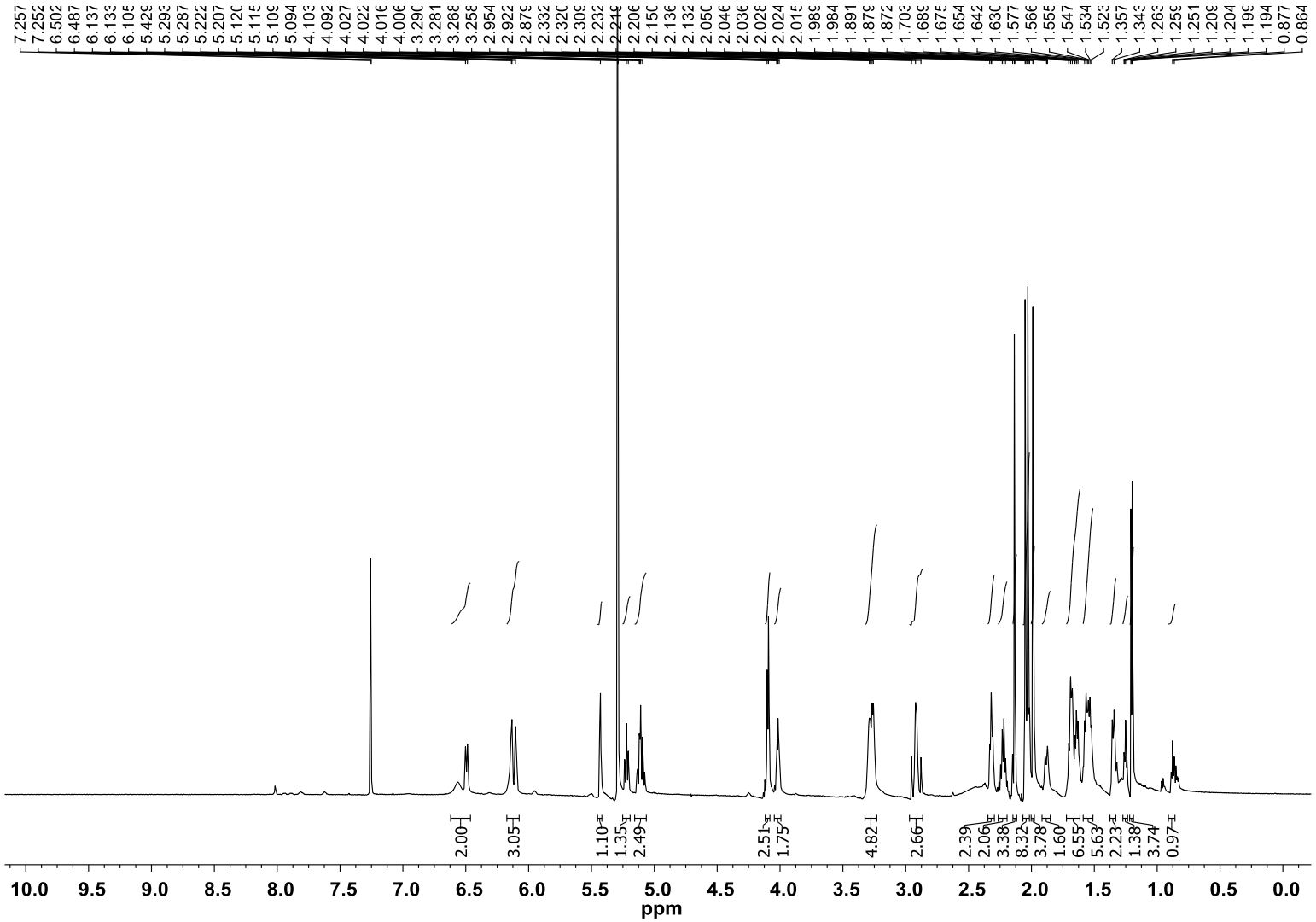

A-8: ^{1}H NMR spectrum of NB-(ava)$_2$-Acy-Gal, 14

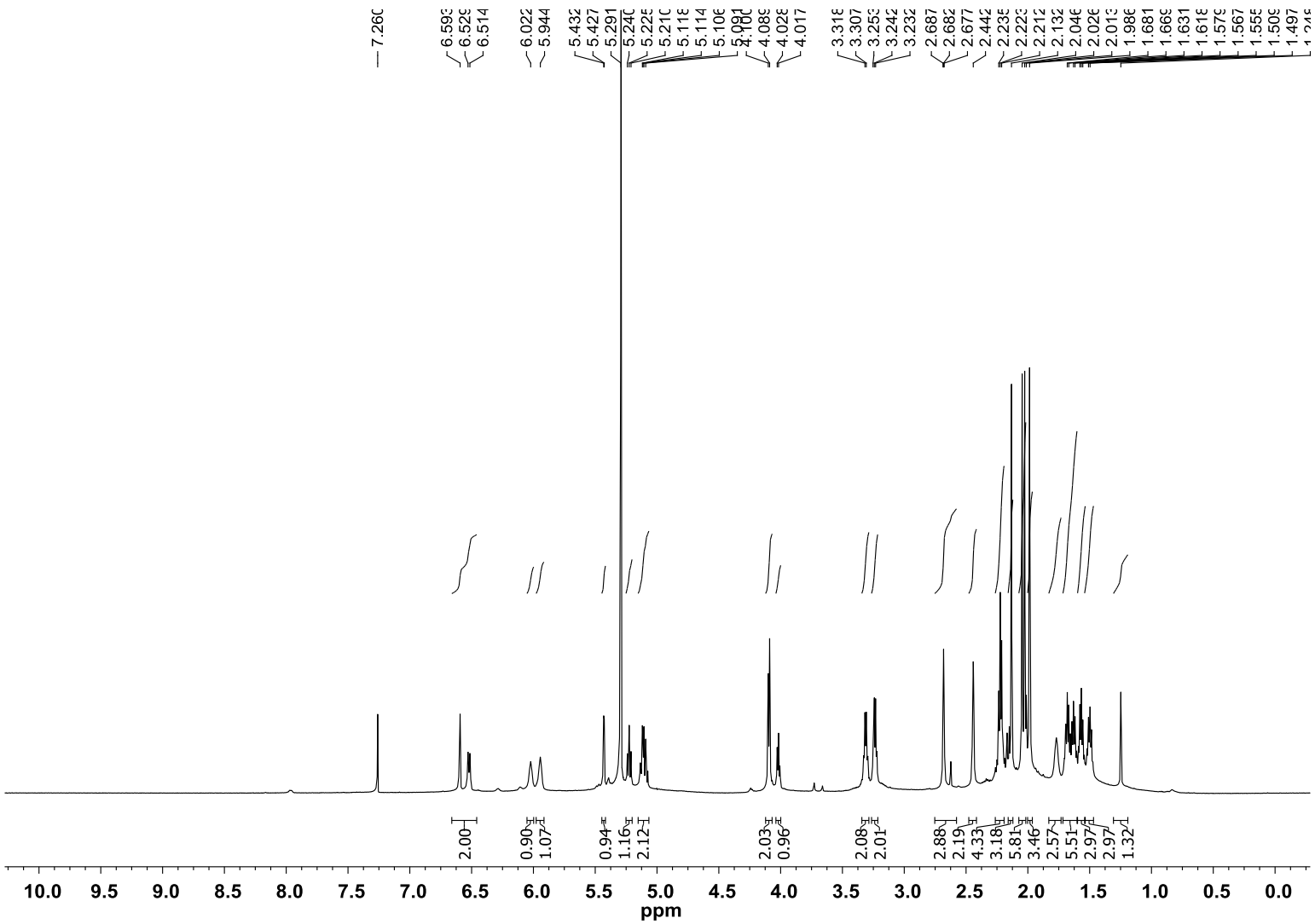

A-9: ^{1}H NMR spectrum of CB-(ava)$_2$-Ac$_y$-Gal, 15

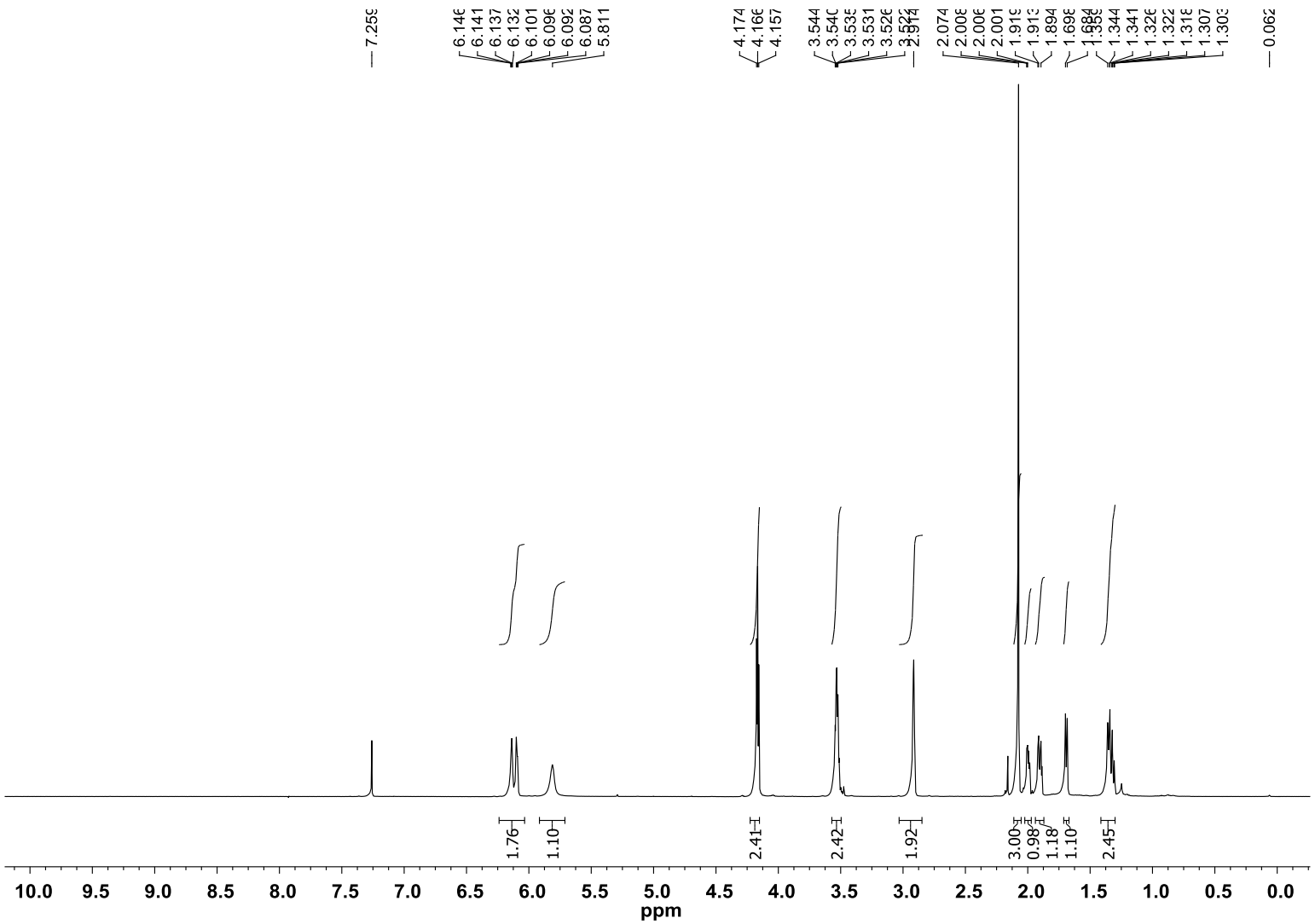

A-10: ^{1}H NMR spectrum of NB-$(CH_2)_2$-OAc, 17

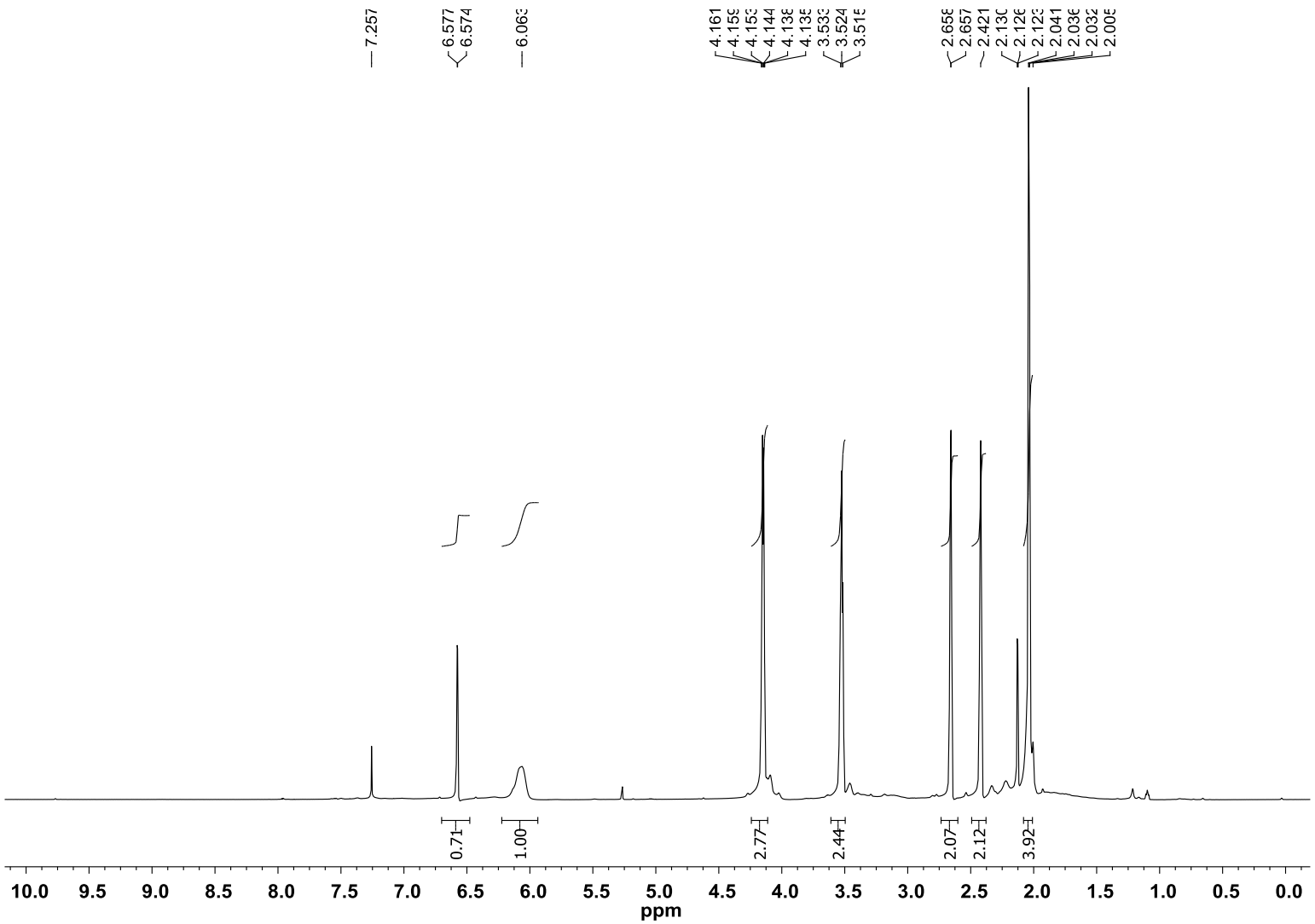

A-11: ^{1}H NMR spectrum of CB-$(CH_2)_2$-OAc, 18

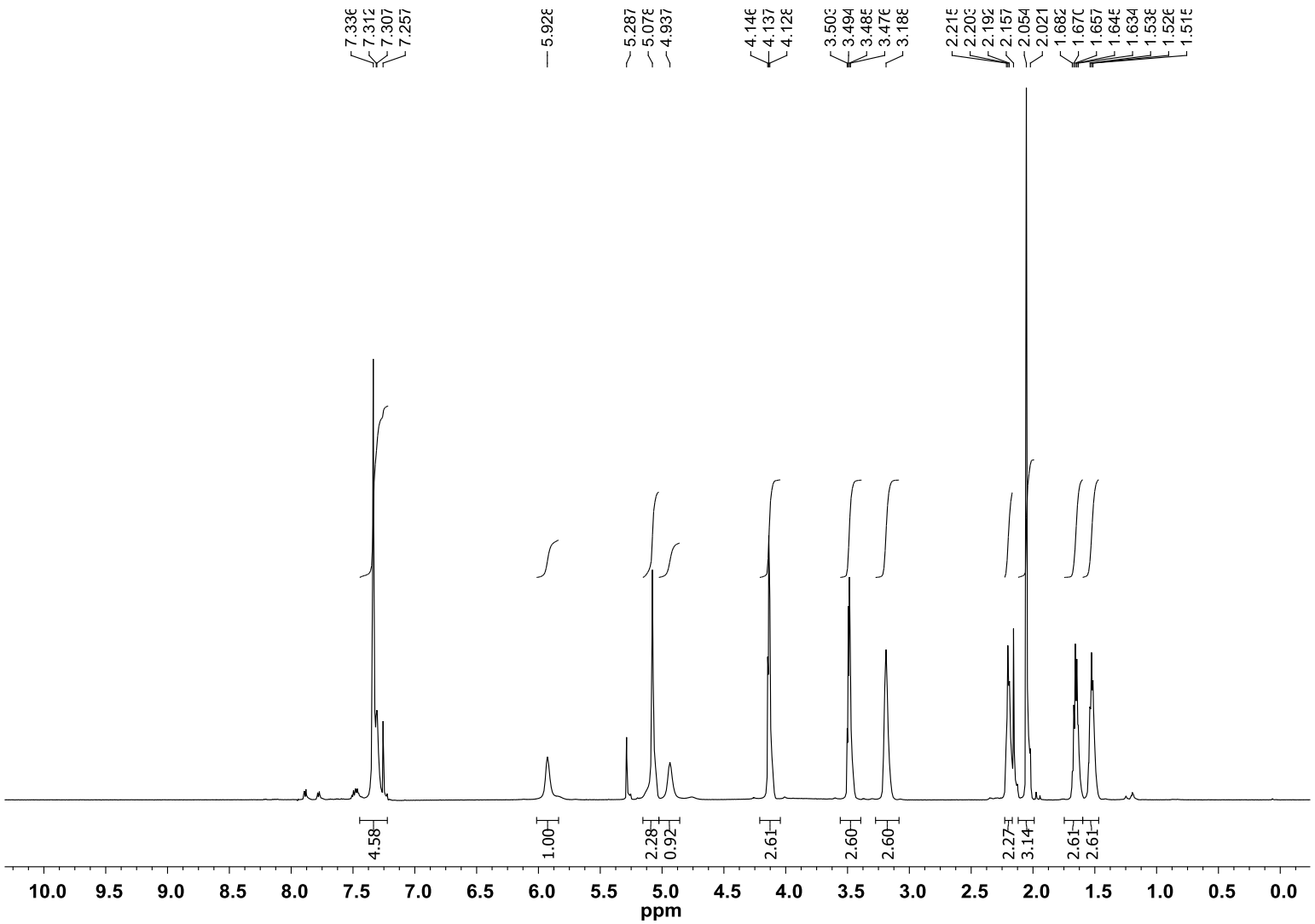

A-12: ^{1}H NMR spectrum of Z-ava-$(CH_2)_2$-OAc, 19

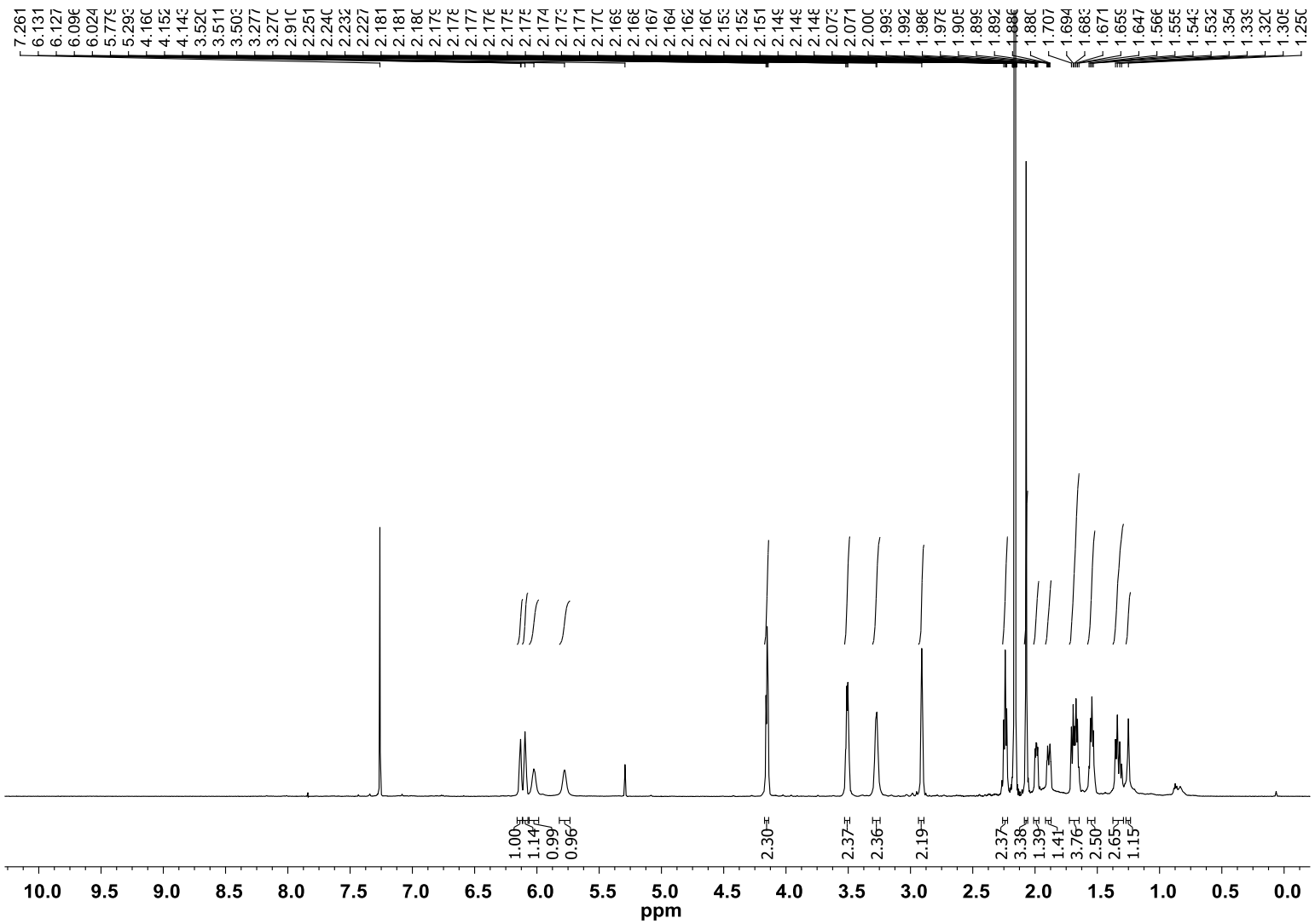

A-13: ^{1}H NMR spectrum of NB-ava-$(CH_2)_2$-OAc, 20

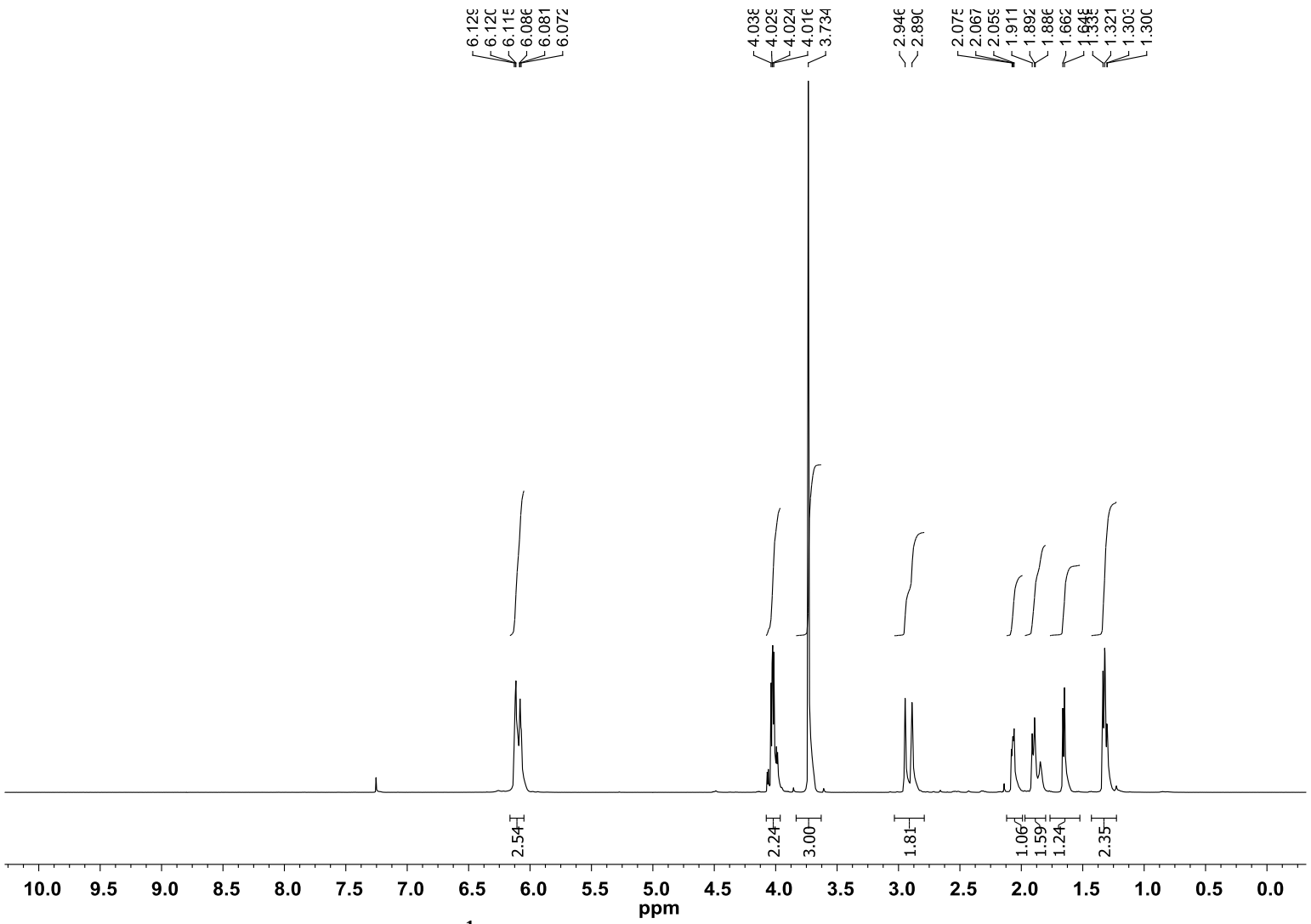

A-14: ^{1}H NMR spectrum of NB-Gly-OMe, 21

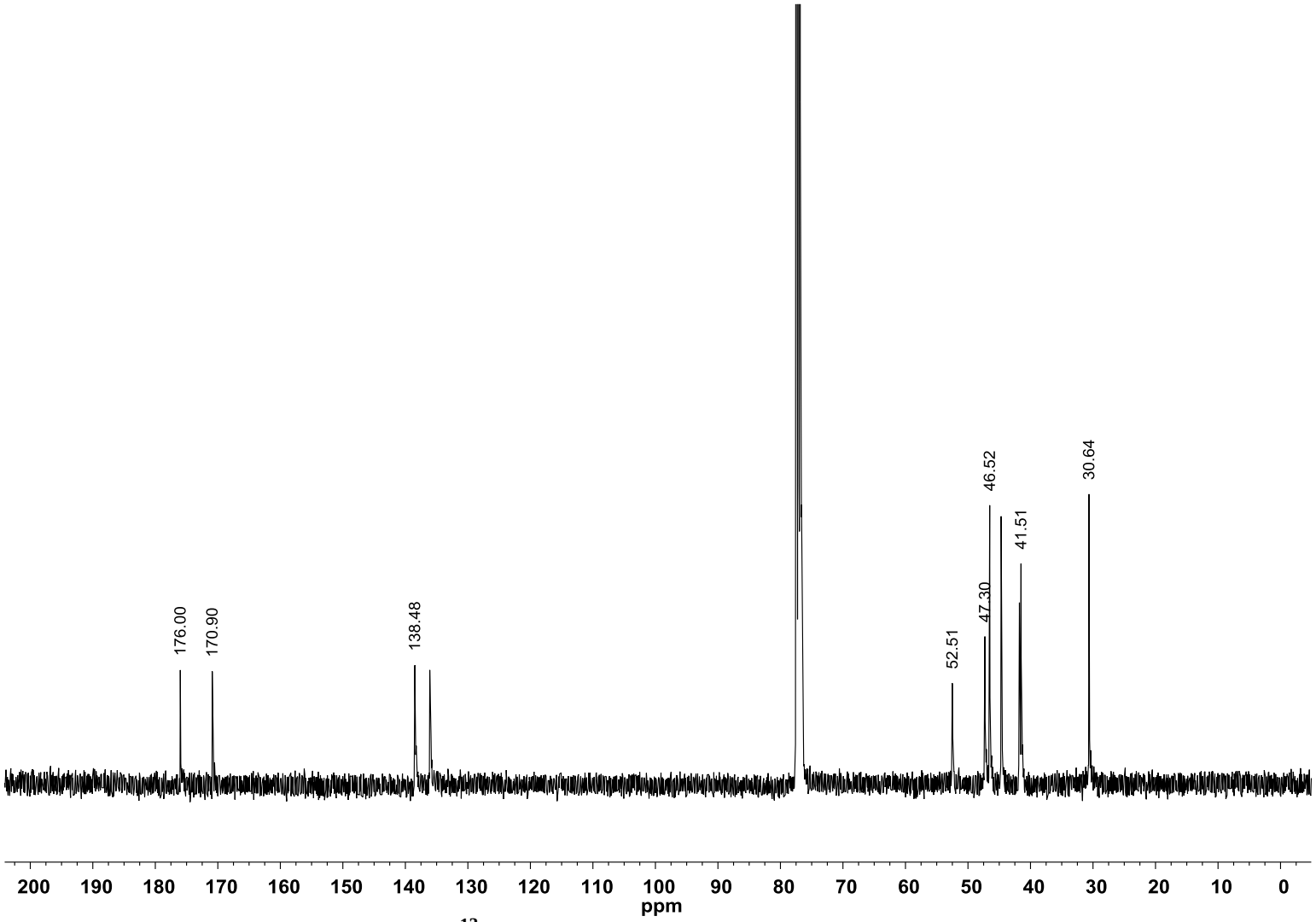

A-15: ^{13}C NMR spectrum of NB-Gly-OMe, 21

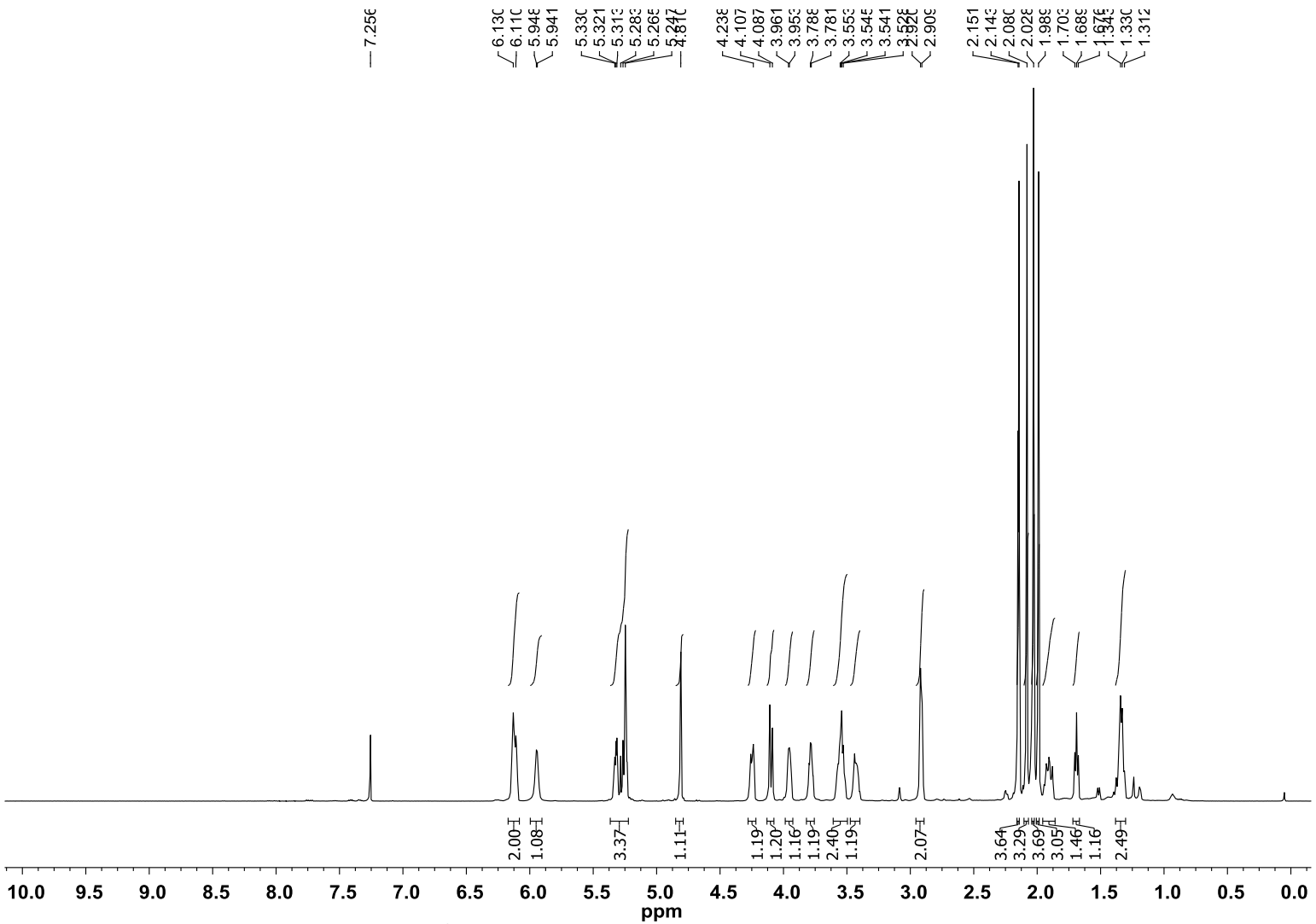

A-16: ^{1}H NMR spectrum of NB-AC$_y$-mannose, 22

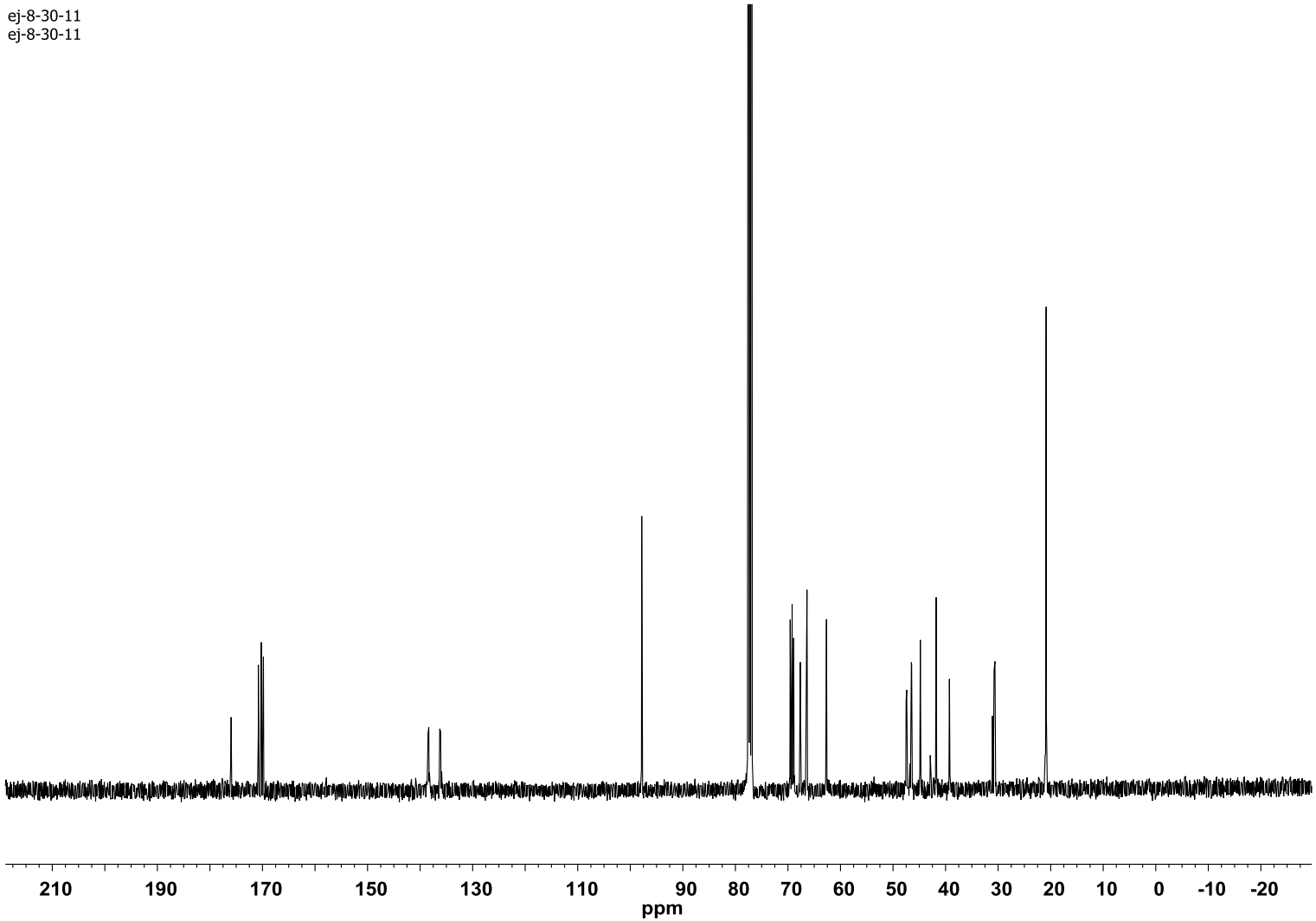

A-17: ^{13}C NMR spectrum of NB-AC$_y$-mannose, 22

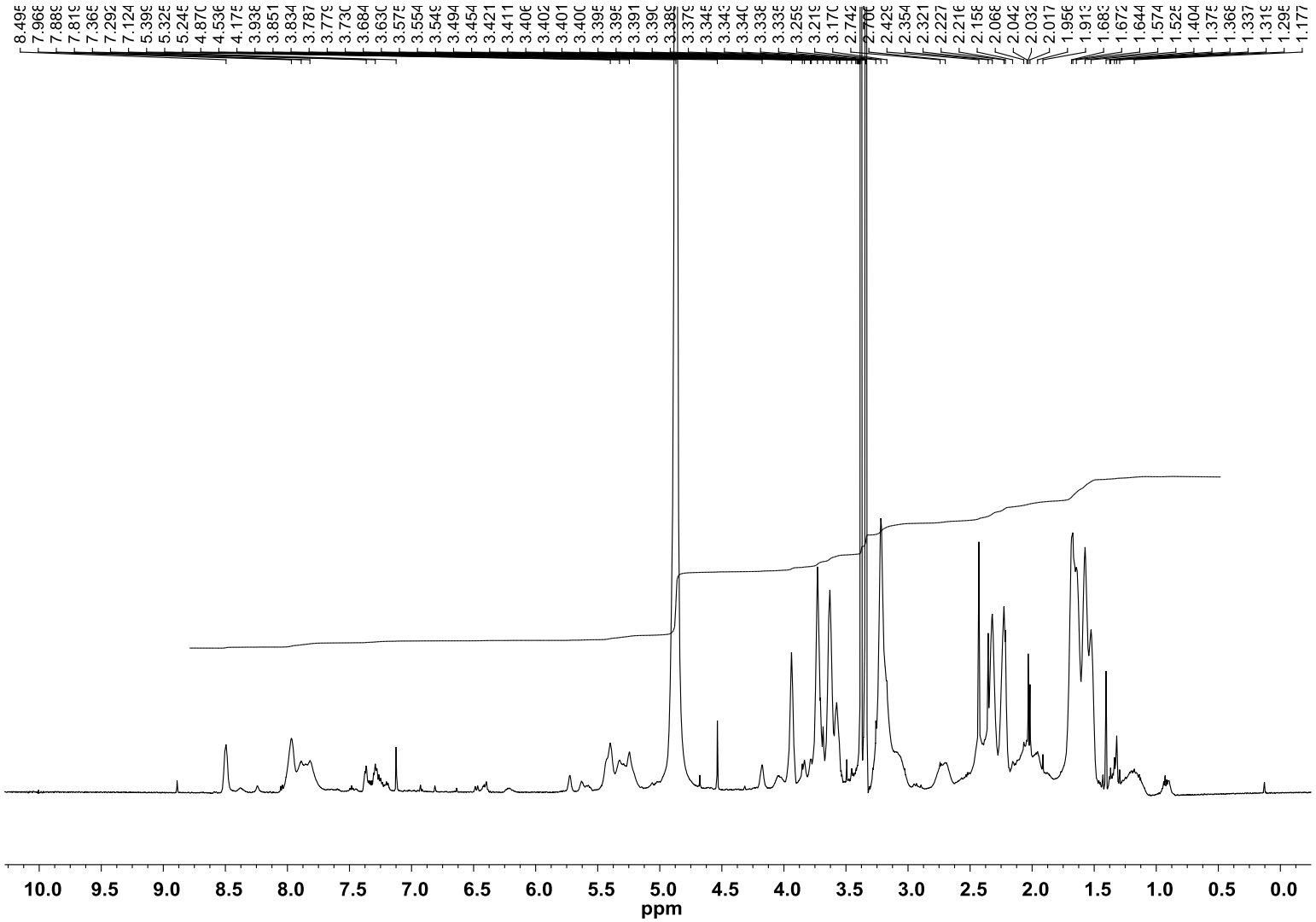

A-18: ^{1}H NMR spectrum of Homopolymer-1

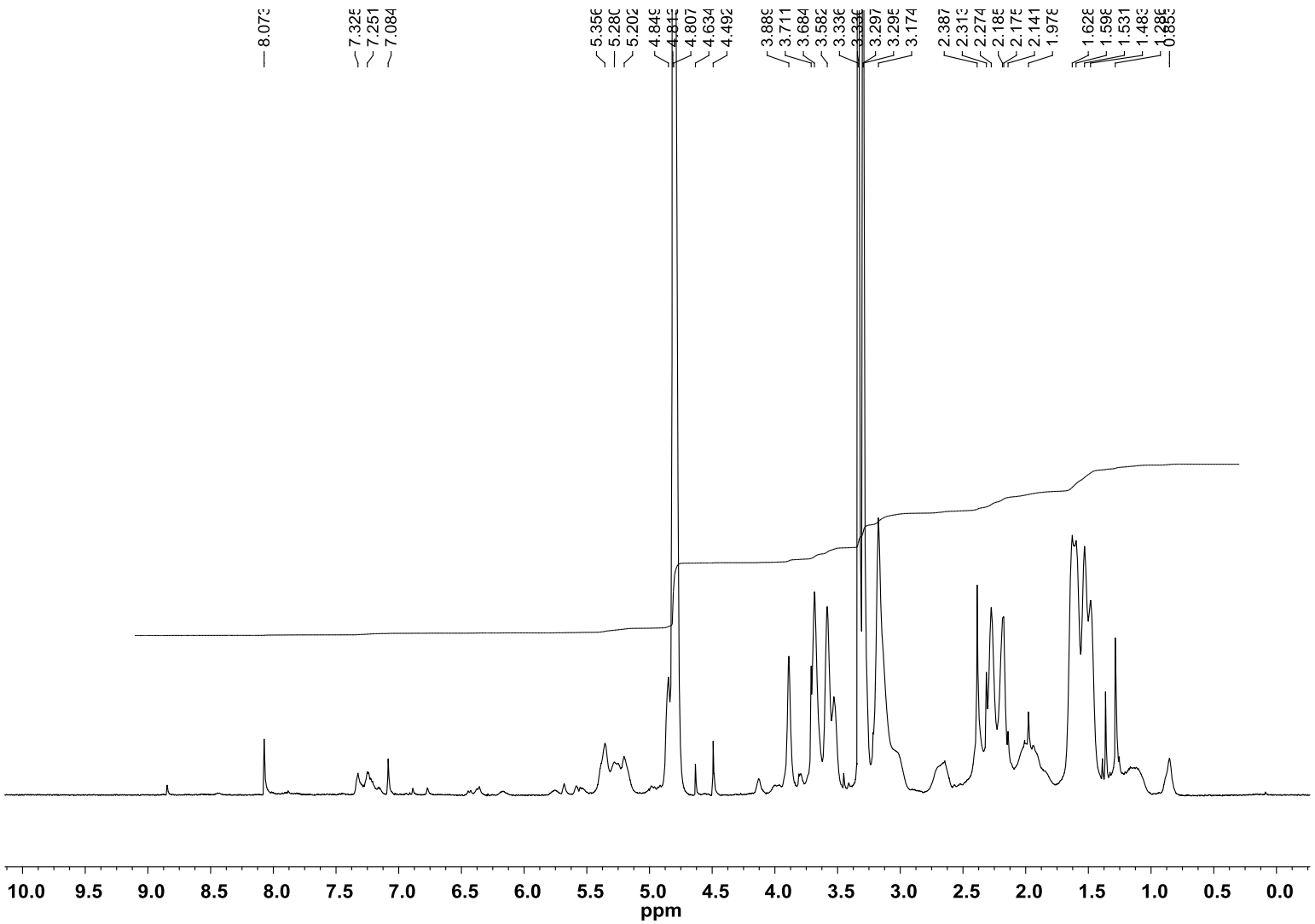

A-18: ^{1}H NMR spectrum of Homopolymer-2

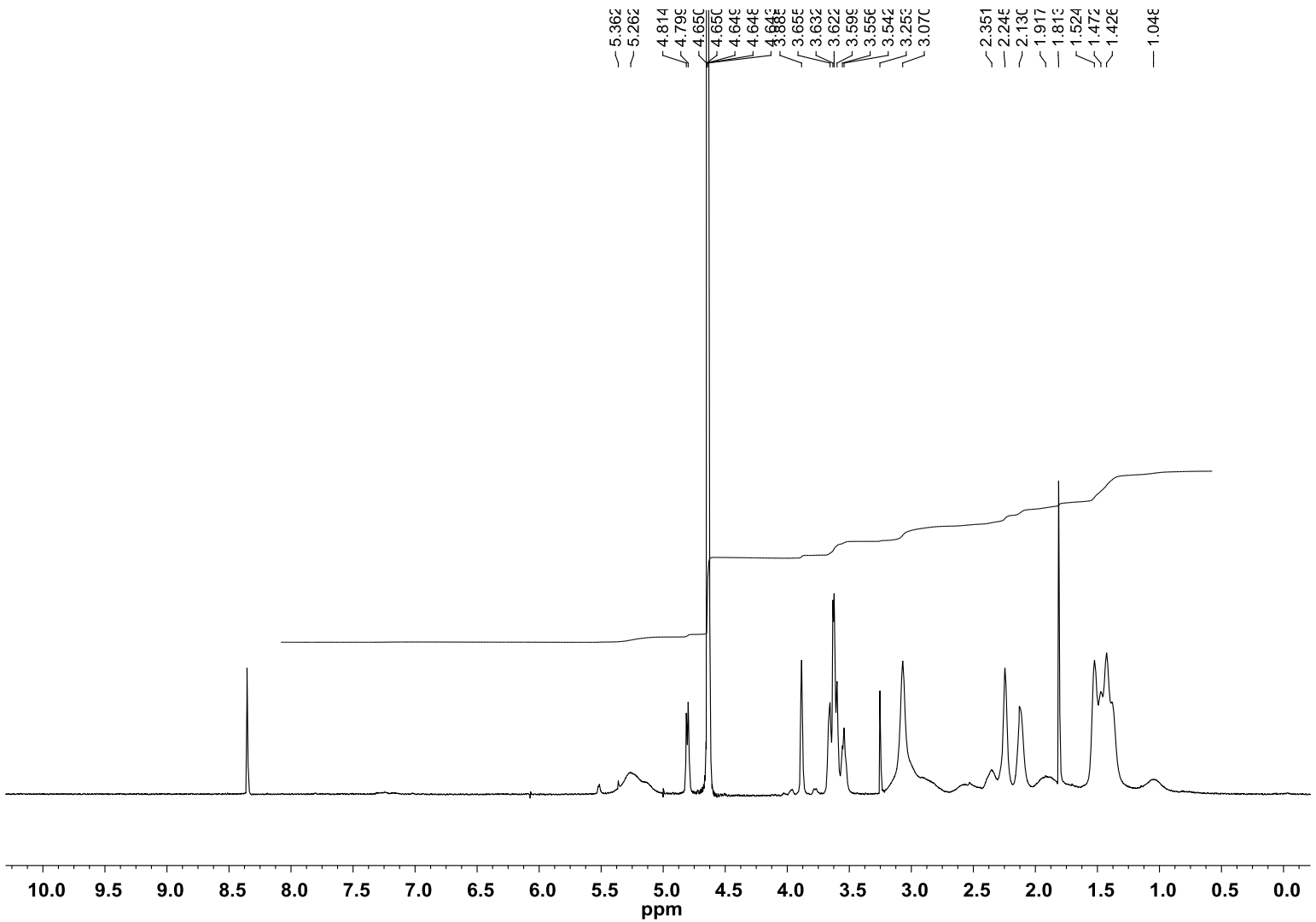

A-19: ^{1}H NMR spectrum of Homopolymer-3

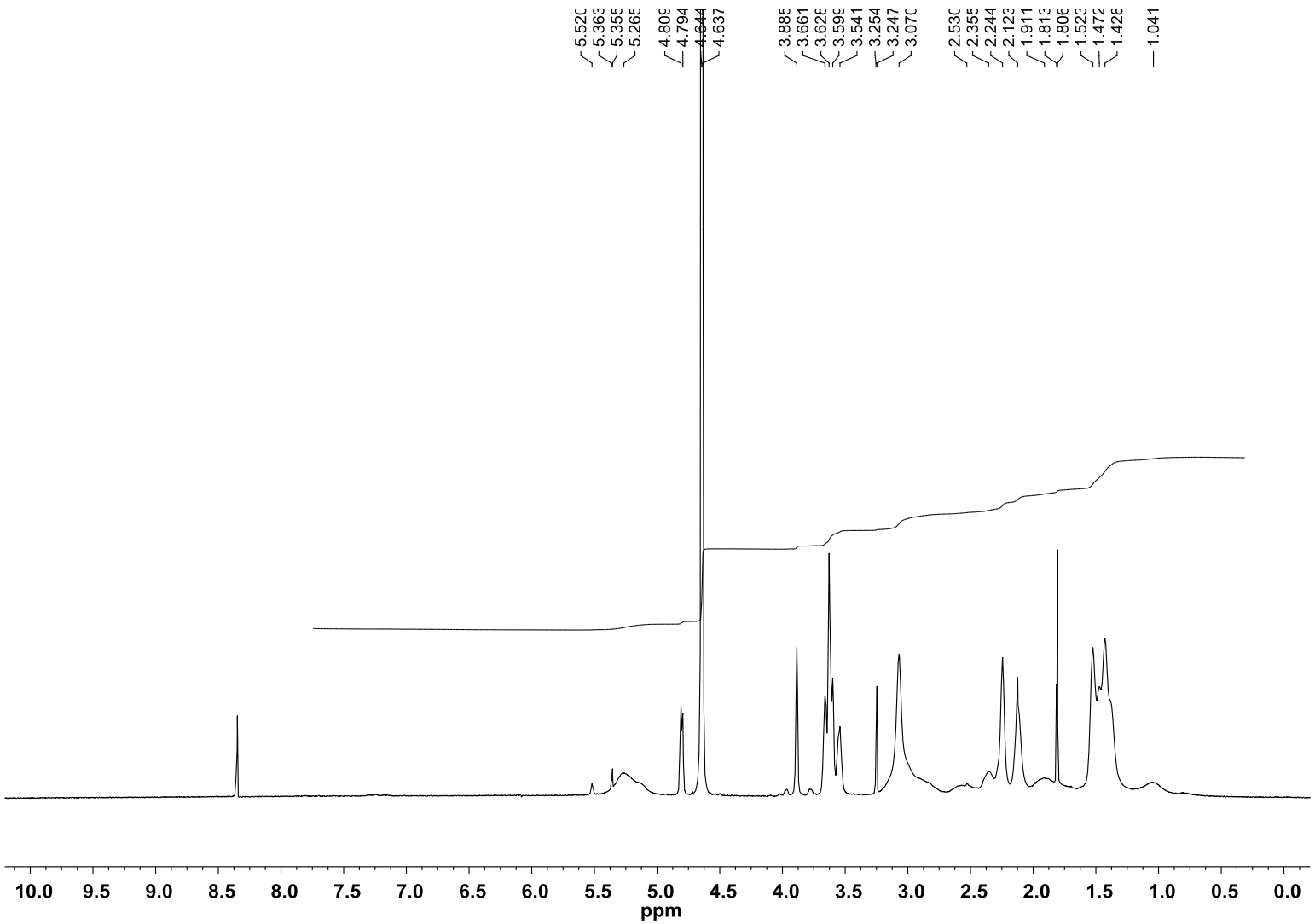

A-20: ^{1}H NMR spectrum of Homopolymer-4

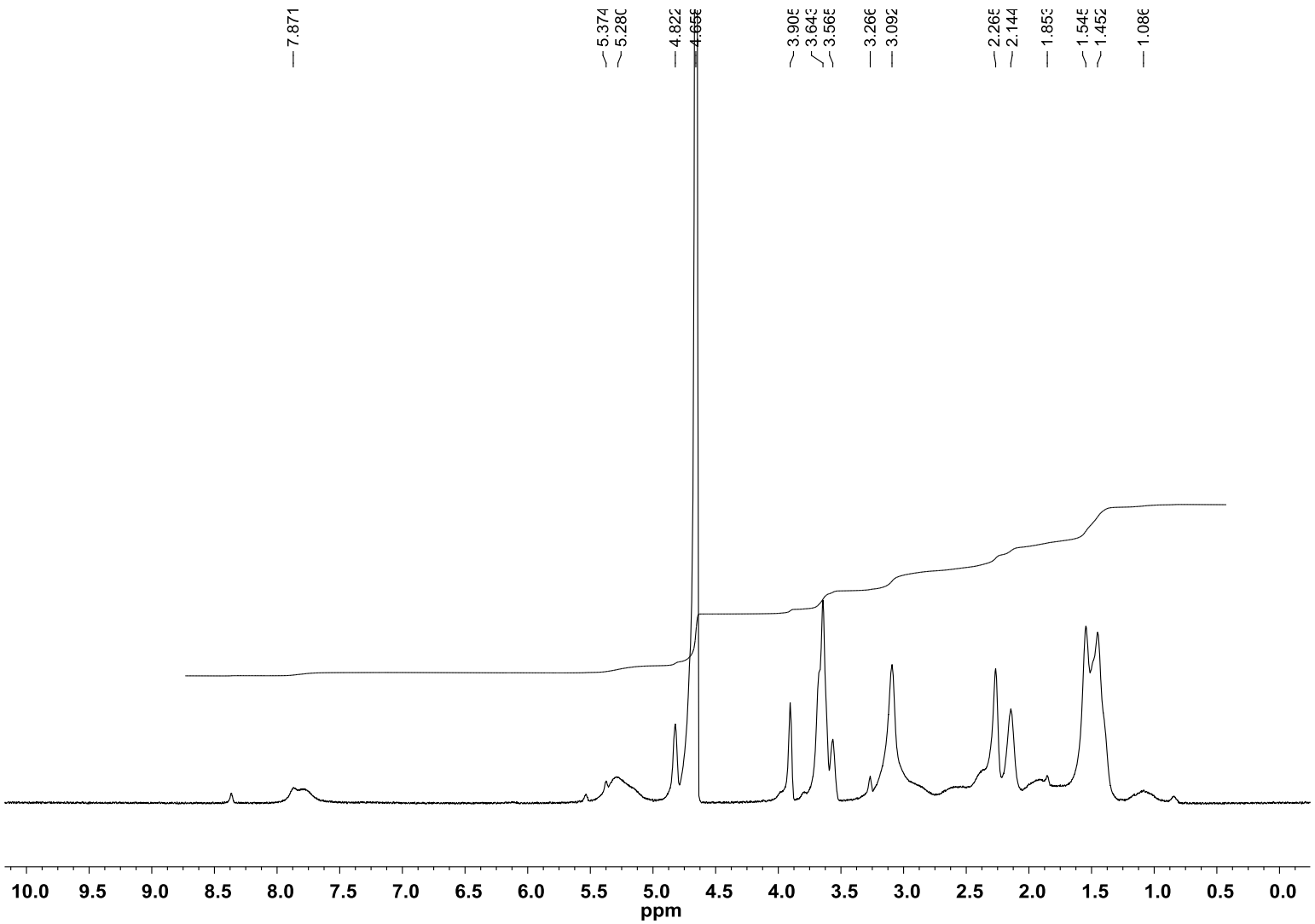

A-21: ^{1}H NMR spectrum of Homopolymer-5

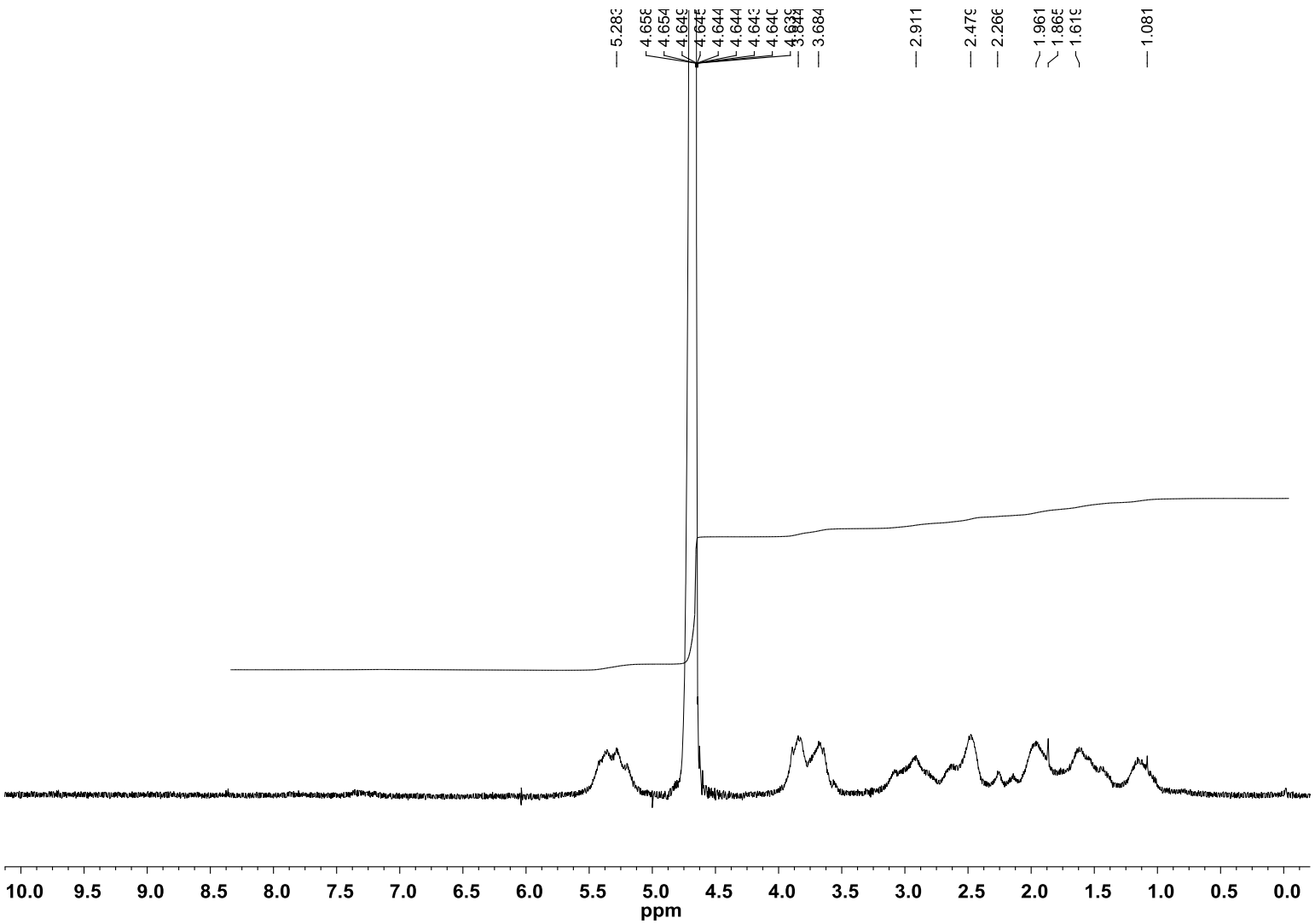

A-22: ^{1}H NMR spectrum of Copolymer-1

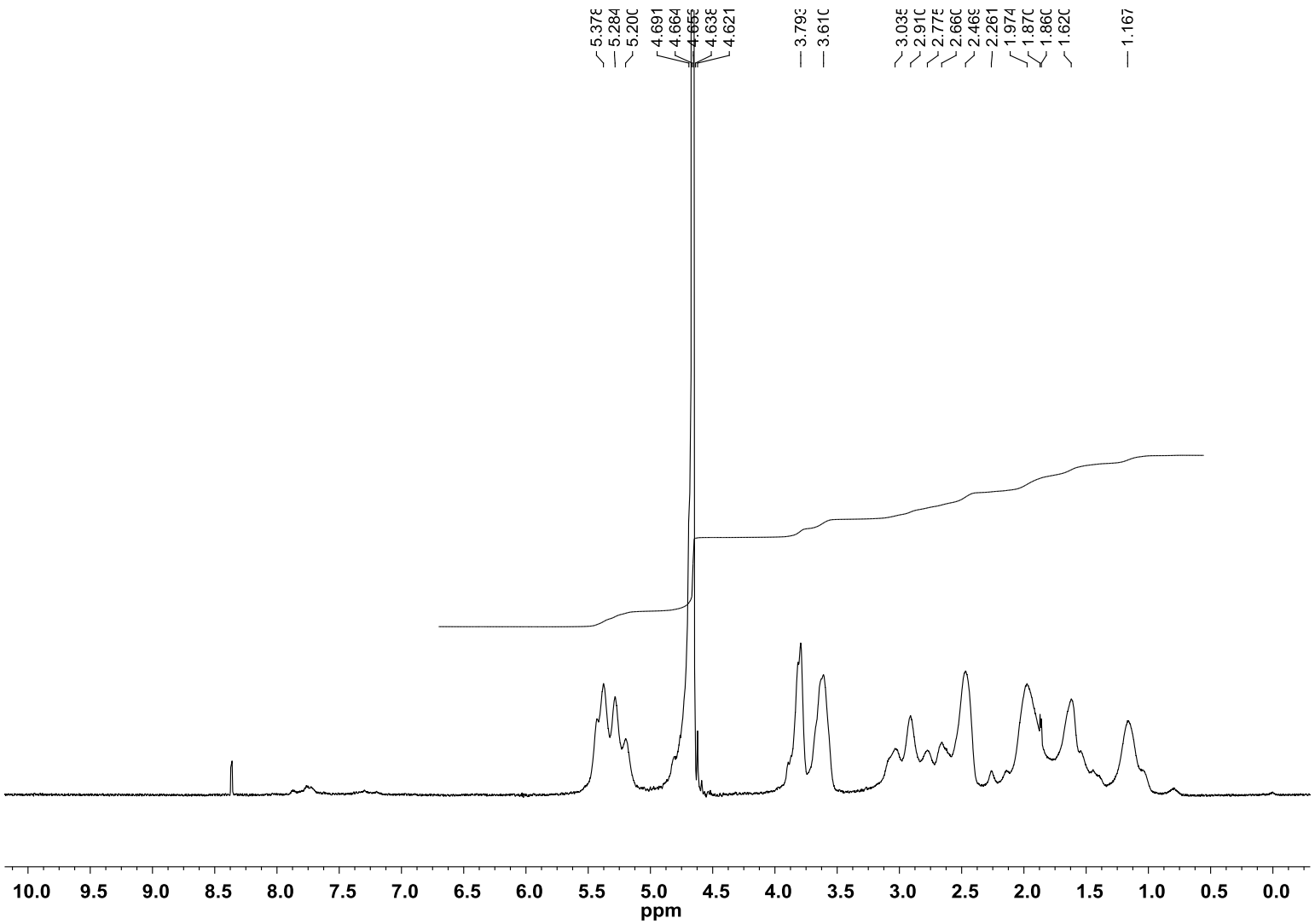

A-23: ^{1}H NMR spectrum of Copolymer-2

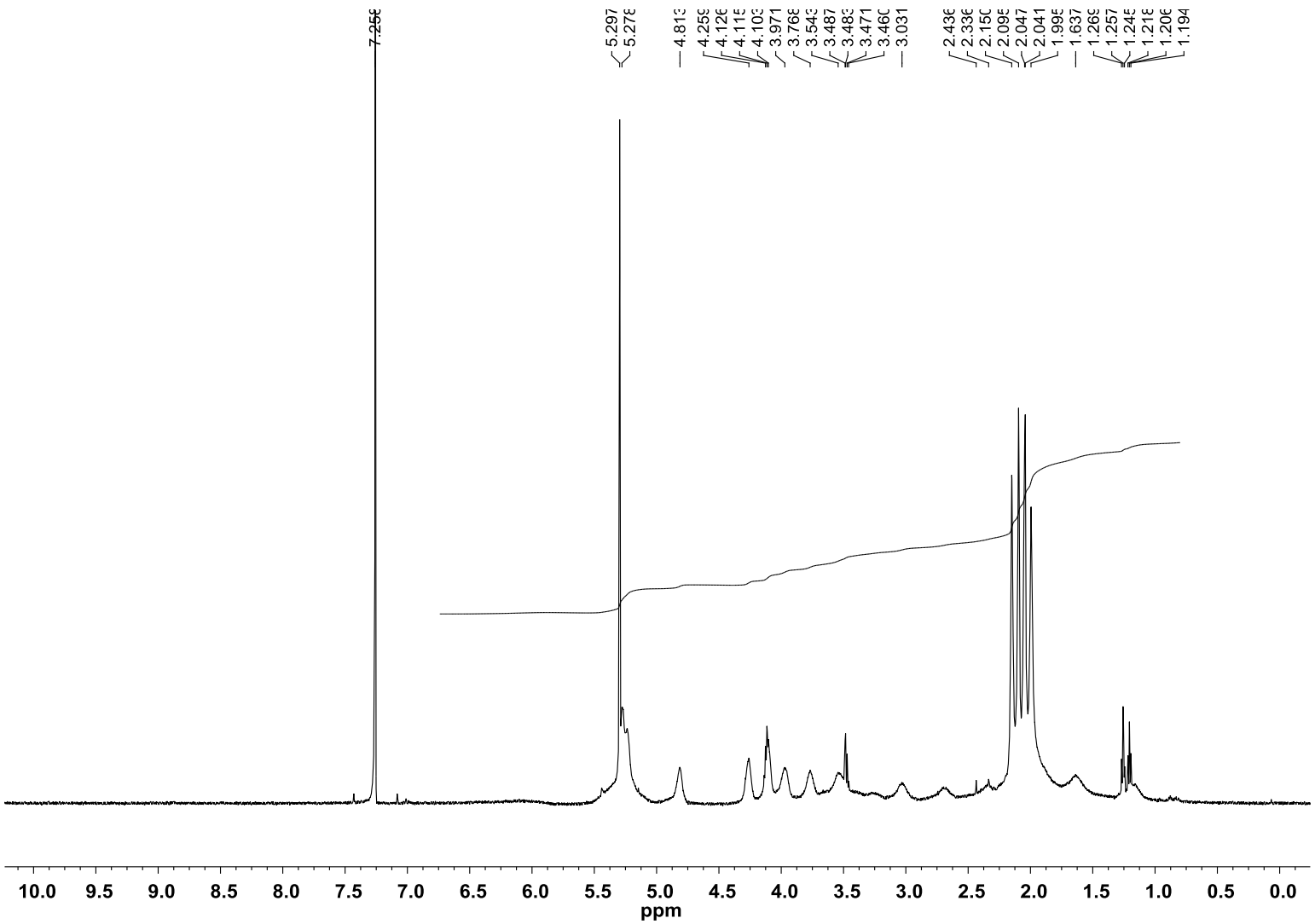

A-24: ^{1}H NMR spectrum of Copolymer-3

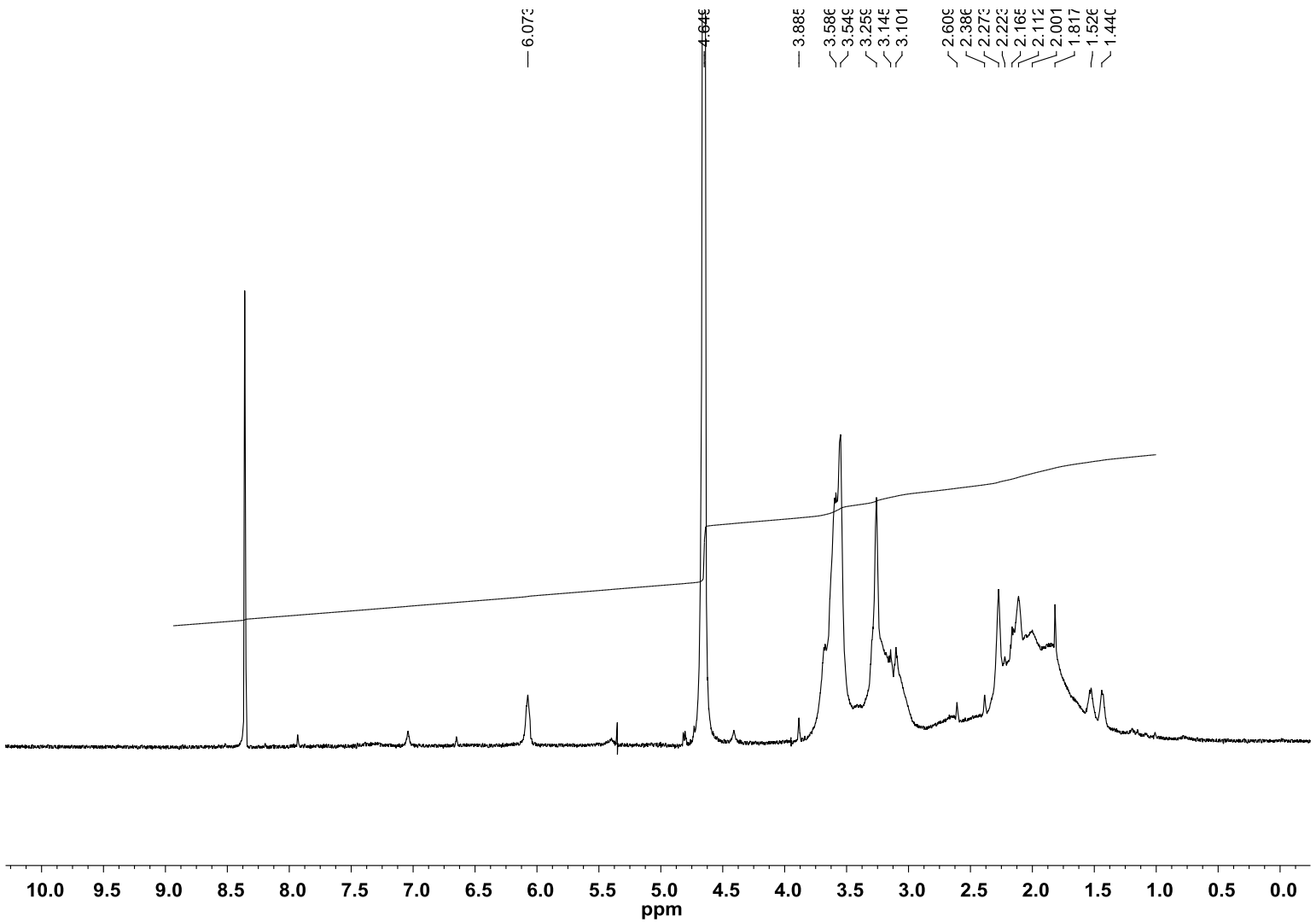

A-25: ^{1}H NMR spectrum of Copolymer-4

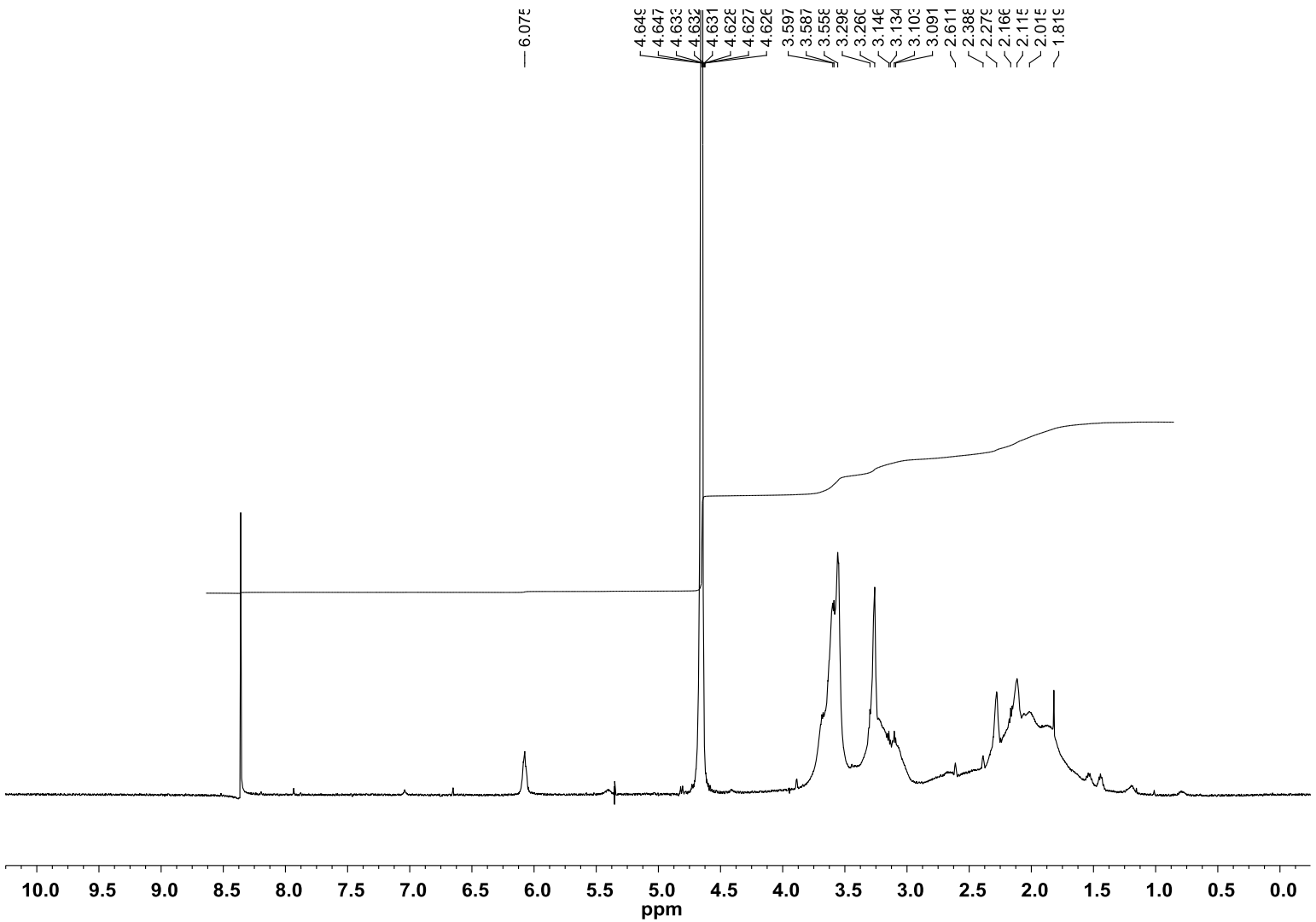

A-26: ^{1}H NMR spectrum of Copolymer-5

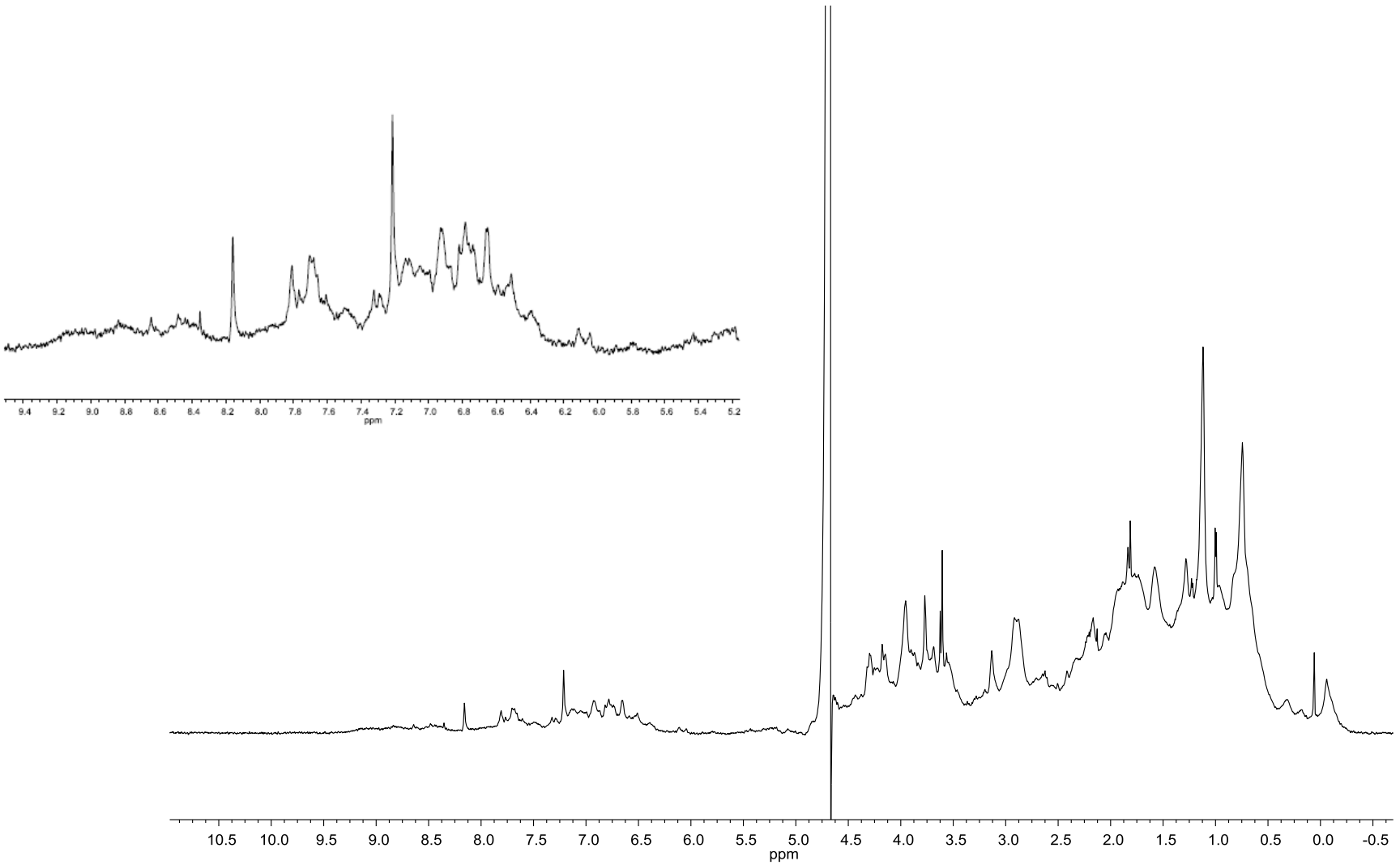

A-27: ^{1}H NMR spectrum of CT B_5

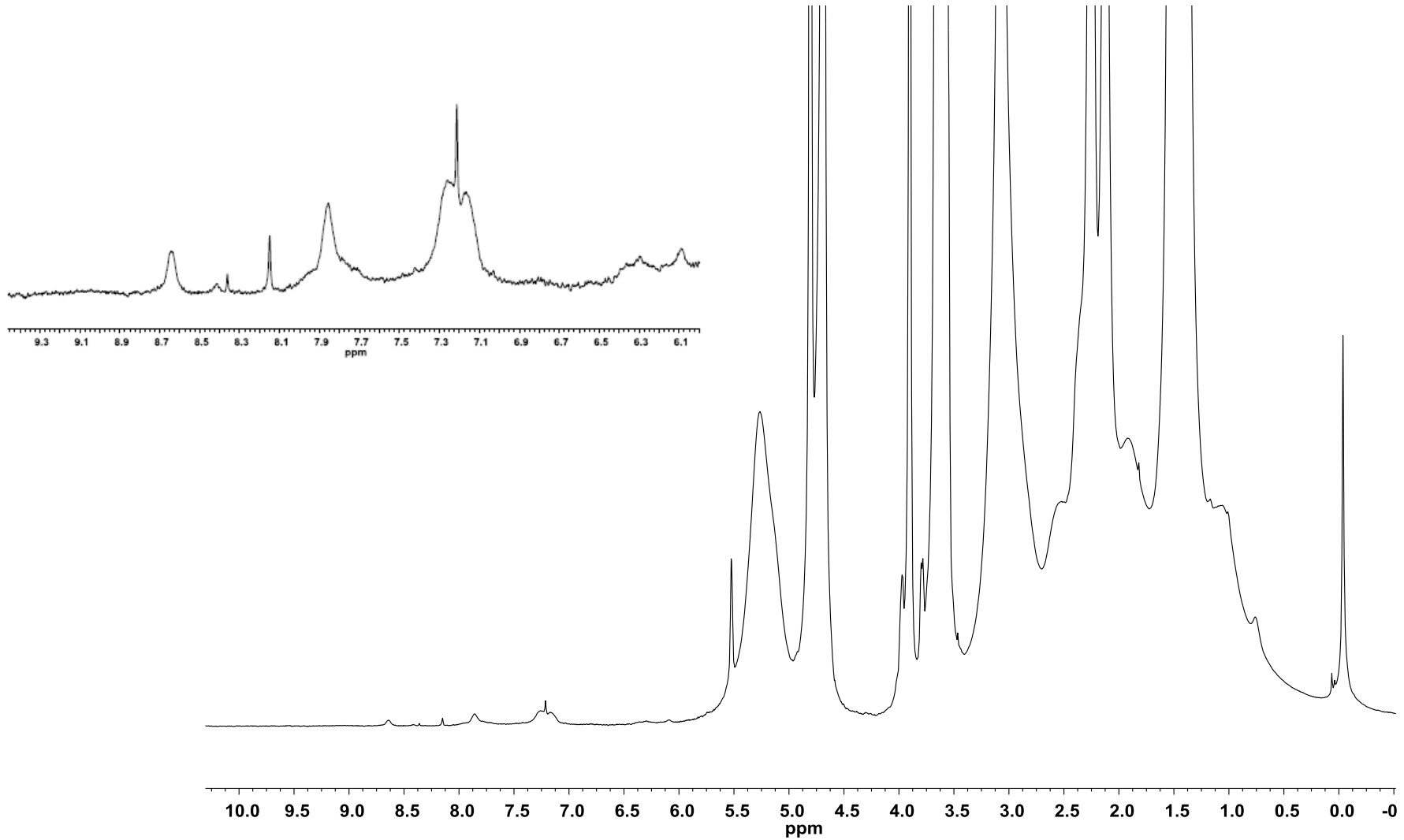

A-28: ^{1}H NMR spectrum of CT B_5 / Homopolymer-4

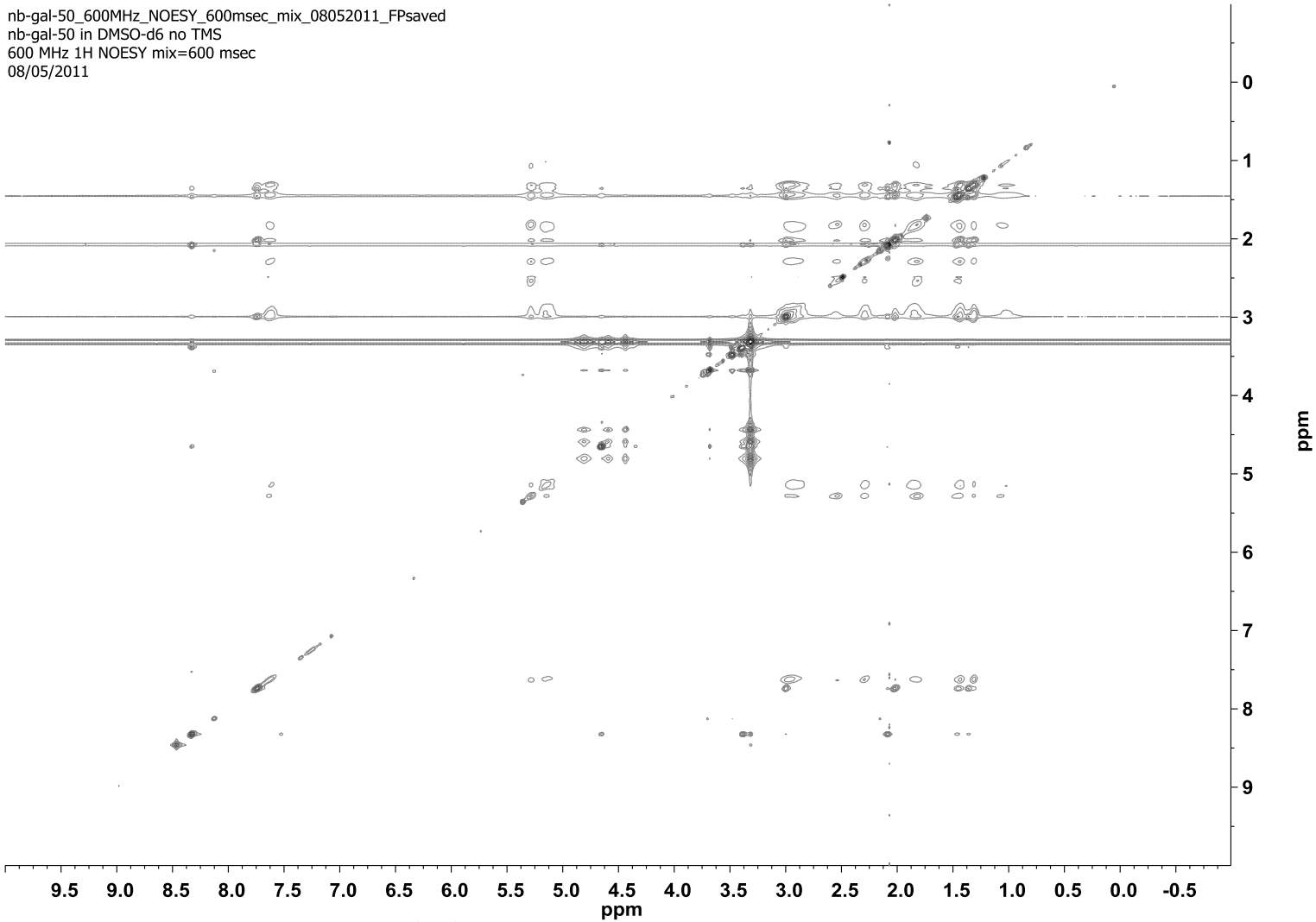

A-29: 2D-^{1}H,^{1}H- NOESY- NMR spectrum of Homopolymer-3